ENVIRONMENTAL VARIABILITY AFFECTS GUT MICROBIOTA AND EXPERIMENTAL OUTCOMES IN MOUSE MODELS

A Dissertation presented to the Faculty of the Graduate School at the University of Missouri- Columbia

---

In Partial Fulfillment of the requirements for the Degree Doctor of Philosophy

---

by AMBER L. RUSSELL

Dr. Aaron Ericsson, Dissertation Supervisor

MAY 2023

The undersigned, appointed by the dean of the Graduate School, have examined the dissertation entitled

ENVIRONMENTAL VARIABILITY AFFECTS GUT MICROBIOTA AND

EXPERIMENTAL OUTCOMES IN MOUSE MODELS

presented by Amber Russell,

a candidate for the degree of Doctor of Philosophy,

and hereby certify that, in their opinion, it is worthy of acceptance.

_____

Professor Aaron Ericsson

_____

Professor Craig Franklin

_____

Professor Elizabeth Bryda

_____

Professor Susan McKarns

_____

Professor Christopher Baines

DEDICATION

This work is dedicated to my loving parents Mark and Bobbie Russell. Thank you for being a constant source of support, for your unconditional love, and for the sacrifices you have made and continue to make, for not only me, but the whole family.

ACKNOWLEDGMENTS

I would like to acknowledge the following people for their efforts and assistance over the course of my degree:

My advisor Dr. Aaron Ericsson for being an excellent mentor and an overall good person. Thank you for the kindness and understanding you have shown me during difficult times.

Members of the Franklin and Ericsson labs, both past and present especially Giedre Turner, Becky Dorfmeyer, Benjamin Olthoff, and Chunye Zhang for continuing my studies during my unexpected medical absence. A special acknowledgment is also due to Zach McAdams for taking the time to troubleshoot my programming and sharing the joy of R coding and programming with me.

Members of my PhD committee Drs. Craig Franklin, Elizabeth Bryda, Susan McKarns, and Christopher Baines for their support and efforts throughout my PhD experience.

Past and present faculty and students of the Department of Veterinary Pathobiology and Comparative Medicine Program.

The staff and technicians of the Organization of Animal Research for their excellent husbandry and care of the animals involved in my research.

TABLE OF CONTENTS

LIST OF FIGURES

LIST OF TABLES

LIST OF ABBREVIATIONS

ANOVA: analysis of viariance

ASV: amplicon sequence variants

BGL: blood glucose level

BR: broad range

BSC: biosafety cabinet

GF: germ-free

GIT: gastrointestinal tract

GM: gut microbiota

IACUC: Institutional Animal Care and Use Committee

IBD: inflammatory bowel disease

IDDM: insulin-dependent diabetes mellitus

MHV: murine hepatitis virus

mpc: mice per cage

NOD: non-obese diabetic

PERMANOVA: permutational multivariate analysis of variance

RA: relative abundance

SFB: segmented filamentous bacteria

SPF: specific pathogen free

T1D: Type 1 diabetes

VAMN: vancomycin, ampicillin, metronidazole, and neomycin mixture

ABSTRACT

The gut microbiome of humans and animals is critical to host health. Mice are used to investigate the microbiome and its influences; however, the predictive value of such studies is hindered by cage effects due to coprophagy. Our objectives were to evaluate the influence of cage density on the statistical power to detect treatment-dependent effects of a selective pressure on microbiome composition. C57BL/6 mice were separated into groups of 2 or 4 mice per cage, and then assigned to groups receiving enrofloxacin, broad-spectrum antibiotics, or control. Fecal samples were collected at weeks 0, 1, and 4, along with contents of the jejunum and cecum. Bacterial DNA was analyzed for microbiome richness, diversity, and variability within and between cages. Statistical analyses revealed that reduced housing density consistently resulted in comparable susceptibility to antibiotics, reduced cage effect, and increased statistical power to detect treatment-associated effects, justifying the practice of reduced housing density.

There is limited understanding of how the microbiota colonizing various maternal tissues contribute to the development of the neonatal gut microbiota (GM). To determine the contribution of various maternal microbiotic sites to the offspring microbiota in the upper and lower gastrointestinal tract (GIT) during early life, litters of mice were sacrificed at 7, 9, 10, 11, 12, 14, and 21 days of age, and fecal and ileal samples were collected. Dams were euthanized alongside their pups, and oral, vaginal, ileal, and fecal samples were collected. This was done in parallel using mice with either a low-richness or high-richness microbiota to assess

the consistency of findings across multiple microbial compositions. Sample were analyzed using 16S rRNA amplicon sequencing. The similarities between matched pup and dam samples were used to determine the contribution of each maternal source to the pup fecal and ileal composition at each timepoint. As expected, similarity between pup and maternal feces increased significantly over time. During earlier time-points however, the offspring fecal and ileal microbiotas were closer in composition to the maternal oral microbiota than other maternal sites. Prominent taxa contributed by the maternal oral microbiota to the neonatal gut microbiota were supplier-dependent and included *Lactobacillus* spp., *Streptococcus* spp., and a member of the *Pasteurellaceae* family. These findings align with the microbial taxa reported in infant microbiotas, highlighting the translatability of mouse models in this regard, as well as the dynamic nature of the gut microbiota during early life.

The Non-Obese diabetic model of type 1 diabetes (T1D) has been the most highly utilized animal model in T1D research, resulting in multiple studies that have furthered the understanding of T1D development. However, this model suffers from inconsistency in disease incidence between studies that has been attributed to environmental variability, resulting in compositional shift in the gut microbiota (GM). It is currently unclear how these variations in GM composition influence the overall T1D phenotype in NOD mice. Therefore, this study aims to determine how sex, GM composition, and exposure to specific pathobionts previously suspected to alter T1D incidence interact to influence the T1D phenotype in NOD mice. Two cohorts of NOD mice were utilized to analyze diabetic and pre-diabetic timepoints of disease development for T1D incidence and insulitis severity respectively. The

GM composition of these mice were then analyzed to identify shifts in beta diversity and predicted metabolic function associated with pathobiont inoculation. Results show all three factors interact to effect T1D incidence, insulitis severity, and GM beta diversity. Most prevalent, *H. hepaticus* shifted beta diversity in all groups and tended to exacerbate disease onset and severity. This *H. hepaticus* driven shift in beta diversity was associated with predicted changes in metabolic functions related to T1D.

CHAPTER 1 – VARIABILITY IN TRANSLATABILITY OF MOUSE MODELS

Introduction

Utilization of animal models in scientific research has profoundly increased understanding of human biological systems and disease pathogenesis. The house mouse, *Mus musculus*, has historically been the choice animal for observational study, with its use in scientific research starting as early as the 16th century[1]. By the 18th century, the study of mice became increasingly popular for observational studies due to their small size, short gestation periods, and ease of maintenance[1]. During the 20th century laboratory mouse models became commercially available for experimental research, and inter-individual variability between mice became a concern for scientists[2]. This resulted in scientist controlling for as much variability between mice as possible. Thus, in the 1960's, suppliers of mouse models began the exclusion of specific pathogens within laboratory mouse colonies to reduce transmission of pathogens that may produce undesirable research results[3]. This establishment of a specific pathogen free (SPF) setting for commercially available mice, in hindsight, contributes to confounding variability between mouse studies due to supplier differences in pathogen exclusion, as well as supplier and institutional differences in maintaining a SPF environment[3,4]. However, the ramifications for the implementation of the SPF mouse model were not understood until the 21st century, with the discovery of several significant revelations, the

most relevant to this manuscript being the discovery of supplier-dependent differences in the gut microbiota (GM) composition of laboratory mice[5]. Additional studies, expanded upon later in Chapter 1, have confirmed that these differences in GM composition have a significant effect on various experimental outcomes in mouse studies, and that changes within each GM composition can be further driven by various environmental differences related to husbandry. The research detailed in this dissertation provides further explanation of how GM composition interacts with various environmental factors to influence study outcomes on the topics of housing density and statistical power (Chapter 2), maternal transfer of the neonatal GM development (Chapter 3), and type 1 diabetes model phenotype (Chapter 4). The overarching goals of these studies is to emphasize the role of the GM in experimental outcomes, to highlight the importance of considering the GM in experimental design, and to prompt further investigation into the complex interactions of the GM in animal models and humans alike.

Considerations of animals in experimental research

Animals have been utilized to better understand human physiology since as early as 6 BCE, when Alcmaeon of Croton studied dogs and discovered that the brain was the source of intelligence and sensory integration[6]. Galen, the credited founder of experimental medicine, during the 2nd century, utilized both human and animal subjects in his

experimentation[7]. The ethicality of human experimentation has always been a concern due to the unknown or negative physical and psychological effects novel scientific intervention can have on humans. Therefore, animal models have served as experimental subjects in lieu of humans and played a significant role in informing our understanding of human biological processes since the establishment of modern science. The use of animals in scientific research is so prevalent now, that their use is legally required in the field of medicine for the advancement of novel therapies to clinical human trials[8]. However, despite their historic use, there is concern from the public and scientists regarding the ethical use and translatability of animals in scientific research.

Public opinion and ethics surrounding animal welfare, or an animal's quality of life, have evolved since the founding of modern science. The overall public opinion on animal experimentation is important for scientist to consider as these viewpoints help shape government legislature that effects how animals can be used in research. In ancient Greece, where many of the first known reports of animal experimentation began, there was not much consideration for animal welfare in general[9]. It was not until the enlightenment period in the 17th century that philosophers such as Baruch Spinoza, John Locke, and Immanuel Kant, reflected on an animal's ability to feel and the cruelty of inflicting harm to animals without reason[10]. However, these philosophers did not feel that humans have direct ethical duties toward animals, nor did they attribute animals with any moral

standing[10,11]. This framework allowed for animal experimentation with little consideration of the harm inflicted upon the animal, but also founded animals as sentient beings[10].

It was not until the 18th century that moral standing for animals were proposed by philosophers such as Jean-Jacques Rousseu and Jeremy Bentham, and sentiments of animal welfare were introduced into experimental practice[10]. Animal experimentation was deemed largely justifiable based on the benefits humans can derive from experimental findings, so long the experimental outcomes outweigh the harm to the animals[9]. In the early 19th century, Claude Bernard revolutionized scientific research by stating that only highly controlled and rigorous animal experiments could provide reliable medical information on human physiology and pathology[10]. By the end of the 19th century, as animals became increasingly popular as research subjects, so did the concern for animal welfare from the public and scientists. This concern resulted in the first government legislation in 1822 regarding the use of animals in experimentation[12], and the movement for animal welfare regulation was later greatly justified by Bernard's rationale with the finding that stress can affect the outcomes of experiments and lower translatability to humans[13].

Throughout the 20th century, research continued to inform best practices in the use of animal modeling, and further regulations and guidelines for appropriate animal experimentation were implemented throughout the world. One guiding principle introduced during the 20th

century that is still an important consideration for animal experimentation is a concept that combines both principles of animal welfare and experimental replicability, referred to as the "Three R's tenant"[14]. This principle revolves around the reduction, replacement, and refinement of animal models in experimental research. In short, animal use should be limited within research whenever alternatives are applicable (reduction). When there is no appropriate alternative in an experiment (replacement), the chosen model should be as optimally translatable to humans as possible while also having the lowest level of attributed pain perception out of applicable model choices. Additionally, animal models should be given the highest quality of life possible throughout experimentation, with the least amount of harm inflicted, and new validated findings should inform best care practices (refinement). This ideology is currently accepted by a majority of the public and continues to encourage new innovations in scientific research[15].

A challenge in animal modeling identifiable through the three R's tenant is a limited ability to replicate animal model findings across studies, and the inconsistent ability of these animal models to predict human clinical outcome. These discrepancies lower the feasibility of the use of animal models in comparative medicine, and thus the three R's tenant encourages replacement studies, so other less controversial models have been explored, such as *in vitro* and *in silico* methods[16]. Many of these alternative models are currently utilized by scientists, but no alternative model allows for the research of multi-organ diseases. Therefore, it is not feasible to

completely phase out animal experimentation without a proper whole organism model, as many alternative models are complementary to, but not replacements for animal testing[16]. Following the R tenant, refinement of animal models is an ongoing responsibility of comparative medicine scientists, and it is our duty to continue to improve animal model studies by identifying the diverse range of factors that can limit reproducibility and translatability to humans, and then subsequently developing techniques to control for these factors.

Improving translatability of animal models

When discussing animal models, translatability is broadly defined as the ability of experimental outcomes utilizing an animal model to reflect a specific aspect of human biological function or mechanism. It is critical to consider translatability of an animal model for ethical and practical implications, for failure to correctly assess translatability of experimental findings can be catastrophic. In 2006, an anti-CD28 monoclonal antibody, TGN1412, was administer to six healthy male humans[17]. This antibody had previously shown therapeutic effects in rodent models for a variety of ailments such as inflammatory bowel disease (IBD) by stimulating and expanding T regulatory cells[18,19], but in humans, it resulted in a devastating cytokine storm[17]. However, more recent studies by Rosshart et al. in a novel mouse model later accurately recapitulated the cytokine storm seen in the human clinical trials[20]. This was achieved through improving the

translatability of the conventional laboratory mouse model by acknowledging more recent findings within the field that showed a stark deficit in SPF laboratory mouse translatability relating to an underdeveloped immune system[21], and then creating a novel model that applied those findings by diversifying antigen stimulation of the SPF laboratory mouse[20]. This is just one example of a recent breakthrough in animal modeling and the importance of continuously innovating techniques and considering recent literature to improve translatability.

It can be challenging to determine the most optimal model when designing a project, and there is no currently implemented standard for determining model translatability or proper study design. Tangible ways to determine the translatability of an animal model have been proposed such as the animal model quality assessment outlined in Storey et al. which is a semi-quantitative tool for assessing the overall validity of an animal model[22]. The animal model quality assessment tool is useful for determining gaps in knowledge by presenting a series of questions that are essential to consider during study design development. The remainder of this section will restate the considerations proposed by storey et al. in the context of models of disease and highlight the importance of these considerations when developing hypothesis-driven animal model experiments.

First, it is important to consider what is known about the human condition and the variability of manifestations of that condition[22]. A major contributing factor to limited translatability of animal models to humans is

the lack of variability in experimental design[23]. This is due to the controlled environment of experimental studies, where variation between subjects within a treatment group are reduced as much as possible to avoid confounding factors. However, variability of the condition can still be incorporated into experimental study design by utilizing different sexes, environmental factors, and genotypes[22,23].

Second, it is important to consider the differences between the physiology of the human and candidate animal model or models[22]. These differences can limit the applicability of the findings to human studies and the complexity of animals makes exact translation impossible[24], but proper consideration of models can determine the most conserved species in relation to the mechanism of interest. For the highest translational probability, the animal model must be capable of modeling the specific biological mechanism of interest that is seen in humans[23]. The overall physiological differences between the chosen model or models can then be carefully considered throughout the study to determine their potential effects on experimental outcomes and overall translatability.

Third, when working with a model of disease, it is important to consider the differences between humans and candidate models for disease pathogenesis and etiology[22]. A disease with a complex mechanism of onset, rather than a direct initiator, can be difficult to properly model. Many models of disease rely on interventions to induce disease that are not concurrent with disease pathogenesis in humans. For example, in Smad3

knockout (KO) mice, IBD is induced through inoculation with *Helicobacter* species[25]. This mechanism of disease pathogenesis has not been confirmed in humans[26]. In this instance, this model would not be appropriate to study mechanisms of disease onset or interventions that prevent onset of disease in relation to humans but could be more properly utilized in a study that examines the downstream effects of a therapy or intervention on IBD severity and symptoms.

Fourth, it is important to consider the reproducibility of the study design and animal model phenotype. For a study to be reproducible, all stages of the experiment including data analysis must be explained thoroughly enough that others may properly recapitulate the study. The ability to properly reproduce study results strengthens the confidence that the observed results are legitimate. It is of utmost importance to properly standardize techniques before commencing experimentation, and to publish all data collected from each animal. Through access to this data, others may find these data useful for exploring trends related to their hypotheses. Further, if an animal model has inconsistent phenotypic outcomes, the contributing factors to the variability in phenotypic outcome should ideally be identified before attempting to translate results to humans.

Overall, a properly designed study paired with the most appropriate animal model is essential for optimizing translatability to humans. The greater our understanding of the underlying mechanism of interest, the greater our ability is to design an experiment that properly models that

mechanism[23]. If a biological mechanism is not well understood, confounding factors are likely unaccounted for and the applicability of the experimental findings will have low reproducibility across studies, as well as poor translatability to humans. Often novel findings of low-probability experiments attract much interest, but these findings should not be applied to humans until the mechanism is recapitulated in additional studies and preferably with multiple animal models. Through rigorous experimentation and reporting of bio metrics, uncontrolled variables capable of altering results can be identified, and paradigms can be strengthened through confirmatory results[24].

The gut microbiota and host interactions

In this dissertation the authors aim to improve the translatability of the laboratory mouse by increasing the understanding of how a significant driver of variability within the laboratory mouse model population, the GM, and its interactions, can affect the overall results of an experimental study. Without proper understanding of the mechanisms in which the GM interacts with the host, and the GM's role in various diseases, unaccounted differences within the GM will continue to lead to conflicting and uninterpretable results, thereby reducing the applicability of animal studies to humans. Continued efforts to determine the complex interaction of the GM on and within the populations of animal models are required to increase

the understanding of the GMs diverse role in healthy biological function as well as its role in various diseases.

The GM is the community of microorganisms that colonize the gastrointestinal tract (GIT) of various animals ranging from insects like *Drosophila*, to fish like *Danio rerio*, to mammals like *Homo sapiens*. These communities have coevolved with their hosts[27] and consists of a large variety of organisms, such as bacteria, archaea, viruses, bacteriophages, fungi, and protozoa. The composition of the GM typically consists of both zoonotic colonizers as well as species-specific microorganisms[28], and is constantly undergoing changes in composition to adapt to environmental influences while remaining relatively stable during adulthood[29].

The GM and the host share a largely symbiotic relationship[30], as the host provides the GM with an appropriate environment and energy source[31], and the GM promotes host health by aiding in digestion[32], modulating the immune system[33], promoting gut barrier functions[34], and protecting against colonization of pathogens[30,35]. However, perturbation of the GM and certain GM compositions can contribute negatively to host health through these same mechanisms. The overall composition and functionality of the GM is dependent on a large range of factors including species[36], genetics[37], sex[38], and a variety of environmental factors[30].

Although the GM harbors many microorganisms, the most well characterized component of the GM, and of interest in this dissertation, is the bacterial population. This is due to the relative ease in which scientist

are able to identify various bacterial communities through amplification and sequencing of bacterial DNA, and the high functional capacity of bacteria to alter host pathways. Bacteria account for a predicted 90% of GM mediated host function relative to other microorganisms[39]. Bacteria are highly abundant within the GM and are hypothesized to reach numbers of 10^{13}-10^{14} in the human gut[40]. The bacterial composition of the GM depends largely on the host, but human and mouse GM compositions are markedly similar at the phylum level, with both hosts sharing the same dominant phyla, *Bacillota* and *Bacteroidota*[41]. At the genera level, studies have reported an overlap of around 62% between the bacterial composition of humans and laboratory mice, and even less similarity at the species level with only 10% of bacterial species shared[42].

Many studies have attempted to resolve GM differences between laboratory mice and humans through creation of humanized mice, which are often created by inoculating gnotobiotic mice with a human fecal slurry. These humanized mice often have incomplete transfer of the human bacterial GM and do not fully model the human host response[41]. This should not come as a surprise due to the coevolution of bacterial strains with their specific host, the loss of potentially important bacteria, and the physiological differences between the human and mouse GIT such as differences in villi length and relative size of cecum[41].

Despite differences between bacterial species and GIT physiology, increasing evidence supports a high overlap in the functionality of bacterial

species between humans and mice, with functional gene-overlap predicted to be between 82.1% and 95%[39,43]. These studies also revealed that closely related species of bacteria do not necessarily share the same function, but functional databases are in development to aid in finding bacterial species in mice that provide the same functions as those in humans, which is predicted to improve functional translatability more so than finding human-mouse species equivalents[39] or utilization of humanized-mice[41]. Results support the use of laboratory mice GM as models for the human gut microbiota, so long as special consideration is taken into account for how divergencies in physiological architecture of the gut and functional GM differences could affect study translatability.

Implications of gut microbiota diversity

It has long been known that the GM is not directly pertinent to survival, as seen in gnotobiotic germ free (GF) animal models, who are devoid of any colonizing microorganisms. However, being devoid of detectable microorganisms causes adverse alterations in physiological functions[44]. GF murine models cannot synthesize vitamin K and B without a GM present, and therefore without supplementation of these vitamins into their diet they suffer from hemorrhaging[44,45]. GF animal models have also been found to have alterations in an extensive list of biological functions including a blunted immune response[46], as well as alterations in metabolism, stress, digestion, and nervous system regulation[45]. The

mechanisms in which these alterations occur is not currently known, but it is clear that the GM is essential for the development of a healthy individual.

The relationship between the GM and the host is generally beneficial to the host, but certain characteristics of the GM have been attributed to poor health. The diversity of the GM composition within an individual is one such attribute repeatedly correlating with host fitness and disease susceptibility[47]. Diversity is a measurement that accounts for the overall number of taxa present in the GM (richness), and how evenly distributed each taxa present is compared to the rest of the community (evenness). A low diversity GM is a GM with a lower number of microorganisms, and/or a GM where a specific taxon is overrepresented compared to the rest of the population. Low GM diversity has continuously been shown to be associated with dysbiosis, or a perturbed and unstable state of the GM[47,48]. A low diversity GM in a dysbiotic state is commonly found in a variety of diseases which directly affect the GIT such as IBD[49], Crohn's disease, and colorectal cancer[48], as well as diseases that indirectly effect the GIT such as autism[50], allergies[51], and chronic stress[52]. The dogma of low diversity and dysbiosis leading to disease is recognized in the literature, but the exact mechanism has yet to be elucidated in many diseases. However, there is increasing evidence that altered metabolism and decreased immune tolerance are consequences of the low GM diversity profile, which are likely involved in increasing susceptibility to disease.

In contrast to a low diversity GM, a high diversity GM is attributed as being more beneficial to the host and is associated with the typical complexity of a healthy individual. Evidence supports that a high diversity GM can exert protective effects on host health through promotion of immune tolerance and colonization resistance. However, recent studies show that animal models such as the laboratory mouse model suffer from decreased GM diversity compared to their wild-caught or pet store bought counterparts[20,21,53]. A study by Beura et al. shows that pet store and wild-caught mouse GMs harbor a high diversity GM that stimulates antigen experience and CD8+ T cell diversification through microbe-host cross-talk, while conventional laboratory mice harbor low diversity GM composition and a CD8+ T cell repertoire comparable to a human neonate[21]. Thus, the naivety of the laboratory mouse immune system has largely been attributed to the highly controlled and sanitized laboratory setting and the maintenance of a SPF environment[3].

When mice in the Beura et al. study were challenged with *Listeria monocytogenes*, an intracellular pathogen, the individuals with the high diversity GMs were more primed to protect against pathogen colonization than the low GM diversity individuals, resulting in a >10,000 fold reduction in bacterial burden by day 3[21]. The level of colonization resistance in the high diversity GMs were comparable to that of low diversity mice immunized against *L. monocytogenes*. This study and other confirmatory studies highlight the importance of considering the gut microbiota diversity as a

factor with potential to drive variability within the laboratory mouse population and targets the GM of SPF laboratory mouse as a factor that decreases the overall translatability of the model due to the lowered diversity and naivety of the immune system compared to adult humans.

Scientists are now searching for ways to correct the discrepancy in translatability between human adults and SPF laboratory mice. Cohousing of wild-caught or pet store mice with laboratory mice has shown promise in increasing GM diversity of co-housed laboratory mice and improving diversification of the immune system[21,53], however the current parameters of biosafety implemented by many mouse suppliers and institutions prohibit the admission of many organisms highly prevalent in the commensal wild-mouse and pet store mouse GM such as *Helicobacter species*, murine hepatitis virus (MHV), mites, and pinworms[53,54]. Studies have shown that quarantine of pet store mice resulted in reduction of microbial richness, which would again serve to lower translatability to adult humans[54]. In addition, many of these excluded organisms have shown adverse effects in immunocompromised models while being largely asymptomatic in healthy mice[55], again serving to lower the feasibility of implementing a wild or pet-store mouse GM as these organisms could adversely affect study outcomes in immunocompromised models, or change the model phenotype altogether[56].

For scientists to resolve the disparities in translation between the mouse model and the human, more research is needed to understand factors that

promote and diminish GM diversity, and the subsequent effects on host health and immunity. One way in which to do so is to utilize the variability in GM diversity already present within the laboratory mouse population. Recent studies have demonstrated that SPF laboratory mice from 3 different mouse suppliers harbor significantly different GM compositions in terms of diversity[57]. Further studies investigating these GM backgrounds report significant variance in model phenotype in the absence of experimental intervention[58]. For instance, mice with lower diversity GM background show increased anxiolytic behavior[58], increased weight[58], and are reportedly more prone to dysbiosis and increased disease susceptibility[59]. These studies support the idea that incorporating varying GM backgrounds into study design may help increase the translatability to humans in multiple aspects. For instance, utilizing multiple GM backgrounds may help reveal GM-mediated differences in experimental outcomes and disease models. Utilizing multiple GM backgrounds may also better model the natural variance of the GM seen in the human population.

Failure to correctly consider GM background in study design or failure to report GM background in a methods section may unintentionally confound study results if GM-mediated variance is significant. Therefore, the use of GMs of varying complexities should become more common place in experimental mouse model research.

The differences in environmental factors between suppliers are the likely drivers of differences between the reported supplier-related GM

diversity. For example, many suppliers have differences in the specific organisms that are excluded from the vivarium, and even have different exclusion criteria for different mouse colonies. This variability in GM composition has been reported to drive differences in study outcomes[60], and inter-experimental comparisons can become confounded by these supplier-related GM differences if mouse obtainment source or GM composition is left unreported in the literature, which is often the case, especially in non-GM focused studies. This warrants further investigation into other environmental factors that can further drive unaccounted GM differences between experiments.

Environment drives GM variability

It is important to consider the diverse range of factors that are capable of driving variability between laboratory mice and humans, as well as investigating inter-individual differences in GM composition that are related to differences between experimental outcomes. Environmental factors are of particular interest as multiple environmental factors can interact, making understanding the direct associations of each variable on the GM and host extremely difficult to determine. Potential and known drivers of environmental variability are often left unexamined, unreported, and uncontrolled for in both animal and human studies, leading to confounding results and reduced understanding of the mechanisms in which the GM interacts with the host.

A vast number of environmental factors have been reported to alter the GM composition in humans. These environmental factors can be either macroenvironmental, having effects on multiple individuals, or microenvironmental, having direct effects on only the individual[30]. Macroenvironmental factors associated with altering the GM include geography[61], air pollution[62], housing environment[63], and socioeconomic environment[64]. Microenvironmental factors associated with altering the GM include smoking[65], alcohol dependence[66], and diet[67]. These environmental factors interact with the GM and result in a unique GM composition for each individual. Similarities in environmental factors between individuals can result in increased inter-individual similarity, but these factors are nearly impossible to control for during clinical trial due to the failure of cooperation of individuals, as well as financial and practical relevance of controlling for environmental factors that affect daily life. Due to these reasons, it is unrealistic to try to determine the effect of each individual variable on GM composition without a more controlled approach. Therefore, animal models such as the laboratory mouse model are a pertinent tool for understanding how these environmental factors interact with the GM to affect various aspect of host health.

Many environmental factors drive conserved changes in the GM composition between humans and the laboratory mouse model. Diets such as a high fat diet (HFD) have repeatedly been reported to alter the GM[68]. A HFD modifies the GM of both mice and humans by driving dysbiosis to

increase *Bacillota* and decrease *Bacteroidota* populations compared to healthy individuals, ultimately leading to decreased GM diversity[68]. These GM alterations result in phenotypic changes and increased susceptibility to various diseases such as obesity[69,70] and type II diabetes[71]. A HFD likely drives this disease susceptibility through a combination of GM-host interactions resulting in increased inflammation, increased intestinal permeability, and alteration of the host metabolism[72]. A non-exhaustive list of other common environmental factors capable of inducing conserved changes in the GM between species include caloric restriction[73], antibiotics[74], and probiotics[75]. These seemingly affect the GM composition regardless of host GM background[76].

Other environmental factors such as exposure to specific pathogens or pathobionts drive a more varied response within the population of both humans and mouse models. *Helicobacter hepaticus* is a common commensal bacterium of wild mice, however in multiple mouse strains it can lead to various diseases such as colitis in Smad3-/-[25] and IL-10$^{-/-}$ mice[77]. Studies examining this response found that colitis severity was dependent on the background GM composition[59]. Differences in GM diversity drove differential colonization resistance to *H. hepaticus* and differential colitis severity between GM backgrounds[59]. In IL-10 deficient *H. hepaticus* monocolonized mice, colitis does not manifest, suggesting an interaction of *H. hepaticus* and the commensal GM are necessary for disease onset[78]. The appearance of *H. hepaticus* in non-gastrointestinal tissue such as the

liver in mice or the gallbladder in humans[79] suggest *H. hepaticus* is escaping the GIT, likely through mechanisms of increased intestinal permeability. The specific organisms or communities within each GM composition implicated in these interactions have yet to be elucidated, indicating more studies are needed to determine driving mechanisms.

There is also a growing number of environmental factors that are capable of driving variance within a mouse model GM background and subsequent experimental results that are not directly translatable to the human. These factors include differences in husbandry methods such as the type of housing used for neonatal immunocompromised mice[80], transportation of animals between facilities[81], choice of GM transfer method[82], differences in bedding material[60], and differences in water decontamination methods[60]. These environmental factors drive changes in GM composition which may go undetected for long periods of time but are still ultimately capable of altering the GM composition and diversity. For example, water decontamination and bedding methods in a study by Bidot et al. detected alterations in the cecal composition rather than the fecal composition of mice[60]. Cecal composition is less explored in mice due to the inability to sample cecal content without euthanasia and thus the inability to sample one animal longitudinally. These studies highlight the importance of monitoring mouse colonies for changes in GM composition in gastro-intestinal locations less utilized in studies such as the ileum and jejunum as well as the cecum and support the need to explore additional

husbandry methods that could further drive alterations in GM composition that are currently unaccounted for. More knowledge on the effect of husbandry methods on the mouse GM composition will serve to better inform best husbandry practices to maintain more consistent and reproducible GM compositions.

CHAPTER 2 – REDUCED HOUSING DENSITY IMPROVES STATISTICAL POWER OF MURINE GUT MICROBIOTA STUDIES

Introduction

Standardization, reproducibility, and translatability are three key components of any biomedical research experiment. Efforts to improve those aspects demonstrate good scientific practices and reflect the ethical considerations underlying replacement, refinement, and reduction of animal models. For these reasons, it is essential to look at all potential variables within an experiment, particularly those in which animal models are used and those which translate to human medicine. One such variable that has gained considerable attention over the last couple of decades is the gut microbiome. In the context of mouse models, factors such as differing husbandry practices[60,83], different animal sources[5,84], and the use of antimicrobials[76] can significantly alter the microbiome and impact the results of a study [85-87]. While assessing differences within the microbiome in murine studies has become critical to understanding its influence on human health and disease susceptibility, it is important to understand the treatment effect size in the context of the inherent within-group variability, both of which may be altered by factors such as housing density.

Because mice are subject to the effects of their microenvironment within each cage due to close contact and coprophagy, it is reasonable to assume that the microbiome of cage-mates will begin to resemble each

other over time more closely than the microbiome of mice in the same treatment group but in other cages. Indeed, the cage has been proposed, justifiably, as the biological unit, with each mouse being a technical replicate within the cage[88]; however, the vast majority of peer-reviewed literature treat each mouse as a biological unit in statistical analyses. While single-housing mice would completely eliminate the possibility of cage effects, mice are social animals[89] and animal welfare considerations preclude housing mice individually unless there is a strong scientific rationale. Additionally, mice are traditionally housed with greater housing densities (typically 4 or 5 mice per cage) to reduce housing costs when per diems are charged on a per cage basis, resulting in a 4 to 5-fold increase in housing costs for mice housed individually. In an effort to decrease cage effects (defined here as an increased intra-cage similarity within treatment groups), a rational compromise would be to house two mice per cage, allowing mice to express social behaviors, while only doubling the housing costs (compared to four mice per cage).

However, it is unclear whether reduced housing density would render mice more susceptible to the effects of an experimental pressure, such as antibiotics, due to the lack of cage-mates to help re-inoculate the gut. It is also not known whether the data would reflect increased intra-cage similarity in microbiome composition (i.e., cage effects) or whether any difference in cage effects between data generated in mice housed two or four mice per cage (mpc) would result in an increased ability to detect the

effect of an experimental pressure. Without a demonstrated benefit in statistical power, it is difficult to justify the increased housing costs.

With this in mind, the goals of this study were to determine whether mice housed at a cage density of two or four mpc would be differentially affected by a selective pressure (antibiotics) on their microbiome and whether experimental designs using the two different housing densities would differ in their ability to detect an effect of antibiotics on the microbiome. Accordingly, adult mice arriving at our institution (Cohort 1, *N* = 48, Cohort 2, *N* = 72) were randomly divided into two housing densities (2 or 4 mpc) and two (Cohort 1) or three (Cohort 2) treatment groups in fully crossed study designs. Cohort 1 comprised control and enrofloxacin treatment groups, while Cohort 2 comprised control, enrofloxacin-treated, and a third group receiving a combination of vancomycin, ampicillin, metronidazole, and neomycin (VAMN). This allowed for 12 mice per group in either three cages of 4 mpc or six cages of 2 mpc. DNA from feces collected before treatment (upon arrival), after one week of antibiotic or control exposure, and again four weeks after cessation of antibiotics, along with cecal and jejunal luminal contents collected at endpoint, were subjected to 16S rRNA amplicon sequencing. Here we show that, relative to 4 mpc, a housing density of 2 mpc was associated with reduced cage effects and a consistently increased ability to detect treatment-associated effects on the microbiome, despite effects of the antibiotic pressure on any given individual.

Methods

Study design and mice

This study was performed using two independent cohorts of six-week-old female C57BL/6NHsd mice from Envigo. Mice in Cohort 1 (*N* = 48) were randomly assigned to one of two experimental treatment groups (control or enrofloxacin); mice in Cohort 2 were randomly assigned to one of three experimental groups (control, enrofloxacin, or VAMN). Both cohorts were then further subdivided into two different housing densities (2 or 4 mpc), resulting in a total of six cages at 2 mpc and three cages at 4 mpc in each treatment group (**Figure 1A**). Beginning immediately upon arrival, mice in the control group received untreated water, while mice in the enrofloxacin and VAMN groups received drinking water treated with antibiotics for one week, while mice in the. For mice in the enrofloxacin groups (Cohort 1 and 2), enrofloxacin was added to the drinking water at a concentration of 85 mg/L. For mice in the VAMN group, a combination of vancomycin (500 mg/L), ampicillin (1 g/L), metronidazole (1 g/L), and neomycin (1 g/L) were added. Mice were provided ad libitum access to the treated or untreated water for one week. Following one week of antibiotic exposure, the enrofloxacin and VAMN groups were switched to the same untreated water being provided to the control group and allowed to recover for an additional three weeks. Fecal samples were collected from all mice immediately upon arrival (T0, prior to co-housing), on day 8 as antibiotic-treated water was being switched to untreated water in the enrofloxacin

group (T1, immediately post-antibiotic exposure), and four weeks after cessation of treatment at necropsy (T2, **Figure 1B**). Jejunal and cecal luminal contents were also collected at necropsy to determine if long-term cage effects differed at various GIT sites.

Mice were housed conventionally in polycarbonate microisolator cages on individually ventilated racks (Thoren, Hazelton, PA) under positive pressure. Each cage contained compressed pelleted paper bedding and nestlets (Ancare, Bellmore, NY), *ad libitum* access to irradiated chow (Labdiet 5058, LabDiet, St. Louis, MO), and *ad libitum* access to acidified, autoclaved water, while under a 14:10 light/dark cycle. Cages were changed and cleaned bi-weekly, using barrier procedures inside a primed class II biosafety cabinet (BSC), by the care staff of the MU Office of Animal Resources. All procedures were performed under the approval of the University of Missouri Institutional Animal Care and Use Committee and according to the guidelines of the Guide for the Care and Use of Laboratory Animals.

Sample Collection

Sample collection at T0 and T1 occurred inside a class II BSC. The home-cage containing mice was removed from its rack and placed in the primed BSC, alongside an empty, autoclaved cage. Individual mice were placed in the empty cage and allowed to defecate normally. Freshly evacuated pellets were collected using autoclaved toothpicks and placed in sterile 2 mL round-bottom tubes containing a 0.5 cm diameter stainless

steel bead. At T2, the mice were euthanized and fresh fecal pellets along with jejunal and cecal luminal contents were collected *post mortem* and stored in the same manner. All samples were collected between the hours of 8 a.m. and 1 p.m. Once collected, samples were stored at −80°C until DNA extraction took place.

DNA Extraction

Fecal DNA was extracted using PowerFecal kits (Qiagen) according to the manufacturer's instructions. DNA yields are quantified via fluorometry (Qubit 2.0, Invitrogen) using quant-iT BR dsDNA reagent kits (Invitrogen).

16S rRNA library preparation and sequencing

Extracted fecal DNA was used to generate libraries at the MU DNA Core Facility (Columbia, MO). Bacterial 16S rRNA amplicons were constructed via amplification of the V4 region of the 16S rRNA gene using dual-indexed universal primers (U515F/806R) previously developed against the V4 region [90], flanked by Illumina standard adapter sequences. PCR was performed in 50 µL reactions containing 100 ng metagenomic DNA, primers (0.2 µM each), dNTPs (200 µM each), and Phusion high-fidelity DNA polymerase (1U, Thermo Fisher Scientific). Amplification parameters are $98°C^{(3\ min)}$ + [$98°C^{(15\ sec)}$ + $50°C^{(30\ sec)}$ + $72°C^{(30\ sec)}$] × 25 cycles +$72°C^{(7\ min)}$. Amplicon pools (5 µL/reaction) were combined, mixed, and purified by addition of Axygen Axyprep MagPCR clean-up beads to an equal volume of 50 µL of amplicons and incubated for 15 minutes at room temperature. Products were then washed multiple times with 80% ethanol and the dried

pellet resuspended in 32.5 µL elution buffer (Qiagen), incubated for two minutes at room temperature, and then placed on the magnetic stand for five minutes. The final amplicon pool was evaluated using an Advanced Analytical Fragment Analyzer automated electrophoresis system, quantified using quant-iT HS dsDNA reagent kits, and diluted according to Illumina's standard protocol for sequencing on the MiSeq instrument.

Informatics analysis

Amplicon sequences were filtered, trimmed, and annotated at the MU Informatics Research Core Facility (Columbia, MO). Primers were designed to match the 5' ends of the forward and reverse reads. Cutadapt[91] (version 2.6; https://github.com/marcelm/cutadapt) was used to remove the primer from the 5' end of the forward read. If found, the reverse complement of the primer to the reverse read was then removed from the forward read as were all bases downstream. Thus, a forward read could be trimmed at both ends if the insert was shorter than the amplicon length. The same approach was used on the reverse read, but with the primers in the opposite roles. Read pairs were rejected if one read or the other did not match a 5' primer, and an error-rate of 0.1 was allowed. Two passes were made over each read to ensure removal of the second primer. A minimal overlap of 3 with the 3' end of the primer sequence was required for removal.

The QIIME2[92] DADA2[93] plugin (version 1.10.0) was used to denoise, de-replicate, and count amplicon sequence variants (ASVs), incorporating the following parameters: 1) forward and reverse reads were truncated to

150 bases, 2) forward and reverse reads with number of expected errors higher than 2.0 were discarded, and 3) chimeras were detected using the "consensus" method and removed. R version 3.5.1 and Biom version 2.1.7 were used in QIIME2. Taxonomies were assigned to final sequences using the Silva.v132 database, using the classify-sklearn procedure[92].

Statistical analysis

Differences in richness (represented by ASVs) and alpha-diversity (Shannon index) of fecal samples were performed using a mixed effect model. For fecal samples from three time-points, we included the interaction of treatment and time as fixed effect, and cage and individual mouse nested in cage as random effects. The model for cecal and jejunal samples collected at necropsy included treatment as fixed effect, and cage as random effect. Differences in beta-diversity under Bray-Curtis distances were determined using non-parametric multivariate analysis of variance (PERMANOVA), with cage nested within treatment. Comparisons between inter- and intra-cage similarity were performed using Welch's t-test.

Results

One library yielded only 187 reads and was removed from all further analyses. The next lowest number of sequences recovered was 28,190 sequences, so all data were randomly rarefied to a uniform read count of 28,189 sequences per sample. The baseline gut microbiota (GM) present in mice upon arrival from the supplier was relatively consistent, with no

suggestion of inherent differences between randomized groups prior to housing (**Supplemental Figure 2.1A**). Principal coordinate analysis of the GM upon arrival showed substantial overlap between samples from mice randomly assigned to each group (**Supplemental Figure 2.1B**) and no significant difference in β-diversity was detected between groups at baseline (p = 0.10; F = 1.5). The mice in Cohort 2 showed similar homogeneity upon arrival (**Supplemental Figure 2.2**).

Assessments of richness (i.e., the number of observed amplicon sequence variants (ASVs) in samples from each group) revealed similar antibiotic-mediated reductions in mice housed four mice per cage (4 mpc) (**Figure 2.2A**, **Supplemental Figure 3A**) and two mice per cage (2 mpc) (**Figure 2.2B**, **Supplemental Figure 2.3B**) immediately after administration of enrofloxacin (T1) which were variably sustained four weeks after cessation of antibiotics (T2). In all comparisons, p values obtained in mice housed 2 mpc were lower than in mice housed 4 mpc. Richness was similarly reduced at T1 in VAMN-treated mice (**Figure 2.3C-D**) but remained lower at T2 only in mice housed 2 mpc. Surprisingly, similar comparisons of Shannon diversity failed to detect significant enrofloxacin-associated differences in the mice housed 4 mpc in either cohort (**Figure 2.2E**, **Supplemental Figure 2.3C-D**), while significant differences were detected in mice housed 2 mpc at T2 in Cohort 1 (p = 0.0012) (**Figure 2.2F**). Shannon diversity was similarly reduced in mice housed 4 mpc (**Figure 2.2G**) or 2 mpc (**Figure 2.2H**) at T1, but remained lower selectively in mice housed 2 mpc. Collectively, these

data suggest that either the effect of antibiotics on richness and alpha-diversity was greater in mice housed two per cage than in mice housed four per cage, or that the statistical power to detect treatment-associated effects had changed due to reduced contribution by cage as a factor.

Similarly, comparison of antibiotic-induced effects on beta-diversity in the two housing densities revealed significant differences between samples from antibiotic-exposed and control mice housed 2 mpc at both T1 (p = 0.0198, F = 10.05) and T2 (p = 0.0099, F = 7.72) (**Figure 2.3A**) while the same analysis of samples from mice housed four per cage failed to achieve significance at T1 (p = 0.089, F = 5.73) or T2 (p = 0.059, F = 4.04) (**Figure 2.3B**), indicating that mice housed two per cage are either more susceptible to enrofloxacin-induced changes in beta-diversity than mice housed four per cage, or the reduction in cage-mediated influence has enhanced the ability to detect treatment-mediated effects. Notably, these findings were reproducible in the second cohort of enrofloxacin-treated mice (**Supplemental Figure 2.4**), as well as VAMN-treated mice (**Figure 2.3C-D**).

To assess the influence of housing density on the effect size of cage as a variable, mean intra- and inter-cage similarity between all possible sample pairs was calculated within each group and time-point. For the purposes of this study, we defined a significant influence of cage as a significantly greater intra-cage similarity compared to inter-cage (within treatment and housing group) similarity. Analysis of samples collected upon

arrival revealed no difference between the mean intra- and inter-cage similarity in all but one group (**Supplemental Figure 2.5**) indicating each sample was, on average, no more similar to samples from cage-mates than samples from other mice in the same treatment group. One week later, control mice demonstrated increased intra-cage similarity relative to inter-cage similarity in mice housed 2 mpc (p = 0.023), while antibiotic-exposed mice showed a general reduction (Cohort 1) or no change (Cohort 2) in both intra- and inter-cage similarity, but no significant differences between intra- and inter-cage similarity (**Figure 2.4A**, **Supplemental Figure 2.6A**). Control mice in Cohort 2 showed no difference between intra- and inter-cage similarity in either housing group at T1, and VAMN induced substantial reduction in both intra- and inter-cage similarity, but no difference between the two (**Figure 2.4B**). Notably, at three weeks after cessation of exposure, mice exposed to enrofloxacin demonstrated significantly increased intra-cage similarity relative to inter-cage similarity in mice housed 4 mpc (p < 0.001) while control mice housed 2 mpc showed a modest, albeit significant (p = 0.047) cage effect (**Figure 2.4C**). Enrofloxacin was associated with strong cage effects in Cohort 2 (**Supplemental Figure 2.6B**), while control mice in Cohort 2 again showed modest cage effects (p = 0.016); VAMN-treated mice demonstrated pronounced cage effects at T2 (**Figure 2.4D**).

Comparing the mean intra- and inter-cage similarities across all three time-points, the effects of housing density on enrofloxacin-induced cage effects were apparent. While enrofloxacin-exposed mice housed 4 mpc

retained greater intra- and inter-cage similarity at T1 compared to mice housed 2 mpc, intra-cage similarity was greatly increased in mice housed 4 mpc and a steep reduction in inter-cage similarity was observed at T2 (**Figure 2.4C**, **Supplemental Figure 2.6C**).

Assessment of other regions of the GIT revealed significant enrofloxacin-induced reductions in richness of the cecal microbiota (p = 0.006 with 4 mpc, $p = 5.2\times10^{-6}$ with 2 mpc, **Figure 2.5A**) at T2, but no significant differences in richness of jejunal microbiota (**Figure 2.5B**). While mean cecal and jejunal richness were reduced in enrofloxacin-treated mice in Cohort 2, the reduction did not achieve significance (**Supplemental Figure 2.7**). VAMN induced significant reductions in both cecal richness (**Supplemental Figure 2.7A**) and jejunal richness (**Supplemental Figure 2.7B**) in mice housed 2 mpc, while neither comparison achieved significance in mice housed 4 mpc. Statistical comparison of cecal community structure detected significant enrofloxacin-associated effects in mice housed 2 mpc (p = 0.020, F = 4.7) but not mice housed 4 mpc (p = 0.079, F = 3.7, **Figure 2.5C**), which was reproduced in Cohort 2 (**Supplemental Figure 2.7C**). A similar pattern was seen in jejunal beta-diversity, with significant treatment-associated effects detected only in mice housed 2 mpc (p = 0.020, F = 2.7, **Figure 2.5D**). Enrofloxacin failed to induce significant change in beta-diversity in mice housed 4 mpc or 2 mpc in Cohort 2 (**Supplemental Figure 2.7D**). VAMN induced a significant difference in cecal beta-diversity in mice housed 2 mpc, but not 4 mpc

(**Supplemental Figure 2.7E**). There were no VAMN-associated differences in jejunal beta-diversity in either housing density (**Supplemental Figure 2.7F**). Interestingly, evaluation of intra- and inter-cage similarity within the cecal microbiota at T2 revealed significant cage effects in all groups (i.e., both treatment groups and both housing densities) (**Figure 2.5E**), while increased intra-cage similarity of jejunal communities was only detected in mice exposed to enrofloxacin ($p < 0.001$ with 4 mpc, $p = 0.047$ with 2 mpc, **Figure 2.5F**). Interestingly, evidence of cage effects within the cecal (**Supplemental Figure 2.7G**) and jejunal (**Supplemental Figure 2.7H**) microbiome in Cohort 2 was stronger in mice housed 2 mpc, most notably in VAMN-treated mice.

Discussion

A number of studies have assessed the effects of housing density from the perspective of animal welfare. Outcome measures have included anxiety-related and aggressive behavior[89,94-97], proxies of autonomic signaling such as adrenal weight[89,96-98] and corticosterone levels[95,96,99,100], and other physiological parameters[89,95-97,100-102]. The goal of these studies was to develop data-driven guidelines whereby housing density could be maximized without causing any adverse effects, implying that each mouse within a cage routinely served as the biological or experimental unit.

There are no published reports of the influence of cage density on the gut microbiota, although the practice of coprophagy has been shown to alter

the gut microbiota, even in singly housed mice[103]. Recognizing that the cage is also a significant variable nested within other treatments[104], the current study approached the question from the perspective of statistical power, and the partitioning of these independent factors. Collectively, the data presented here indicate that, while the GM of mice housed at either housing density is similarly affected by antibiotic exposure in terms of richness, alpha-, and beta-diversity, the cage effects were stronger in mice housed four per cage, and treatment-associated effects (in the fecal microbiome) were stronger in mice housed two per cage. Cage effects were most prominent in samples collected four weeks post-cessation of antibiotic exposure, despite comparable rebounds in richness, alpha-, and beta-diversity. We speculate that the antibiotic-mediated depletion of bacteria was comparable among groups, but resulted in the establishment of different cage-based GM populations based on the semi-stochastic effects of the antibiotic. Whether the different housing densities affected the antibiotic-mediated influence on the microbiome was not determined, but the public availability of these and other datasets represents a resource for researchers investigating particular taxonomies of interest.

It is unclear whether the greater antibiotic-induced differences in richness, alpha- and beta-diversity detected in mice housed two per cage were due to reduced efficacy of the antibiotics in the context of a larger ‘cage microbiota’, or reduction in the contribution of ‘cage’ as a statistical variable. Intuitively, with 4 mpc, there is a greater amount of total fecal

biomass, continuously re-inoculating the cage, relative to mice housed 2 mpc. At the same time, mice housed with three other mice, rather than one other mouse, presumably experience a greater degree of cage-associated influence relative to other experimental pressures. Ultimately, the two effects are intertwined and it is not possible to completely separate them. We were intrigued by the increased antibiotic-associated cage effects observed at the final time-point, suggesting that, after cessation of the antibiotic pressure and reduced intra-cage similarity, mice within each antibiotic-exposed cage assumed highly similar compositions, with a substantial divergence between cages. This effect was greatly mitigated in mice housed two per cage.

At the institutional *per diem* of $0.72 per cage per day, housing costs for mice maintained two per cage for five weeks were $241.92, compared to $120.96 for mice housed four per cage in Cohort 1. Considering the identical animal purchase costs of $930 ($38.75 per mouse × 24 mice) and expenses associated with DNA extraction, library preparation and sequencing totaling roughly $2800 per arm of the study, regardless of housing density, the savings of $121 are relatively meager. Rather, the increased ability to detect the effect of a mock experimental pressure (i.e., antibiotics) on various features of the GM would seem to be worth the difference in housing cost, representing a minor portion of the total experimental costs.

Limitations of the current study include the use of a handful of selective pressures on the microbiota, and investigation of a single mouse genetic background. Future studies are needed to confirm these findings in other models, but based on other reports describing the development of cage-dependent features within the GM[104] and the reproducibility of key findings across two cohorts of two different antibiotic pressures, we would anticipate our findings to be widely applicable. One last pragmatic consideration for pair-housing is vivarium space. In smaller vivaria or active multi-PI facilities, housing space is at a premium. Pair-housing basically doubles the amount of caging needed for the same size experiment performed with group-housed mice, and this is simply untenable in some situations. Additionally, in pair-housing scenarios, any time a mouse dies or is removed from study, an individual mouse remains and must be accommodated in some way. In some instances, this can represent an animal welfare issue, and must be addressed in the Animal Care and Use protocol. Those considerations notwithstanding, the current data suggest that a reduced housing density of two mice per cage is associated with an increased ability to detect treatment-associated effects on the gut microbiome by mitigating the effect of cage as an independent variable. These findings add to the growing number of procedural ‘best practices’ for experimental design[105-108] of murine studies of the gut microbiota.

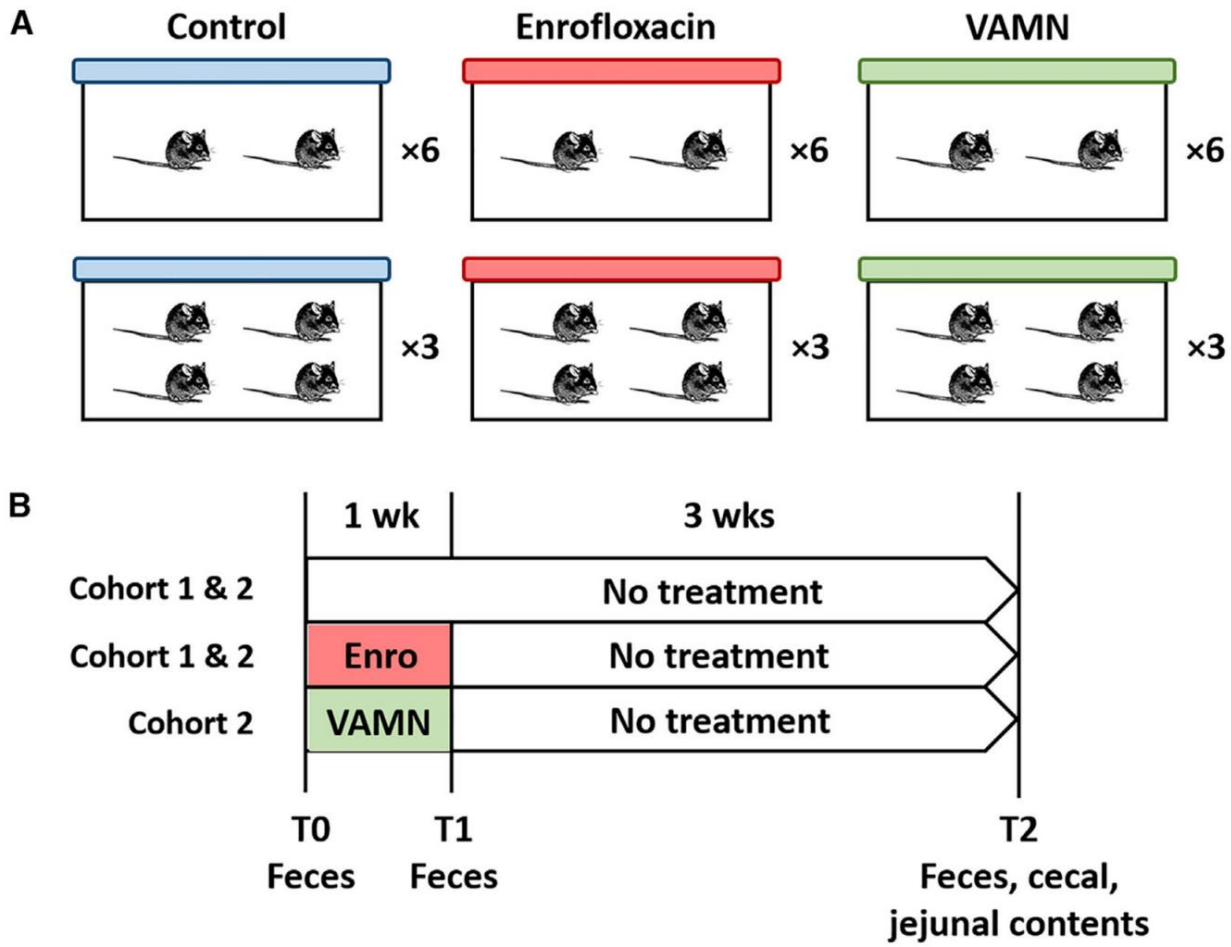

Figure 2.1. Schematic showing experimental design. (A) Depiction of how C57BL/6NHsd mice were randomly assigned to groups receiving nothing (control), enrofloxacin, or broad-range antibiotics (VAMN) in the drinking water, and housed four or two mice per cage (N = 12 mice/group). **(B)** Depiction of treatment and study duration in cohort 1 (N = 48) including control and enrofloxacin-treated groups, and cohort 2 (N = 72) including controls, enrofloxacin-treated, and VAMN-treated groups, and timing and nature of each sample collection.

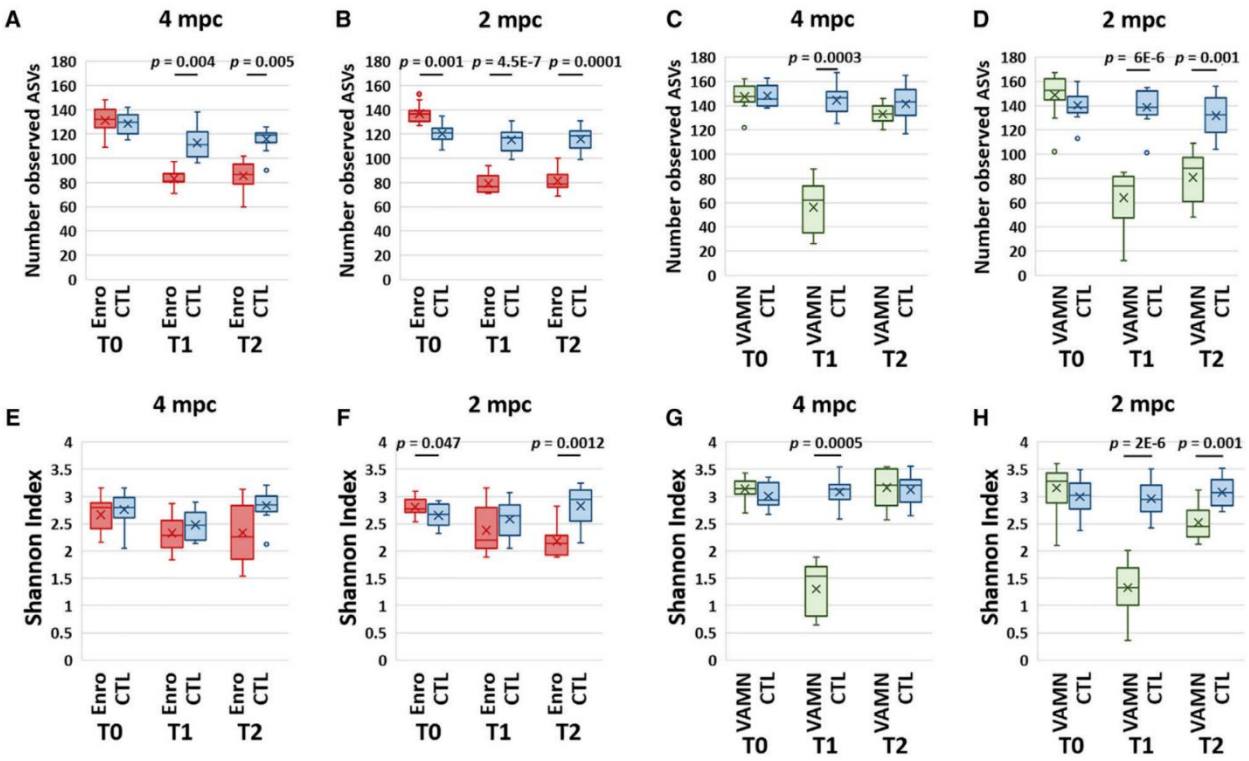

Figure 2.2. Effects of antibiotics on richness and alpha-diversity in different housing densities. Richness of two independent cohorts of mice as represented by the number of distinct observed amplicon sequence variants (ASVs). Mice in cohort 1 received enrofloxacin (Enro) treated water or control (CTL) mice who received untreated water, housed either four per cage **(A)** or two per cage **(B)**. Mice in cohort 2 received broad-spectrum antibiotics (VAMN) in drinking water (or CTL) and were housed four per cage **(C)** or two per cage **(D)**. Feces were collected upon arrival (T0), immediately after one week of exposure to antibiotics or CTL (T1), and three weeks after cessation of exposure (T2). Alpha diversity as estimated by the Shannon diversity index in cohort 1 for mice housed four per cage **(E)** or two per cage **(F)**, and cohort 2 for mice housed four per cage **(G)** or two per cage **(H)**. p-values were obtained from the mixed effect models.

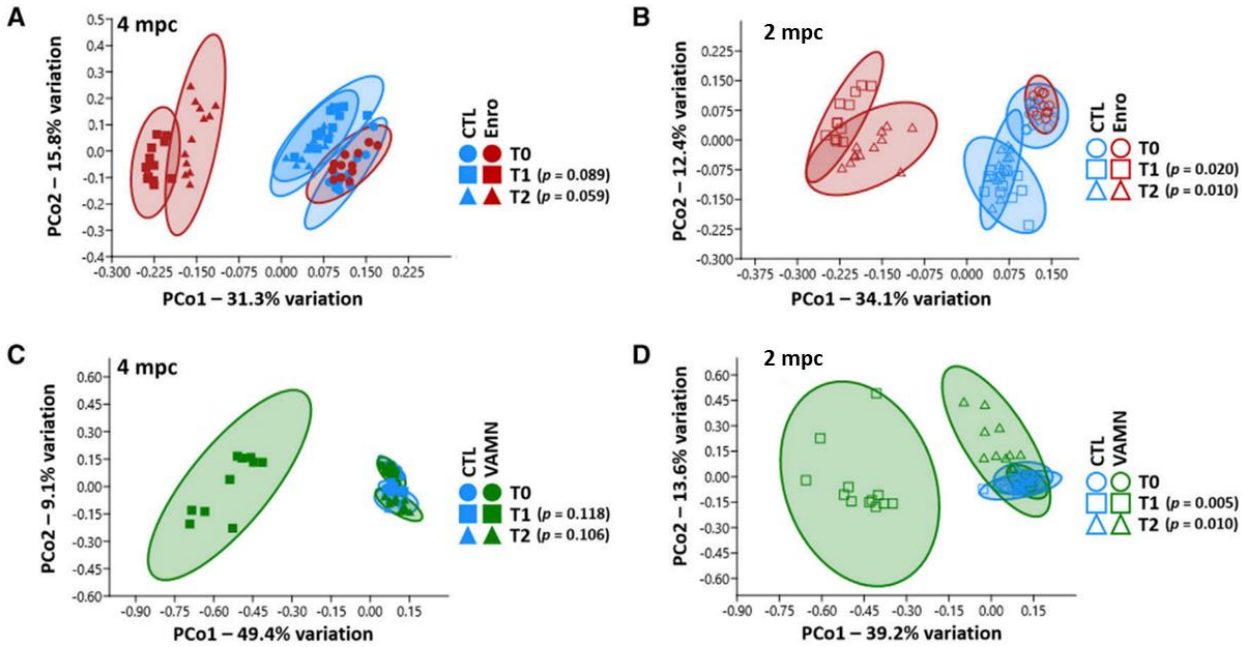

Figure 2.3. Sustained effects of antibiotics on beta-diversity four weeks after cessation of exposure. Principal coordinates analysis of fecal samples from mice receiving enrofloxacin or control, and housed four mice per cage **(A)** or two mice per cage **(B)**; and mice receiving VAMN antibiotics or control, and housed four mice per cage **(C)** or two mice per cage **(D)**. Fecal samples were collected upon arrival from the supplier (T0), immediately after one week of exposure to antibiotics or CTL (T1), and three weeks after cessation of exposure (T2). p-values were obtained from the nested PERMANOVA.

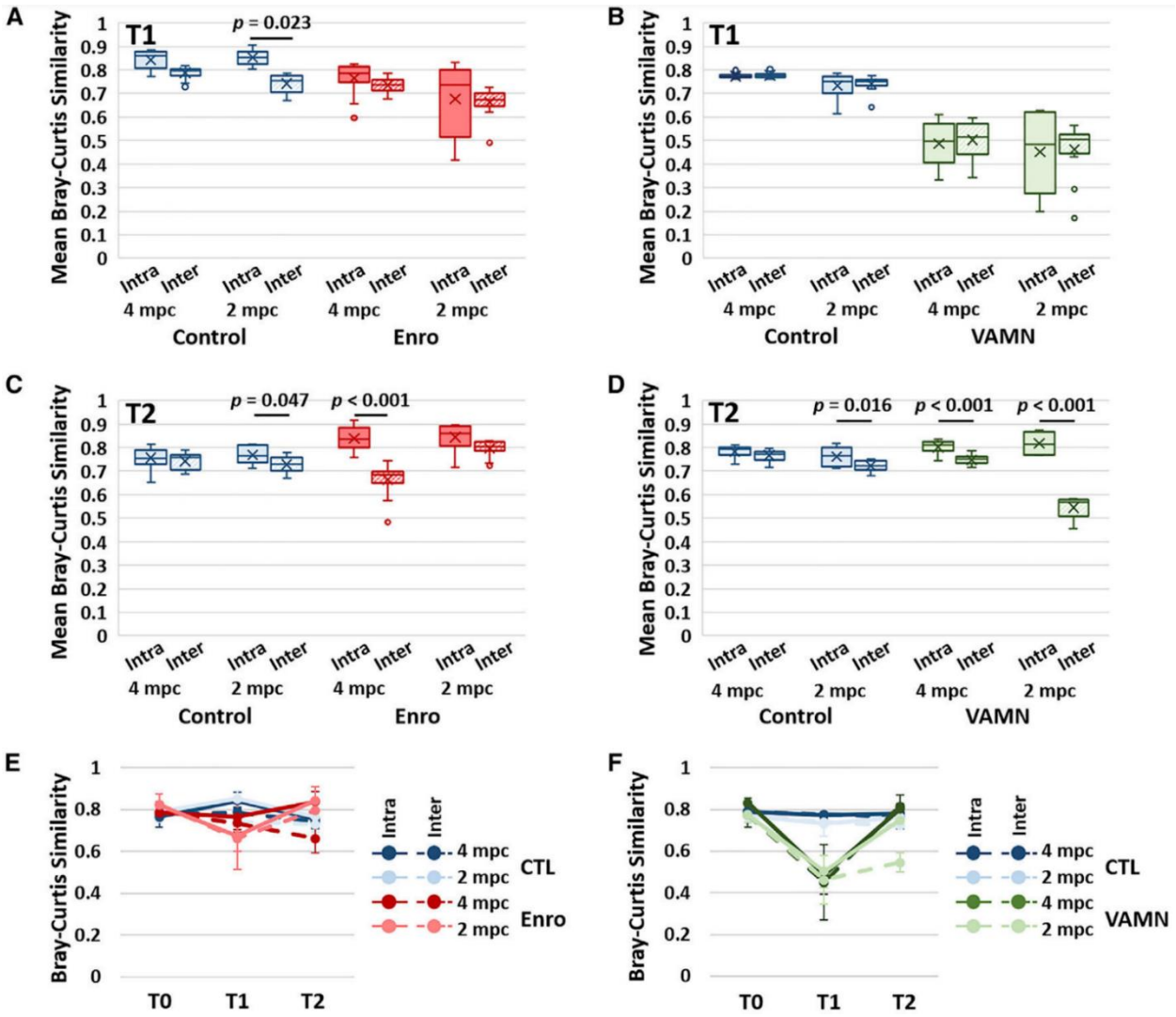

Figure 2.4. Housing density-mediated influence on cage effects. Tukey box plots showing mean intra-cage and inter-cage similarity between all possible sample pairs within a given treatment group and housing density immediately after one week of exposure (T1) to Enrofloxacin (Enro) or control (CTL) in cohort 1 **(A)**, and broad-spectrum antibiotics (VAMN) or CTL in cohort 2 **(B)**. T2 represents fecal samples three weeks after cessation of exposure to antibiotics in cohort 1 **(C)** and cohort 2 **(D)**. Line chart for cohort 1 **(E)** and cohort 2 **(F)** showing the mean ± SD intra- and inter-cage Bray-Curtis similarity upon arrival from the supplier (T0), T1, and T2; figure legends at right of graphs.

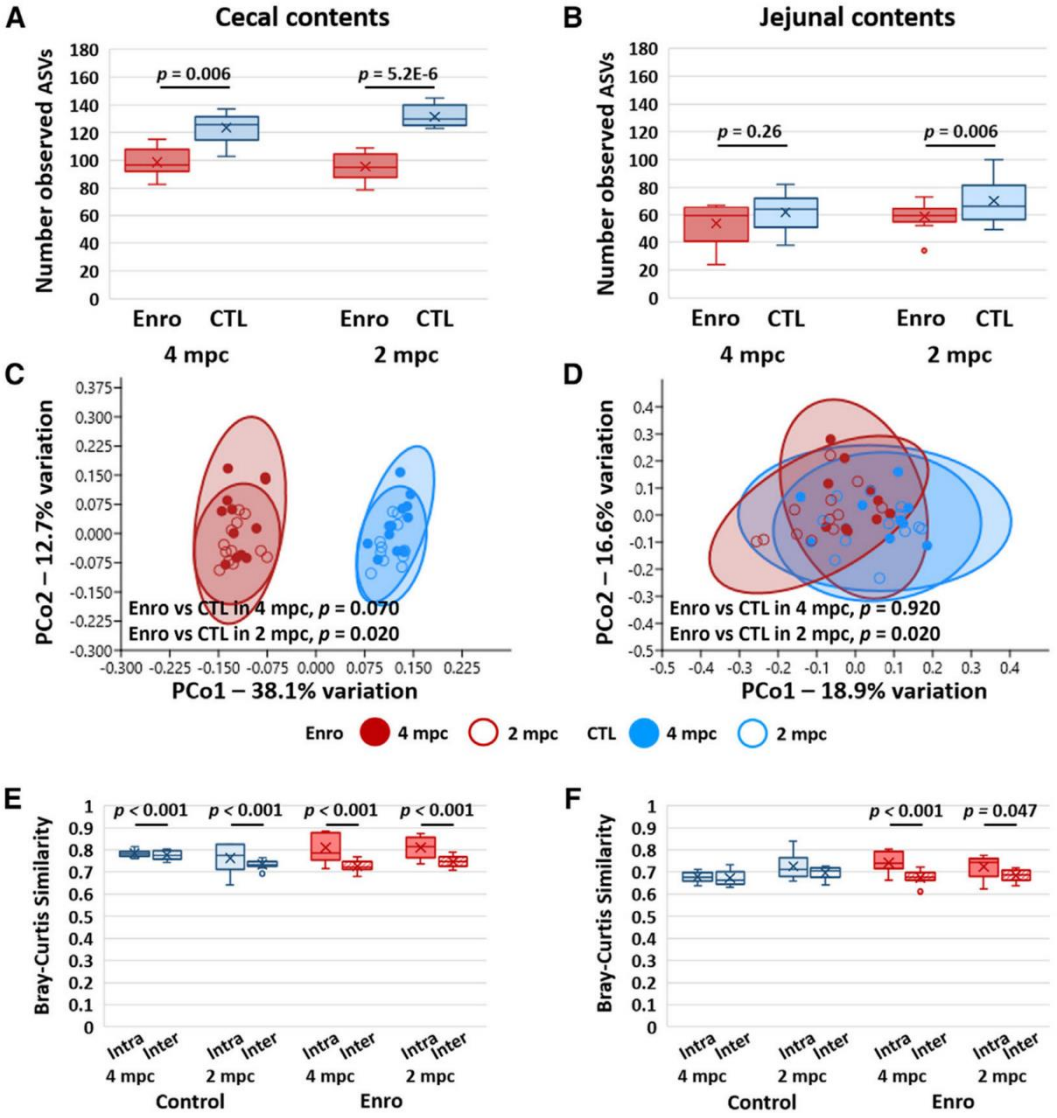

Figure 2.5. Effects of housing density on antibiotic-induced changes in cecal and jejunal richness, alpha- and beta-diversity. Richness as represented by the number of observed amplicon sequence variants (ASVs) in the cecum **(A)** and jejunum **(B)** of mice housed four per cage or two per cage at three weeks after cessation of antibiotics (ABX) or sham (CTL) treatment; *p* values denote ABX-associated effects, based on mixed effect model with cage as a random effect. Principal coordinate analysis plots of Bray-Curtis similarities of cecal **(C)** and jejunal **(D)** microbiota in the mice shown in A and B; *p* values denote treatment-associated effects based on PERMANOVA. Tukey box plots showing mean intra-cage and inter-cage similarity between all possible sample pairs within a given treatment group and housing density, three weeks after cessation of treatment, in the cecal **(E)** and jejunal **(F)** microbiota.

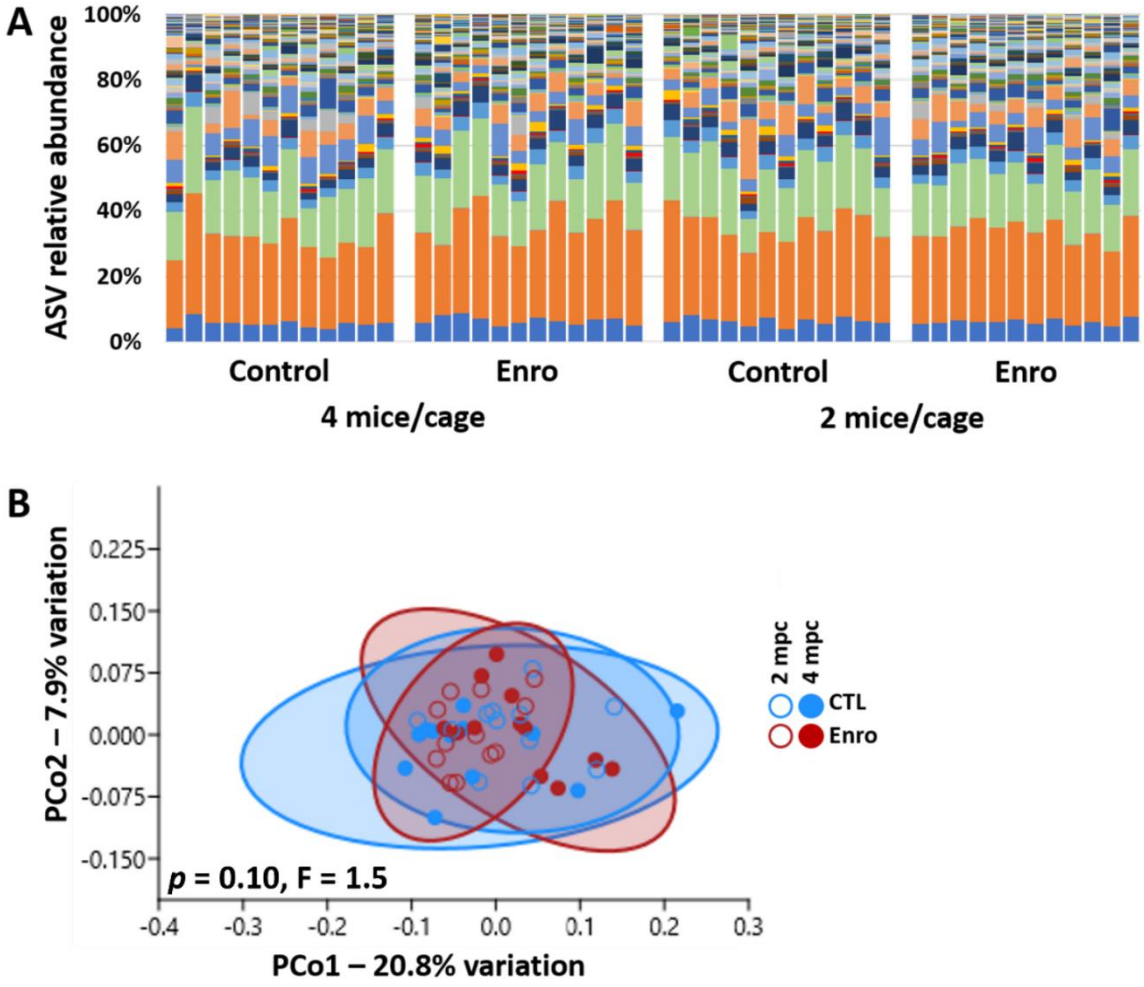

Supplemental Figure 2.1. No differences between groups in GM composition at baseline in Cohort 1, related to Figure 2.1. (A) Stacked bar chart showing the amplicon sequence variant (ASV) relative abundance, in feces from mice prior to treatment who were assigned to housing at 4 or 2 mpc, and to receive either sham (control) or enrofloxacin (Enro) in their drinking water. **(B)** Principal coordinate analysis of the samples shown in A, legend at right; p and F value denotes results of PERMANOVA between all four groups.

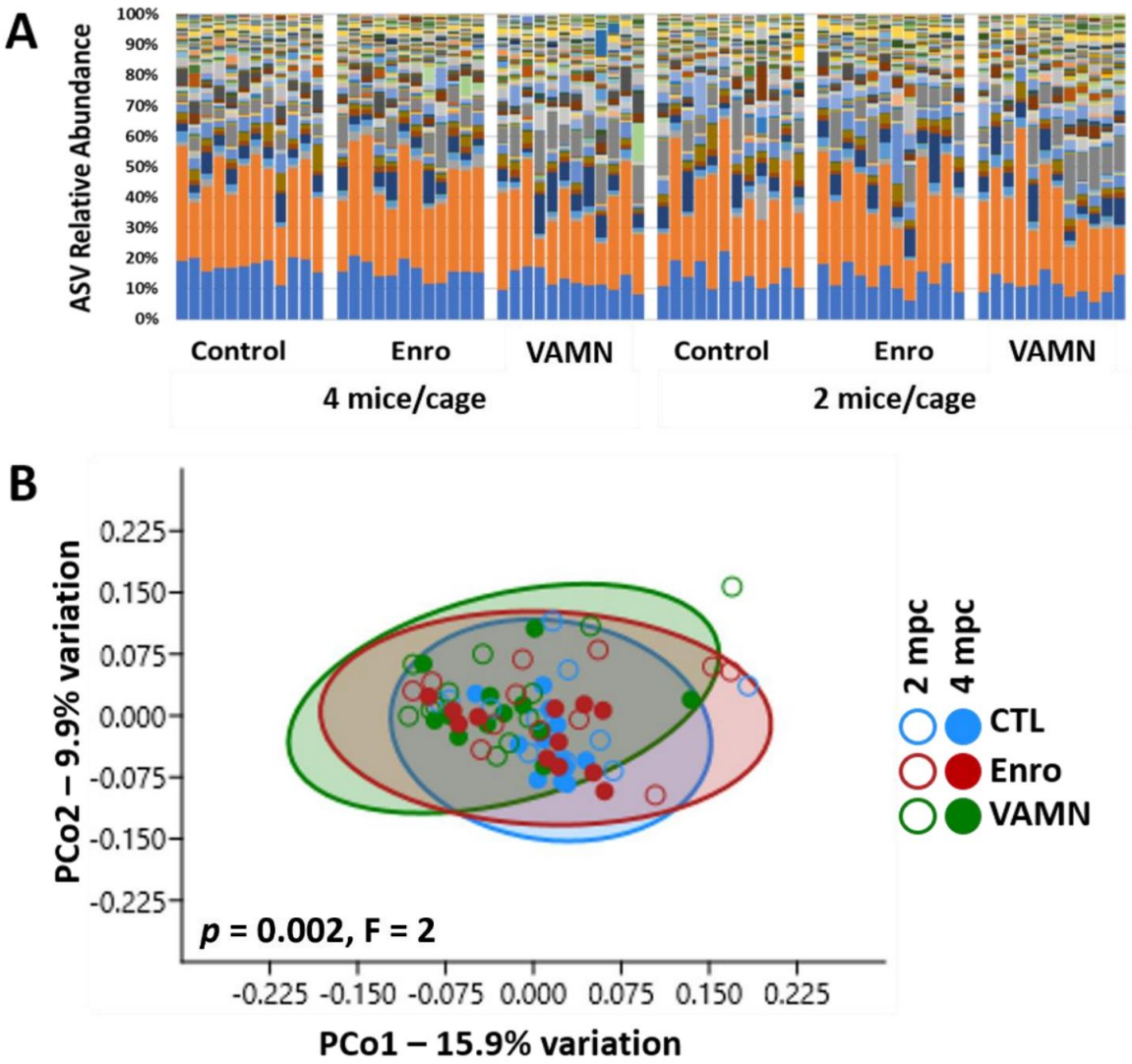

Supplemental Figure 2.2. No differences between groups in GM composition at baseline in Cohort 2, related to Figure 2.1. (A) Stacked bar chart showing the amplicon sequence variant (ASV) relative abundance in feces from mice prior to treatment who were assigned to housing at 4 or 2 mpc, and to receive either sham (control), enrofloxacin (Enro), or broad-range (VAMN) antibiotics in their drinking water. **(B)** Principal coordinate analysis of the samples shown in A, legend at right; p and F values denote results of PERMANOVA between all four groups.

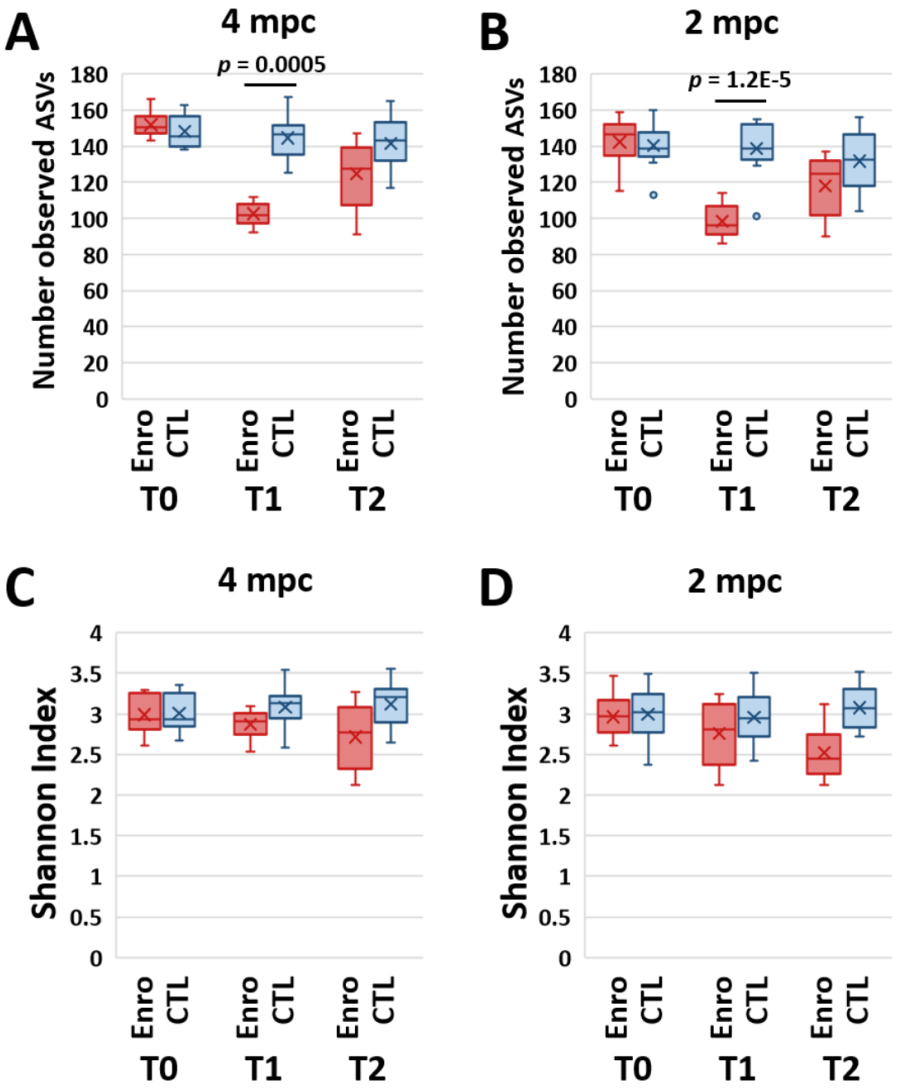

Supplemental Figure 2.3. Effects of enrofloxacin on richness and alpha-diversity in Cohort 2, related to Figure 2.2. Richness as represented by the number of distinct observed amplicon sequence variants (ASVs) in mice housed four per cage **(A)** or two per cage **(B)** upon arrival (T0), immediately after one week of exposure to antibiotics (or control) (T1), and three weeks after cessation of exposure (T2). Alpha diversity as estimated by the Shannon diversity index in mice housed four per cage **(C)** or two per cage **(D)**. p-values were obtained from the mixed effect models.

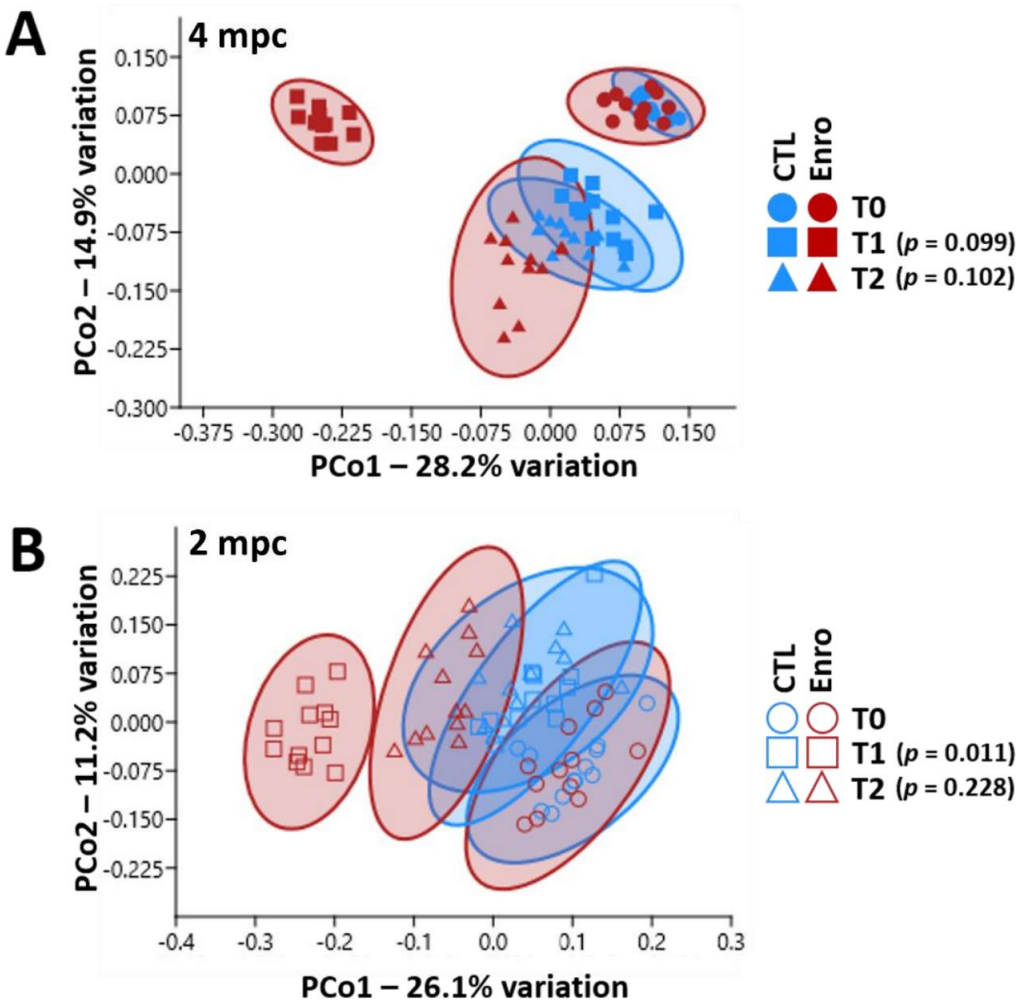

Supplemental Figure 2.4. Enhanced effects of enrofloxacin on beta-diversity in mice housed 2 mpc, related to Figure 2.3. Principal coordinates analysis of fecal samples from cohort 2 mice housed four mice per cage **(A)** or two mice per cage **(B)** and exposed to enrofloxacin (Enro) or control (CTL), collected upon arrival from the supplier (T0), immediately after one week of exposure to enrofloxacin or control (T1), and three weeks after cessation of exposure (T2). p-values were obtained from the nested PERMANOVA.

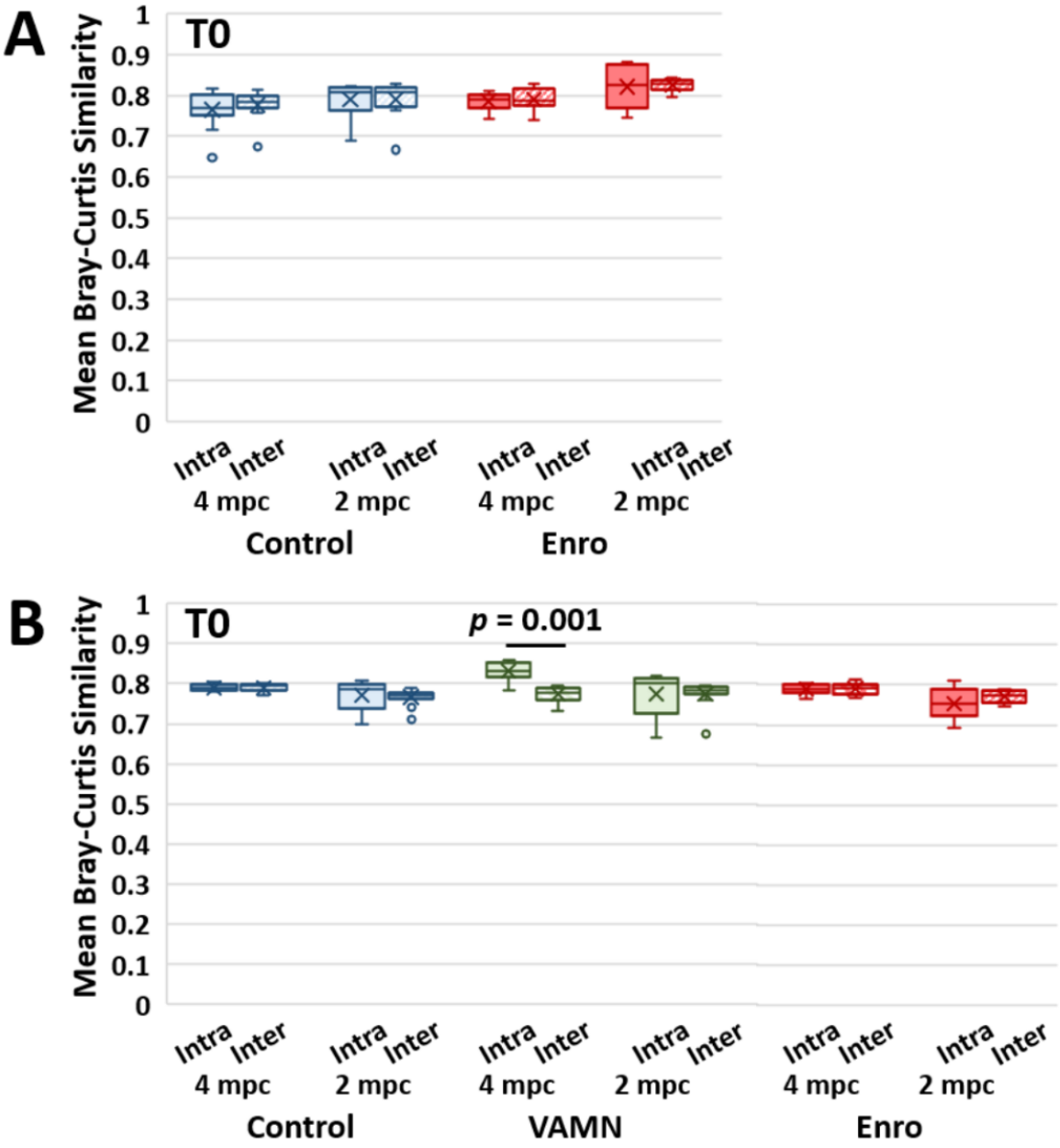

Supplemental Figure 2.5. Few significant cage effects at baseline, related to Figure 2.4. Tukey box plots showing mean intra-cage and inter-cage similarity between all possible sample pairs within a given treatment group and housing density immediately upon arrival at our institution, in Cohort 1 **(A)** and Cohort 2 **(B)**.

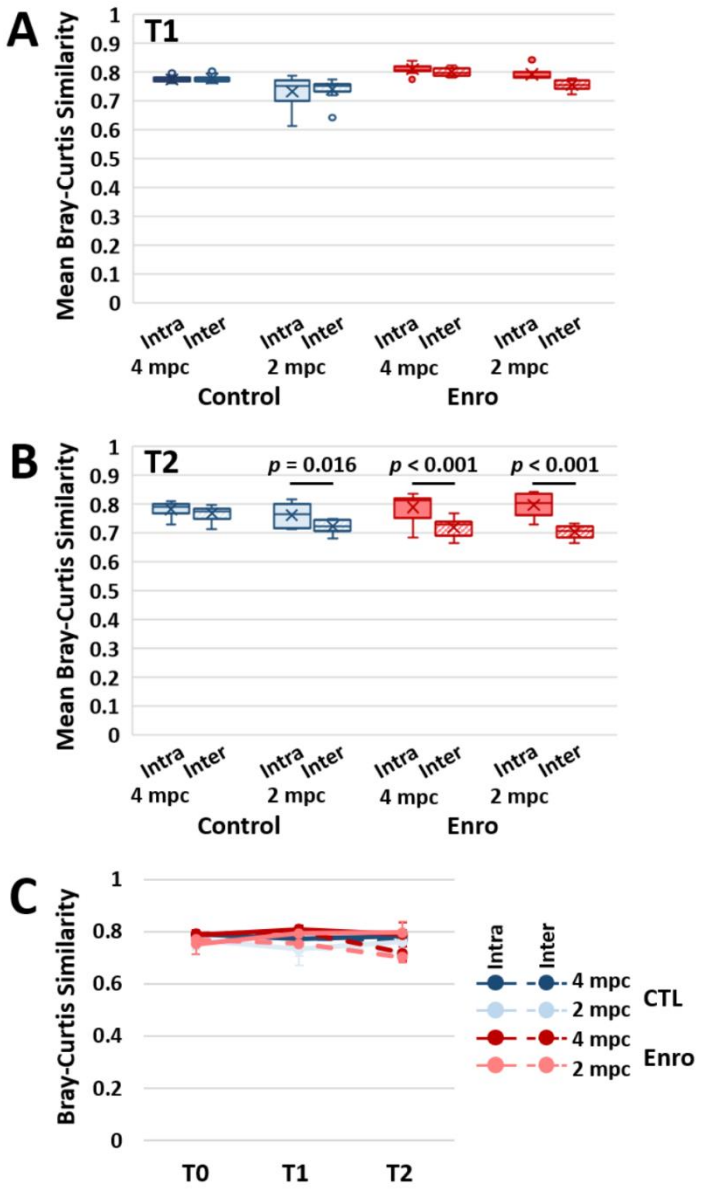

Supplemental Figure 2.6. Housing density-mediated effects on cage effects, related to Figure 2.4. Tukey box plots showing mean intra-cage and inter-cage similarity between all possible sample pairs within a given treatment group and housing density immediately after one week of exposure (**A**, T1) to enrofloxacin (Enro) or control (CTL), or after three weeks of recovery (**B**, T2) in cohort 2. Line chart for enrofloxacin and control groups in cohort 2 **(C)** showing the mean ± SD intra- and inter-cage Bray-Curtis similarity upon arrival from the supplier (T0), T1, and T2. Legend to C to right of C.

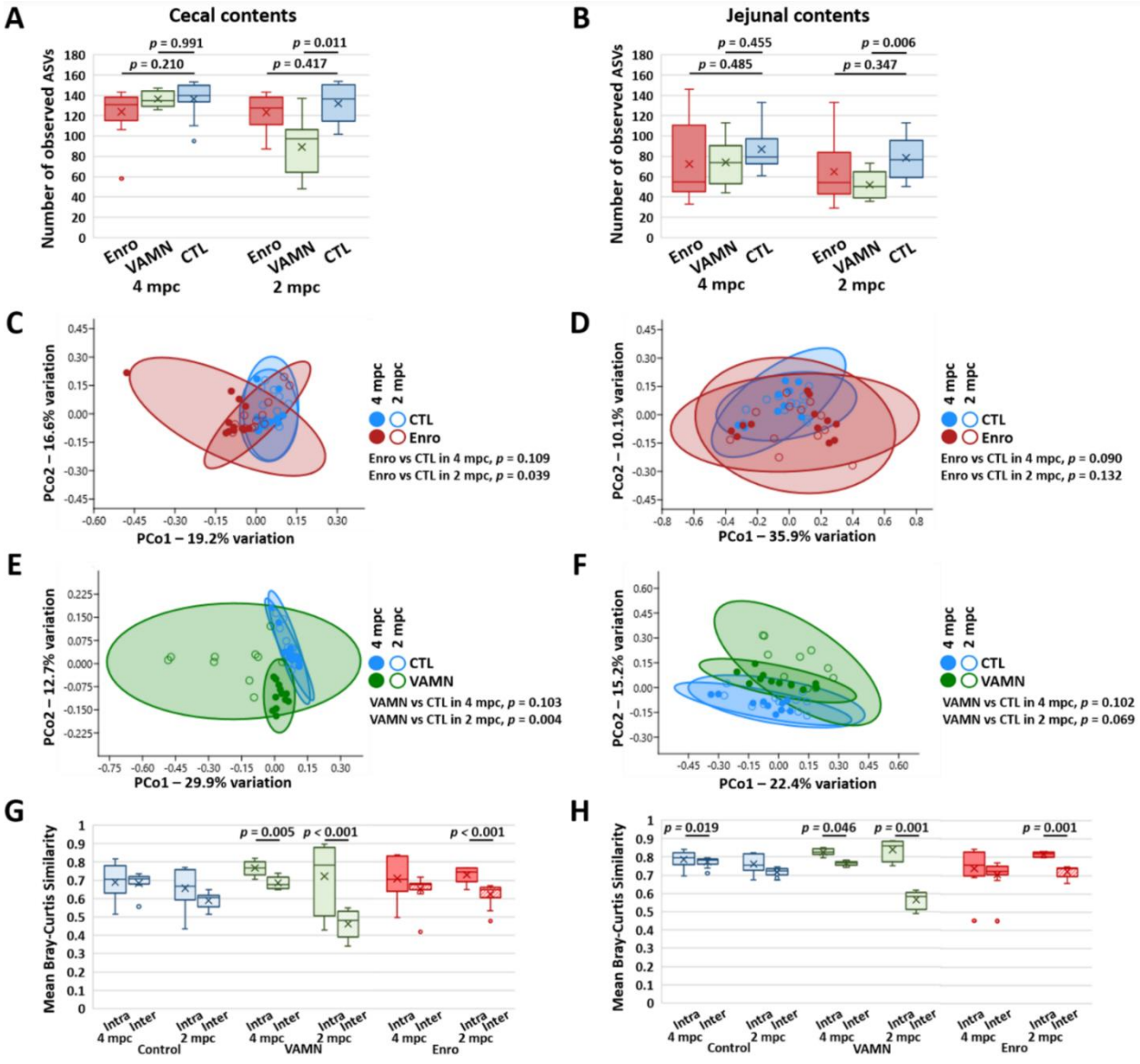

Supplemental Figure 2.7. Effects of housing density on antibiotic-induced changes in cecal and jejunal richness, alpha- and beta diversity (Cohort 2), related to Figure 2.5. Richness as represented by the number of observed amplicon sequence variants (ASVs) in the cecum **(A)** and jejunum **(B)** of mice housed four per cage or two per cage at three weeks after cessation of enrofloxacin (Enro), broad-spectrum antibiotics (VAMN), or sham (CTL) treatment; p values denote ABX-associated effects, based on mixed effect model with cage as a random effect. Principal coordinate analysis plots of Bray-Curtis similarities of cecal **(C)** and jejunal **(D)** microbiota of enrofloxacin and control groups, and cecal **(E)** and jejunal **(F)** microbiota of VAMN and control groups, in Cohort 2; p values denote treatment-associated effects based on PERMANOVA. Tukey box plots showing mean intra-cage and inter-cage similarity

between all possible sample pairs within a given treatment group and housing density, three weeks after cessation of treatment, in the cecal **(G)** and jejunal **(H)** microbiota.

CHAPTER 3 – THE CONTRIBUTION OF THE MATERNAL ORAL, VAGINAL, AND GUT MICROBIOTA TO THE DEVELOPING OFFSPRING GUT

Introduction

The maturation process of the gut microbiota (GM) is an essential process for life-long health that is defined by the acquisition and colonization of microorganisms in the gut and the subsequent immune system induction that occurs during early life. While emerging evidence suggests that initial colonization of the gut may happen as early as *in utero*[109,110], this is controversial, and the conventional understanding is that the first bacterial seeding of the gut begins at birth. Regardless of the timing, the initial bacterial colonization of the neonatal gut undoubtedly derives from a maternal source, emphasizing the importance of understanding how vertical transfer is initiated and influenced during continued exposure to maternal microbial sources over the course of GM maturation[111,112]. During the process of maturation, the neonatal GM is especially susceptible to environmental factors capable of inducing persistent effects on the developing GM[113]. Previously identified factors within both human and mouse model populations associated with significant effects on the composition of the neonatal microbiota include mode of delivery[114,115], breastfeeding[116,117], and antibiotic exposure[118,119]. These factors have the potential to confound research in human neonates, making characterization

of the development and contribution of maternal sources to the neonatal gut microbiota difficult[113].

There is strong agreement across host species regarding the basic characteristics of normal GM maturation that correspond with physiological changes occurring in the gastrointestinal tract[120,121]. During early life, the neonatal gut microbiota of both vaginally born breastfed humans and nursing mouse pups are dominated by members of the *Enterobacteriaceae* and *Lactobacillaceae* families[112,122]. These bacterial populations are transferred from mother during parturition and subsequently colonize the neonatal GM due to the high oxygen availability in the gastrointestinal tract relative to adults[120,123]. Next, as lumenal oxygen tension decreases, and breastfeeding continues, *Bifidobacteriaceae* and *Clostridiaceae* proliferate until weaning, presumably due to their role in metabolism of milk oligosaccharides and facultative anaerobic capabilities[124,125]. With the introduction of solid foods[121], a more diverse and adult-like gut microbiota develops, with *Bacteroidaceae*, *Lachnospiraceae*, and *Ruminococcaceae* being dominant families of the mature gut microbiota[113,121,126], and the maturation process can be considered complete once the GM has reached a richness and composition consistent with that of the maternal feces.

There is limited knowledge regarding the contribution of different maternal source microbiotas in the neonatal mouse gut microbiota. Literature describing the vertical transfer and maturation of the human gut microbiota has relied on noninvasive sampling, and largely ignored the

upper gastrointestinal tract (GIT)[111,112,127]. The few studies of the developing murine gut microbiota that included samples of the upper GIT found compositional and functional differences compared to the lower GIT, but the maternal source of ileal microbes was not investigated[128,129].

To address these knowledge gaps, we characterized the neonatal fecal and ileal microbiota at multiple pre-weaning time-points, alongside the maternal fecal, ileal, vaginal, and oral microbiotas using targeted amplicon sequencing. Core microbiota analyses and similarities between matched neonatal and maternal samples were used to assess the relative contribution of the different maternal sites to the developing neonatal microbiota in both compartments of the GIT. Additionally, considering the significant differences in richness and beta-diversity among SPF microbiotas from different producers, the entire experimental design was replicated in isogenic mice with microbiotas originating from two different U.S. suppliers[57], The Jackson Laboratory and Envigo.

Methods

Animals

All experiments described in this dissertation were approved by the Institutional Animal Care and Use Committee (IACUC) of the University of Missouri (protocol 9587). Outbred CD-1 mice maintained at the University of Missouri harboring either a low richness background GM originating from The Jackson Laboratory, designated GM1, or a high richness background

GM originating from Envigo, designated GM4. A detailed description of these colonies has been previously published[57]. 16 female mice (GM1: n = 8, GM4: n = 8) were bred and their subsequent pups were allowed to age until either day of age 9 (GM1: n = 23, GM4: n = 22), 10 (GM1: n = 13, GM4: n = 21), 11 (GM1: n = 13, GM4: n = 19), or 12 (GM1: n = 19, GM4: n = 16). Two dams and their subsequent pups were euthanized at each timepoint chosen at random, and samples were collected immediately after euthanasia. An additional 12 pup fecal samples were also collected at 7, 14, and 21, days of age from colony pups from both GM backgrounds for comparison to the dam-pup matched samples. Mice were housed at Discovery Ridge in Columbia, MO under barrier condition in microisolator cages on Thoren ventilated racks under a 14:10 light/dark cycle. Each cage contained pelleted paper bedding with nestlets and received *ad libitum* access to irradiated Breeder diet 5053 rodent chow and acidified, autoclaved water.

Sample collection

All maternal samples were collected *post mortem* at days 9, 10, 11, and 12. Oral and vaginal swabs were used to collected oral and vaginal microbiota samples respectively, by inserting a cotton swab into the designated orifice and rotating the swab. Swab samples were then collected into 2 mL round-bottom tubes. Maternal ileal samples were collected by excising roughly 4 cm of ileum proximal to the ileocecal junction and rinsing the luminal contents of the sample into a 2 mL round-bottom tube using

sterile PBS. For maternal fecal samples, the two most distal fecal pellets in the rectum or distal colon were collected and placed in 2 mL round-bottom tubes with a 0.5 cm-diameter stainless steel ball bearing for homogenization of sample. Pup feces were collected as described for dams at days 7, 9, 10, 11, 12, 14, and 21 of age. Pup ileal samples were collected at days 9, 10, 11, and 12 of age by excising 2 cm of the ileum proximal to the ileocecal junction and collecting into a 2 mL round-bottom tube with a 0.5 cm-diameter stainless steel ball bearing due to the small size of the ileal lumen. All samples were placed on ice immediately following collection and samples were stored in a -80° C freezer until DNA was extracted.

DNA extraction

All sample tissue DNA was extracted using PowerFecal Pro kits (Qiagen) according to manufacturer's protocol, with the exception that samples were homogenized using a TissueLyser II (Qiagen) for 10 minutes at 30/sec, in lieu of a vortex adapter as described by PowerFecal Pro kit instructions. DNA yields were quantified by fluorometry via the quant-iT BR dsDNA reagent kits (Invitrogen) and normalized to a consistent concentration and volume prior to submission for downstream processing.

16s rRNA library preparation and sequencing

Tissue sample DNA was processed at the University of Missouri Genomics Technology Core. Bacterial 16S rRNA amplicons were constructed via amplification of the V4 region of the 16S rRNA gene with

the universal primer set (U515F/806R) and flanked by Illumina standard adapter sequences as in a method previously described elsewhere[130,131]. Dual-indexed forward and reverse primers were used in all sample reactions. PCR was initiated in 50 uL reactions containing 100 ng metagenomic DNA, primers (0.2 uM each), dNTPs (200 uM each), and Phusion high-fidelity DNA polymerase (1U, Thermo Fisher). Amplification parameters used were as followed: $98°C^{(3\ min)}$ + [$98°C^{(15\ sec)}$ + $50°C^{(30\ sec)}$ + $72°C^{(30\ sec)}$] × 25 cycles +$72°C^{(7\ min)}$. Amplicon pools of 5 µL/reaction were combined, thoroughly homogenized, and then purified with addition of Axygen Axyprep MagPCR clean-up to an amplicon volume of 50 µL. Amplicons were then incubated for 15 minutes at room temperature and received multiple washes of 80% ethanol. Post-wash, the dried pellet was resuspended in 32.5 µL EB buffer (Qiagen), incubated at room temperature for 2 minutes, and then placed on a magnetic stand for five minutes. The final amplicon pool was then evaluated using quant-IT HS dsDNA reagent kits and diluted according to the Illumina standard protocol for sequencing of 2×250 bp paired-end reads. Amplicon pools were then sequenced on the MiSeq instrument.

Informatics analysis

DNA sequences were assembled and annotated at the MU Bioinformatics and Analytics Core. The primer set was designed to match the 5’ end of both the forward and reverse amplicon reads. Cutadapt4 (version 2021.8.0; https://github.com/marcelm/cutadapt) was then used to

remove the primer from the 5’ end of the forward read, and then if found, remove the reverse complement of the primer to the reverse read from the forward read. Therefore, a forward read could be trimmed at both ends if the insert were shorter than the length of the amplicon. The same method was then utilized for reverse reads, but with the primers in the opposite roles. Read pairs were then rejected if one read or the other did not match a 5’ primer, and the allowed error-rate was 0.1. Two passes over each read count were made to ensure removal of the second primer, and a minimal overlap of three bp with the 3’ end of the primer was required for removal.

The QIIME2 DADA2 plugin (version 1.18.0) was utilized to denoise, de-replicate, and count amplicon sequence variants (ASVs). The following parameters were incorporated: 1) forward and reverse reads were truncated to 150 bases, 2) forward and reverse reads with an expected error higher than 2.0 were ignored, and 3) Chimeras were detected using the “consensus” method and then removed. Python version 3.8.10 and Biom version 2.1.10 were used in QIIME2. Taxonomies were assigned to each of the final sequences using the Silva.v138 database, utilizing the classify-sklearn procedure.

Statistics

To calculate significant changes in alpha diversity and relative abundance (RA) of pup fecal and pup ileal samples, we utilized ANOVA on ranks within each GM, due to a lack of normality. Alpha diversities were quantified by the Chao-1 index using PAST software. ANOVA on ranks was

performed using SigmaPlot 14.0 with a Dunn's *post hoc* analysis for pairwise comparisons.

One-way permutational multivariate analysis of variance (PERMANOVA) was used to test for significant differences in beta diversity of samples and provide pair-wise comparisons of beta-diversity. PERMANOVA testing was performed with PAST software using Bray-Curtis similarities[132]. The Bray-Curtis similarity of pup fecal and pup ileal samples to maternal tissues were tested for significant differences within each GM using two-way ANOVAs for the factors tissue type and age using SigmaPlot 14.0. A Holm-Sidak *post hoc* analysis was used to determine significant differences by pair-wise comparison of each group within each two-way ANOVA analysis via SigmaPlot 14.0 (Systat Software, Inc, San Jose, CA). Spearman correlations between pup fecal and pup ileal Bray-Curtis similarities values were calculated using SigmaPlot 14.0.

Results

Phylum-level composition changes rapidly during gut microbiota development

Neonate feces demonstrated incrementally lower relative abundance (RA) of *Bacillota* and higher RA of *Bacteroidota* at each subsequent timepoint (**Figure 3.1A, B**), with the latter proliferating substantially on day 11 or 12 of life. Prior to day 12, high richness GM4 neonate feces also

contained high RA of *Pseudomonadota*, while this phylum was present at a much lower RA in low richness GM1. The same difference was observed in the neonate ileum (**Supplemental Figure 3.1A, B**). Maternal samples from GM1 (**Figure 3.1C**) also contained lower proportions of *Pseudomonadota* than maternal samples from GM4 (**Figure 3.1D**), while also harboring a greater number of bacterial phyla within vaginal and fecal samples. The vaginal and fecal microbiota of GM4 maternal samples contained populations of *Bacillota*, *Bacteroidota*, *Deferribacterota*, *Verrucomicrobiota*, *Cyanobacteria*, and *Actinomycetota* at proportions of 1% or greater, while GM1 samples contained only *Bacillota*, *Bacteroidota*, and *Pseudomonadota* at proportions of 1% or greater.

An ANOVA on ranks test was used to identify differences in richness within each GM, using the Chao-1 index. As expected, the richness of neonate fecal samples was significantly higher at later timepoints, however within ileal samples, age did not have a significant main effect on richness in either GM. For GM1 mice, fecal richness at day 14 and day 21 was significantly higher than samples from day 7 through day 11 (**Figure 3.1E**), while ileal richness had no clear pattern based on timepoint (**Supplemental figure 3.1**). A similar effect was observed in GM4 neonate richness, where fecal richness at day 21 was significantly higher than day 7 through 12 (**Figure 3.1F**), and no difference in richness was detected in the ileum (**Supplemental figure 3.1**).

Evidence of GM-specific vertical transfer

To better resolve the taxonomic differences between GM1 and GM4 pups within the *Bacillota* and *Pseudomonadota* phyla, we determined the RA of ASVs annotated to the order *Lactobacillales* and the phylum *Pseudomonadota*. The RA of *Lactobacillales* was lower at day 21 compared to day 7 through day 12 in both GM1 and GM4 neonate fecal samples (**Figure 3.2A**). Regarding the different maternal sites (**Figure 3.2B**), the RA of *Lactobacillales* was variable in both GMs, with no statistical difference between sampling sites for either GM1 (H= 17.91, p = 0.001) or GM4 (H = 7.34, p = 0.12). The oral microbiota contained GM-specific species of *Streptococcus*, including *S. danieliae* in GM1, and *S. merionis* in GM4, and this difference was reflected in the neonatal feces. Within the *Pseudomonadota*, an ASV resolved to the family *Pasteurellaceae* was dominant in both GMs, particularly in GM4, reaching a mean RA greater than 50% at day 11 before declining significantly at all later time-points (**Figure 3.2C**). A similar trend was observed in *Escherichia-Shigella,* wherein the RA was higher within GM4 at day 12 compared to earlier timepoints (day 7: p = 0.04, day 9: p = 0.007). On day 14 and 21, *Pasteurellaceae* and *Escherichia-Shigella* were largely replaced by *Parasutterella excrementihominis* in GM1, and an unspeciated *Parasutterella* in GM4 (**Figure 3.2C**). A high RA of the dominant *Pasteurellaceae* ASV was detected in maternal oral samples, but this difference did not reach significance compared to other maternal sites.

The neonatal ileum was distinct from feces but also reflected several trends seen in the neonate feces, including GM1-specific growth of *S. danieliae* (**Supplement Figure 3.2**). Similarly, *Pasteurellaceae* represented the dominant *Pseudomonadota* within the neonatal ileum, showing a similar peak RA approaching 50% in the GM4 neonate ileum at day 11 (**Supplemental Figure 3.2**). Collectively, these data suggest that dominant taxonomies are shared between the maternal oral cavity and neonate mouse gut.

Similarity to maternal tissue depends on neonatal GI sample location

Principal coordinate analysis (PCoA) was used to visualize the beta diversity of neonatal and maternal samples within each GM. Comparison of all maternal sites to neonate feces at the earlier timepoints indicated a greater similarity between oral samples and neonate feces than other maternal sites, in both GM1 (**Figure 3.3A**) and GM4 (**Figure 3.3B**).

Within ileal samples, there was less clustering according to timepoint, and less separation from maternal samples. Within GM1 and GM4 (**Supplemental Figure 3.3**), maternal oral samples clustered more closely to the neonate ileal samples than did the other maternal sites. Collectively, these data suggest that the offspring gut microbiota does not mature until the third week of life, and that the immature gut microbiota is more similar in composition to the maternal oral microbiota than the vaginal microbiota.

The maternal vaginal contribution to neonatal microbiota is negligible

To control for dam-to-dam variation, we also calculated the Bray-Curtis similarity between each pup fecal sample and matched maternal tissue samples. A three-way ANOVA was used to identify main effects and interactions between GM, age of pups, and maternal sampling site. There was a significant main effect of all factors, and significant interactions between all three factors analyzed ($F = 2.38$, $p = 0.005$). In order to analyze pairwise comparison between samples within each GM, data were stratified by GM and a two-way ANOVA was utilized. Within GM1, neonate feces had the highest similarity to maternal fecal samples at all timepoints compared to oral and vaginal samples (**Figure 3.4A**). The similarity between pup feces and the maternal oral and vaginal microbiotas was much lower and favored similarity to the oral microbiota during early life. Within GM4, maternal oral samples had significantly higher similarity to pup feces than maternal vaginal or fecal samples from day 7 to day 12 (**Figure 3.4B**). By day 14, similarity of offspring feces to maternal feces was significantly higher than similarity to oral ($p < 0.001$, $t = 12.48$) or vaginal samples ($p < 0.001$, $t = 14.64$), which remained true on day 21.

Similarities between ileal samples and matched maternal samples were also compared, during the period between days 9 and 12. A three-way ANOVA found an overall main effect of age of pups ($F = 12.30$, $p < 0.001$) and maternal tissue ($F = 13.48$, $p < 0.001$), as well as interactions between all three factors ($F = 6.20$, $p < 0.001$). Two-way ANOVA stratified by GM

found a significant difference between maternal tissue type within GM1 on day 10 and 11 (**Supplemental Figure 3.4**). Within GM4 ileal samples, there was a significant difference between maternal tissue type at each timepoint. While similarity to maternal sites in each GM varied from day to day during this period, the highest similarity was most often to maternal oral or ileal samples.

Next, we utilized Spearman correlation analyses to determine the correlation between maternal tissue similarity to both the neonatal upper and lower GIT. Neonates that had both fecal and ileal samples collected were used for this analysis (n = 146). There was a significant positive association between maternal oral and neonatal GIT similarity (**Supplemental Figure 3.4**). Maternal vaginal similarity to neonatal fecal and ileal samples did not correlate significantly.

Neither maternal vaginal nor maternal fecal samples correlated with neonatal GIT samples in terms of similarity. These data suggest that those mice in which the maternal oral microbiota is most represented in the neonatal ileum, are expected to have the highest similarity between maternal oral and neonatal fecal microbiota as well.

Compositional similarity of the neonatal GIT to the maternal feces increases with age

To determine the number of ASVs consistently shared between the neonatal fecal microbiota and maternal tissue sites over the course of gut

microbiota development, the core microbiota[133] of each maternal tissue within each GM was compared to the core microbiota of neonatal feces at each timepoint within the same GM. An ASV was considered part of the core microbiota if it was detected in 30% or more of samples within a group and had an average group relative abundance of 0.01% or higher. Over the course of fecal microbiota development, the core microbiota of GM1 neonates first undergoes an expansion of ASVs exclusively found in the oral maternal microbiota (**Figure 3.5A**). This event consists of four ASVs detected from day 9 to day 12. The second expansion involves ASVs shared exclusively with the maternal fecal core microbiota starting at day 11. With each consecutive timepoint, the contribution of maternal core fecal ASVs increased up to the final timepoint, with 79 ASVs detected (**Figure 3.5A**). For the neonatal fecal core microbiota in GM4, ASVs shared exclusively with maternal fecal samples were not detected until day 12 with nine ASVs, which increased to 66 ASVs by day 21 (**Figure 3.5B**). The majority of core ASVs detected in GM4 were not exclusive to any maternal tissue core.

The same approach for identifying core microbiota was used for ileal samples. For the GM1 ileal core microbiota, there was only one ASV shared exclusively with the maternal ileal core microbiota at any given timepoint, while the neonatal ileal core microbiota shared up to seven ASVS exclusively with the maternal oral core microbiota at days 9, 10, and 11 (**Supplemental Figure 3.5**). The GM1 neonatal ileal core microbiota was

the only neonatal core microbiota to share ASVs exclusively with the maternal vaginal core microbiota. The core microbiota of GM4 neonatal ileal samples mostly contained ASVs that were shared between all maternal tissue core microbiotas, and there was only one ASV shared exclusively with one maternal source (oral) at any given time.

Discussion

Our results indicate that the gut microbiota of neonatal mice rapidly changes during development to approach the maternal gut microbiota in composition and diversity by three weeks of age (**Figure 3.1**). Within feces, proportions of *Bacillota* and *Pseudomonadota* decrease, while proportions of *Bacteroidota* increase throughout maturation. These changes in phylum level RA are consistent with previous findings indicative of the diversification of the gut microbiota population seen in both humans and mice at weaning[134]. The expansion of *Bacteroidota* is correlated with the onset of consumption of plant derived carbohydrates found in solid foods in both humans and mice[121], likely explaining the increase seen in this study. The decline in the proportion of *Pseudomonadota* and *Bacillota* as pups age may be due to the shift from an aerobic to an anaerobic environment within the intestines due to the decline in oxygen availability as pups age, causing a compositional shift favoring bacteria that are able to utilize anerobic respiration[135].The maturation of the gut microbiota is further exemplified in these pups by the steady increase in fecal alpha diversity over time , as has

been reported previously during early development in both species[112,113,136,137].

The RA of the phylum *Pseudomonadota* was strikingly different between GM1 and GM4 in both neonatal fecal and ileal samples (**Figure 3.2, Supplemental Figure 3.2**). Specifically, GM4 mice harbored higher proportions of *Pseudomonadota* compared to GM1 mice, as two ASVs annotated to *Pasteurellaceae* and one *Escherichia-Shigella* ASV were enriched in GM4 compared to GM1 neonatal feces. Interestingly, maternal *Escherichia-Shigella* was found in highest proportions in oral samples in GM1 but in vaginal samples in GM4. We also found that the RA of *Pseudomonadota* changes in the neonatal gut microbiota over time, but *Lactobacillales* colonization appears less dynamic during the maturation of the gut microbiota. This may be due to intermittent presence of *Pseudomonadota* in the maternal milk microbiota[117,138] and the ability of *Pseudomonadota* to metabolize milk oligosaccharides[139], while the decline in *Pseudomonadota* in neonatal mice has been associated with increased IgA production as neonates age[140]. In contrast, *Lactobacillales* are lactic acid-producing bacteria that utilize carbohydrates and colonize the gut throughout infancy and adulthood and can survive in both anerobic and aerobic conditions[141]. The higher proportions of *Streptococcus danieliae* in GM1 and *Streptococcus merionis* in GM4 in the neonatal gut microbiota were vertically transferred from the maternal oral microbiota. These results suggest that different background GMs are predisposed to harboring not

only different proportions of bacteria, but also experience species-specific gut microbiota vertical transfer of these populations.

As pups age, both fecal and ileal GM beta diversity became increasingly similar to maternal fecal and ileal samples respectively, as well as inter-individual similarity within pups (**Figure 3.3** and **Supplemental Figure 3.3**). This increase in similarity is expected and has repeatedly been reported in the literature of both human and mouse model as a hallmark of GM[122,142]. The contribution of maternal microbial sites to the neonatal gut microbiota varies between different SPF GMs. In terms of beta diversity, the similarity of offspring feces to oral maternal samples remained stable overtime, however in GM4, this similarity was significantly higher than fecal maternal similarity until day 14. This provides evidence that maternal tissue contribution varies between gut microbiota compositions, and we may thus infer that vertical transfer from maternal microbial sites is mediated in part by the composition of the various source microbiotas. The similarity of offspring ileum to maternal tissue samples was inconsistent over time, but findings suggest the same trends seen in the feces.

Analysis of beta diversity similarity (**Figure 3.4**, **Supplemental Figure 3.4**) and the core microbiota of pup samples in relation to the maternal oral, vaginal, fecal, and ileal composition (**Figure 3.5**, **Supplemental Figure 3.5**) revealed high similarity between pup feces and maternal oral samples in early life, with increasing similarity to maternal gastrointestinal samples as pups age. These results are consistent with

recent studies, in which maternal vaginal samples do not colonize the neonatal gut microbiota as well as other maternal sources[111]. As such, this study provides further evidence of conserved events between humans and mice during the maternal transfer of microbes and maturation of the offspring gut microbiota.

Mice fecal samples from each GM were originally collected at day 7, 14, and 21 to examine changes in the fecal microbiota overtime. We found a large compositional shift between day 7 and day 14 in which the neonatal mouse fecal microbiota underwent a dramatic change in composition. To examine this compositional shift in greater detail, we focused on days 9, 10, 11 and 12 to examine the bacterial composition of pup ileum in relation to different maternal sites during this period of transition. Although we do not have ileal data for all timepoints, we found the data pertinent to include in this analysis for a more complete understanding of neonatal gut microbiota development.

The results of this study are overall consistent with recent literature regarding gut microbiota development and vertical transfer of various maternal microbiota sources. Previous maternal transfer studies have focused on human rather than mice, as such our study is the first of its kind to analyze the effect of multiple microbiota sources on gut microbiota development in mice. By utilizing the differing compositions of GM1 and GM4, this study was able to model some of the GM variation seen between individuals in human studies, thus allowing us to find significant differences

in the contribution of various maternal bacterial on the pup GM composition throughout development. These results support the use of the mouse as an appropriate model for gut microbiota development and highlight the importance of utilizing a study design with more than one gut microbiota composition.

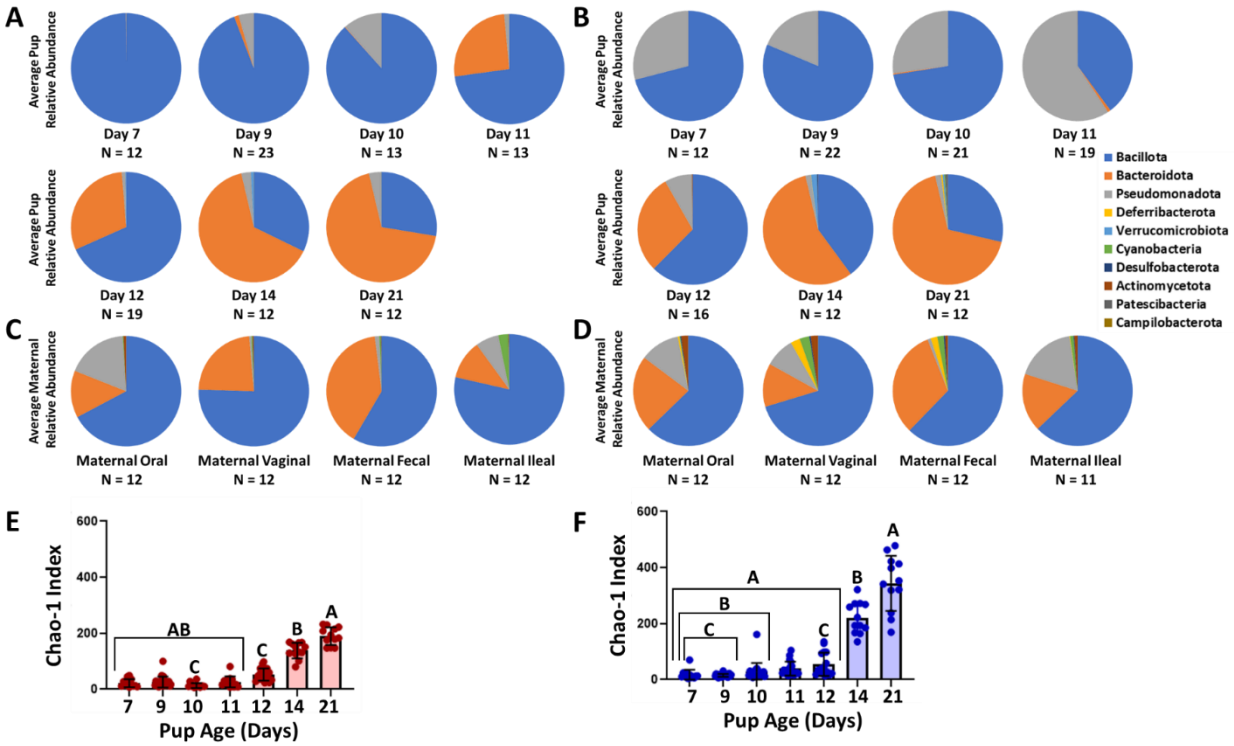

Figure 3.1. Fecal *Bacteroidota* relative abundance and alpha diversity are greater in older pups. (A-D) Circle graphs depicting average relative abundance of samples. Figure key located on right side of panel. (A-B) Pup fecal samples grouped by timepoint from **(A)** GM1 and **(B)** GM4 mice. (C-D) Maternal tissue samples groups by sample tissue type for **(C)** GM1 and **(D)** GM4 mice. (E-F) Bar charts depicting alpha diversity of samples using Chao-1 index with bars representing group averages and error bars representing standard error of mean (SEM). Each symbol represents an individual sample. **(E)** Average GM1 pup fecal alpha diversity grouped by timepoint. **(F)** Average GM4 pup fecal alpha diversity grouped by timepoint. Statistics were calculated using ANOVA on ranks within each GM, like letters within a graph denote a significant difference in pair wise comparisons using Dun's post-hoc.

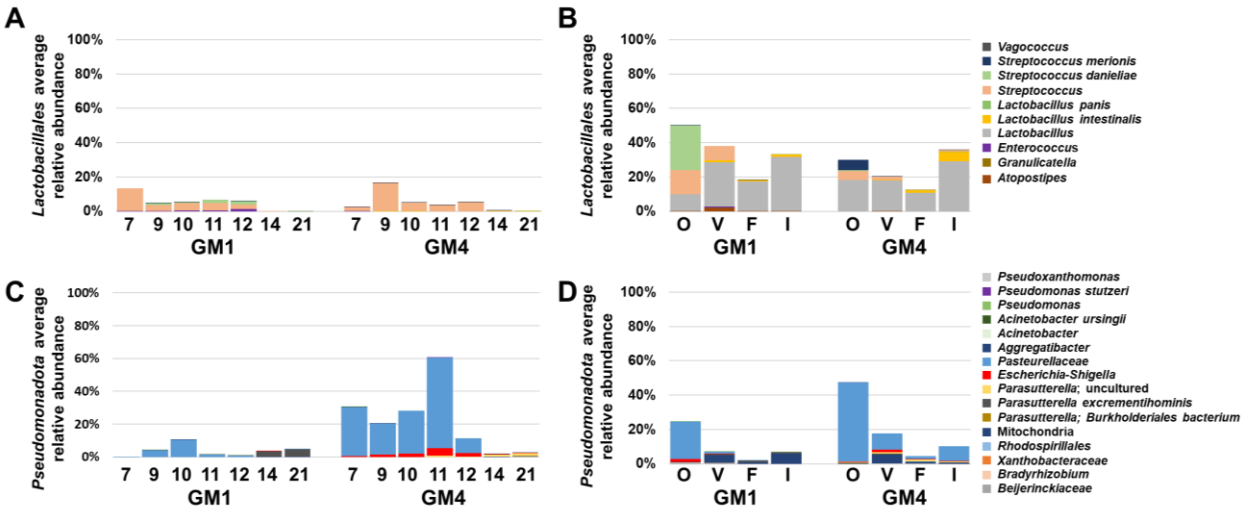

Figure 3.2. GM4 Pup feces harbors a higher proportion of *Pseudomonadota* species than GM1. (A-B) Bar charts depicting the average proportion of taxa annotated to Lactobacillales in study samples. Figure key is located on the right side of panel. **(A)** pup fecal samples grouped by GM and age of pups. **(B)** Maternal samples grouped by GM and tissue type. (C-D) Bar charts depicting the average proportion of ASVs annotated to Pseudomonadota in study samples. Bar charts depicting the average proportion of taxa annotated to Pseudomonadota in study samples. Figure key is located on the right side of panel. **(C)** pup fecal samples grouped by GM and age of pups. **(D)** Maternal samples grouped by GM and tissue type.

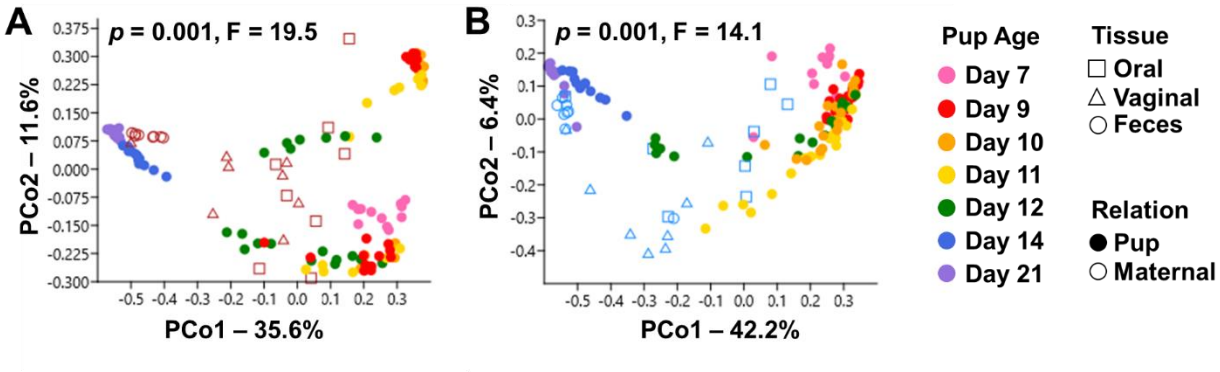

Figure 3.3. Neonatal fecal similarity to maternal tissues shifts dramatically with time in both GMs. Principal coordinate analysis (PCoA) graphs depicting beta diversity using Bray-Curtis similarity index. Figure key to the right side of panel. (A-B) Pup fecal samples with maternal oral, vaginal, and fecal samples from groups **(A)** GM1 **(B)** GM4. Statistics were calculated using a one-factor PERMANOVA for each graph.

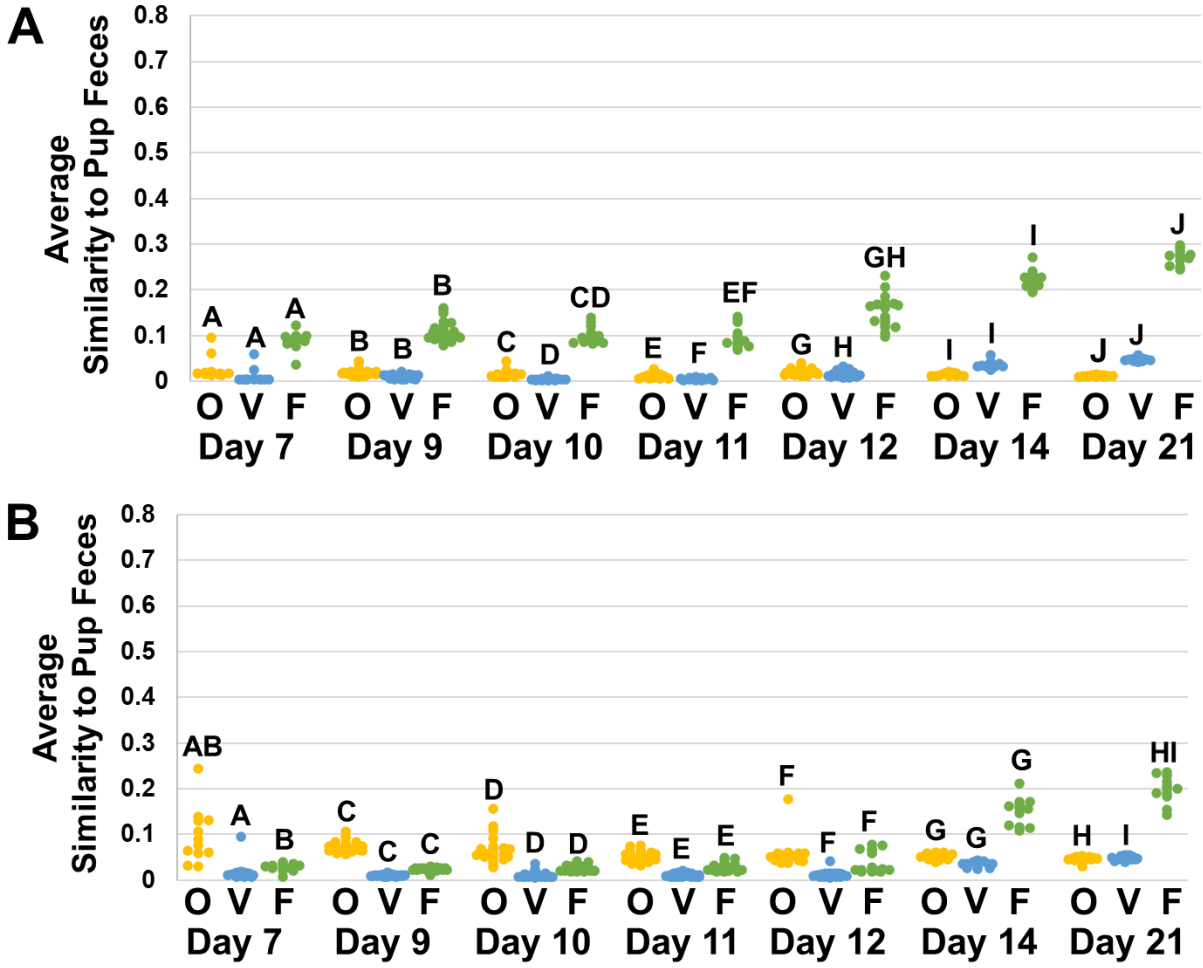

Figure 3.4. Fecal similarity increases over time, but similarity to maternal oral microbiome is GM dependent. (A-B) Dot plots and bar graphs depicting Bray-Curtis similarity of pup feces to maternal tissue. **(A)** Average Bray-Curtis similarity of maternal samples to pup feces in GM1. Each dot represent the average bray-Curtis similarity of one pup fecal sample to all maternal samples of that tissue type in GM1. **(B)** Average Bray-Curtis similarity of maternal samples to pup feces in GM4. Each dot represent the average bray-Curtis similarity of one pup fecal sample to all maternal samples of that tissue type in GM4. Statistics were calculated within each GM using a Two-way ANOVA on tissue type and age of pups. Matching letters denote significant pairwise differences detected during a Holm-Sidak post-hoc analysis. O- Oral, V- Vaginal, F- Fecal.

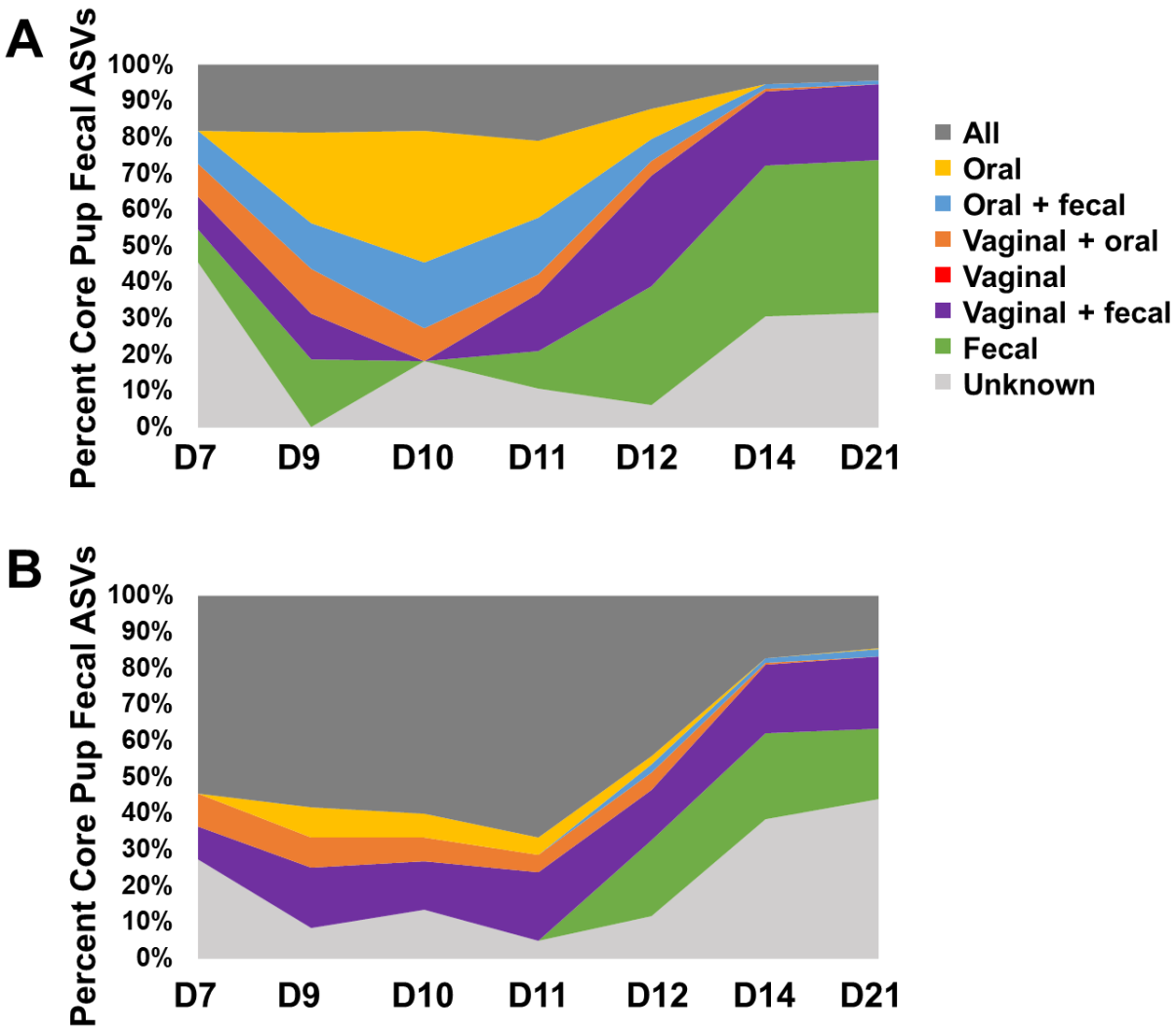

Figure 3.5. Unique maternal vaginal ASVs were not incorporated into pup fecal microbiota. Area graphs depicting the proportion of amplicon sequence variants (ASV)s found in the pup fecal core microbiota at each timepoint, that are also found in maternal tissue core microbiota. Figure key is located to the right of the panel. **(A)** GM1 pup fecal and **(B)** GM4 pup fecal core microbiota.

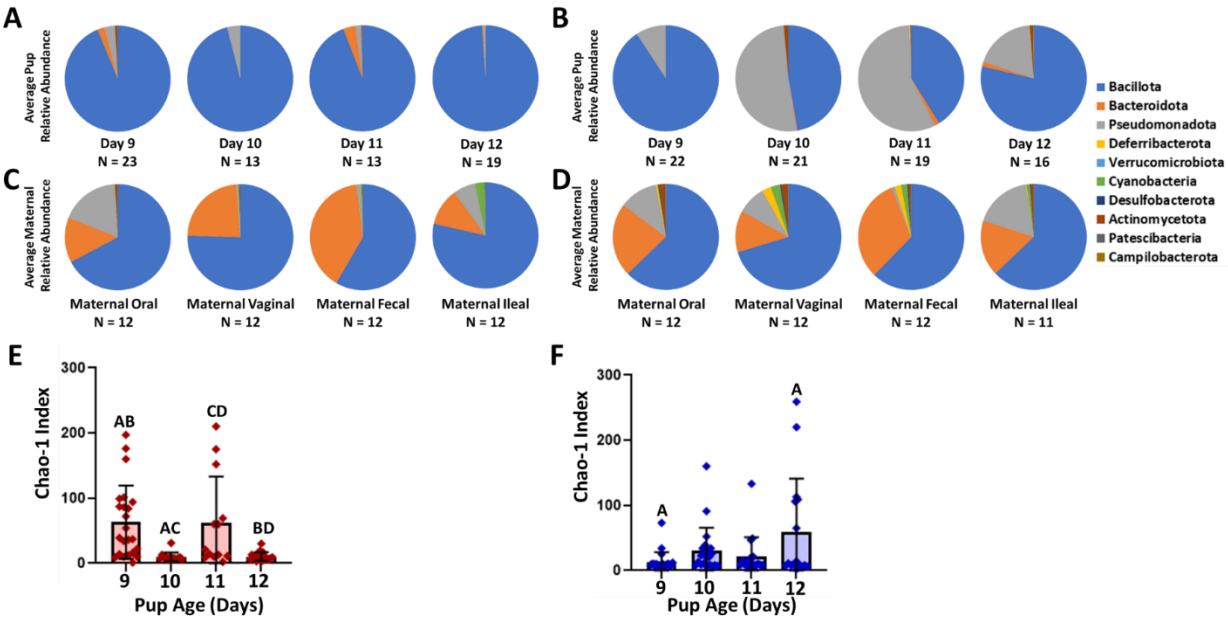

Supplemental Figure 3.1. Pup ileal samples harbor different relative abundances of *Pseudomonadota* between GMs. (A-D) Circle graphs depicting average relative abundance of samples. Figure key located on right side of panel. (A-B) Pup ileal samples grouped by timepoint from **(A)** GM1 and **(B)** GM4 mice. (C-D) Maternal tissue samples groups by sample tissue type for **(C)** GM1 and **(D)** GM4 mice. (E-F) Bar charts depicting alpha diversity of samples using Chao-1 index with bars representing group averages and error bars representing standard error of mean. Each symbol represents an individual sample. **(E)** Average GM1 pup ileal alpha diversity grouped by timepoint. **(F)** Average GM4 pup ileal alpha diversity grouped by timepoint. Statistics were calculated using Two-way ANOVA, like letters within a graph denote a significant difference in pair wise comparisons using a Holm-Sidak post-hoc.

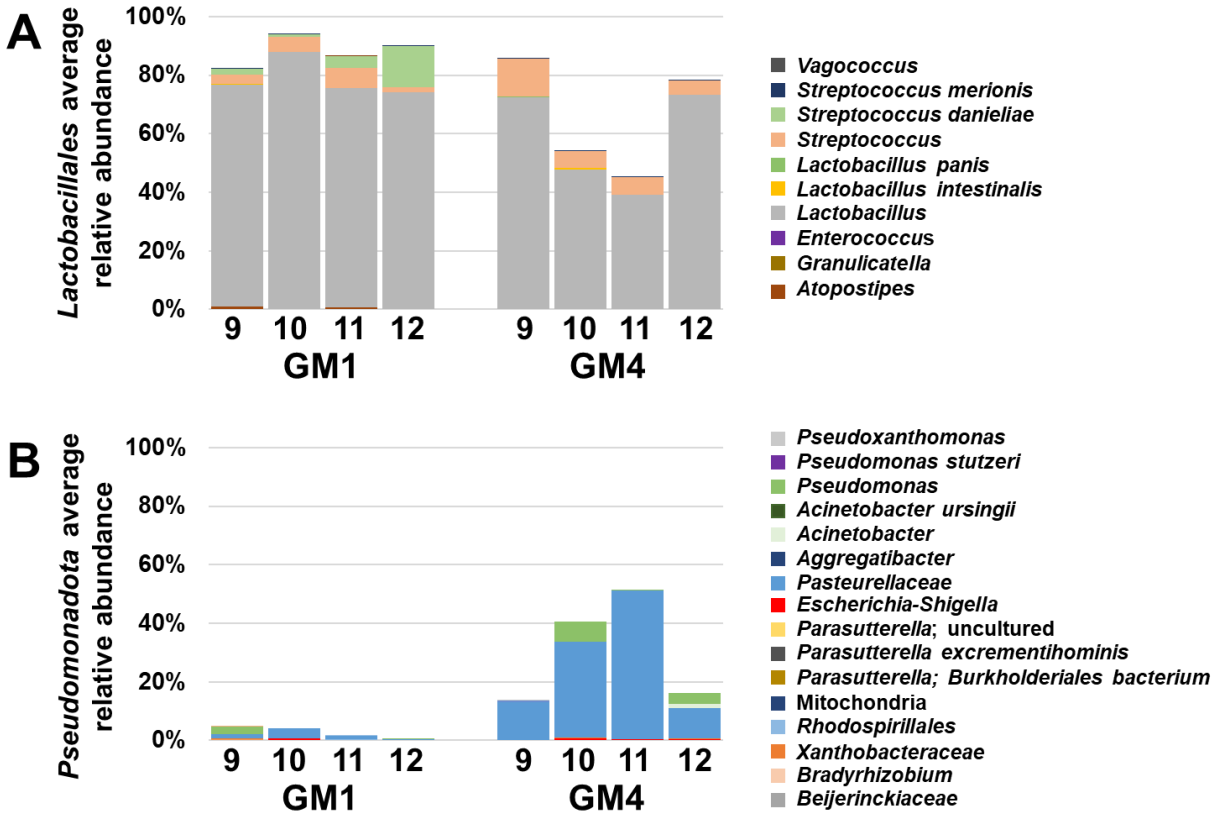

Supplemental Figure 3.2. GM specific ASV transfer from maternal source to pup ileum is observed. (A) Bar charts depicting the average proportion of taxa annotated to *Lactobacillales* from pup ileal samples grouped by GM and age of pups. Figure key is located on the right side of panel. **(B)** Bar charts depicting the average proportion of ASVs annotated to *Pseudomonadota* from pup ileal samples grouped by GM and age of pups. Figure key is located on the right side of panel.

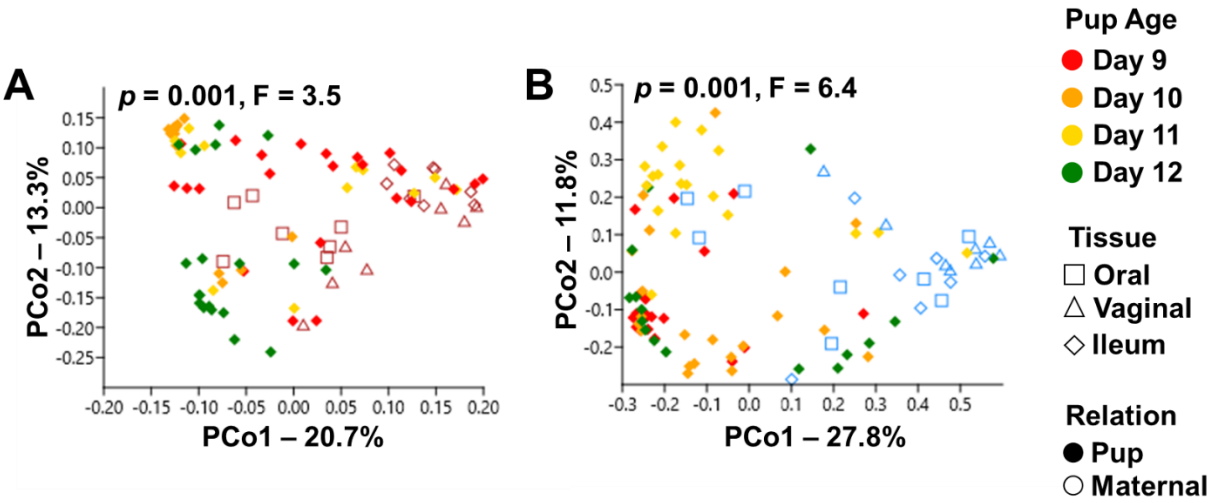

Supplemental Figure 3.3. Developing ileal microbiota closer in composition to maternal oral microbiota than vaginal microbiota. Principal coordinate analysis (PCoA) graphs depicting beta diversity using Bray-Curtis similarities. Figure key to the right side of panel. Pup ileal samples with maternal oral, vaginal, and ileal samples from GM1 **(A)** and GM4 **(B)** mice. Statistics were calculated using a one-factor PERMANOVA within each GM.

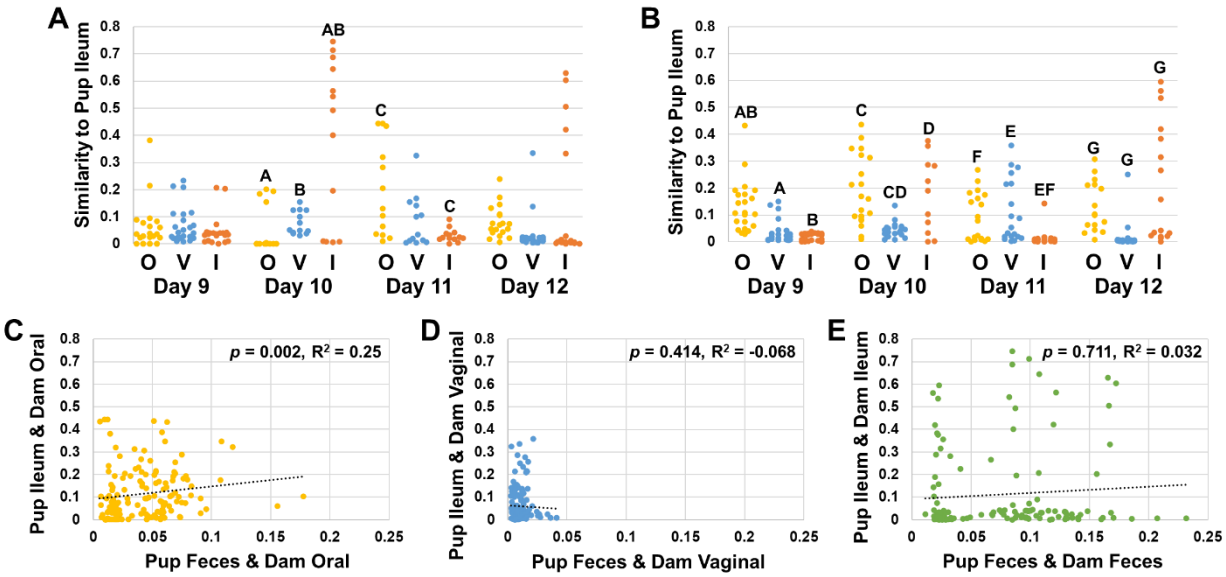

Supplemental Figure 3.4. Neonatal similarity to maternal oral tissue correlates the highest between both GI locations. (A-B) Bray-Curtis similarity of pup ileal sample to the maternal tissue from the dam that birthed the pup, within **(A)** GM1 or **(B)** GM4 colonies. Statistics were calculated within each GM using a Two-way ANOVA on the factors tissue type and age of pups. (C-E) Dot plots depicting the correlation of each pup's fecal versus ileal Bray-Curtis similarity for each maternal tissue source. Statistics were determined using a spearman correlation analysis and located in the right corner of each graph. **(C)** Pup fecal and ileal similarity to maternal oral tissue. **(D)** Pup fecal and ileal similarity to maternal vaginal tissue. **(E)** Pup fecal similarity to maternal feces versus pup ileal similarity to maternal ileal samples. O- Oral, V- Vaginal, F- Fecal.

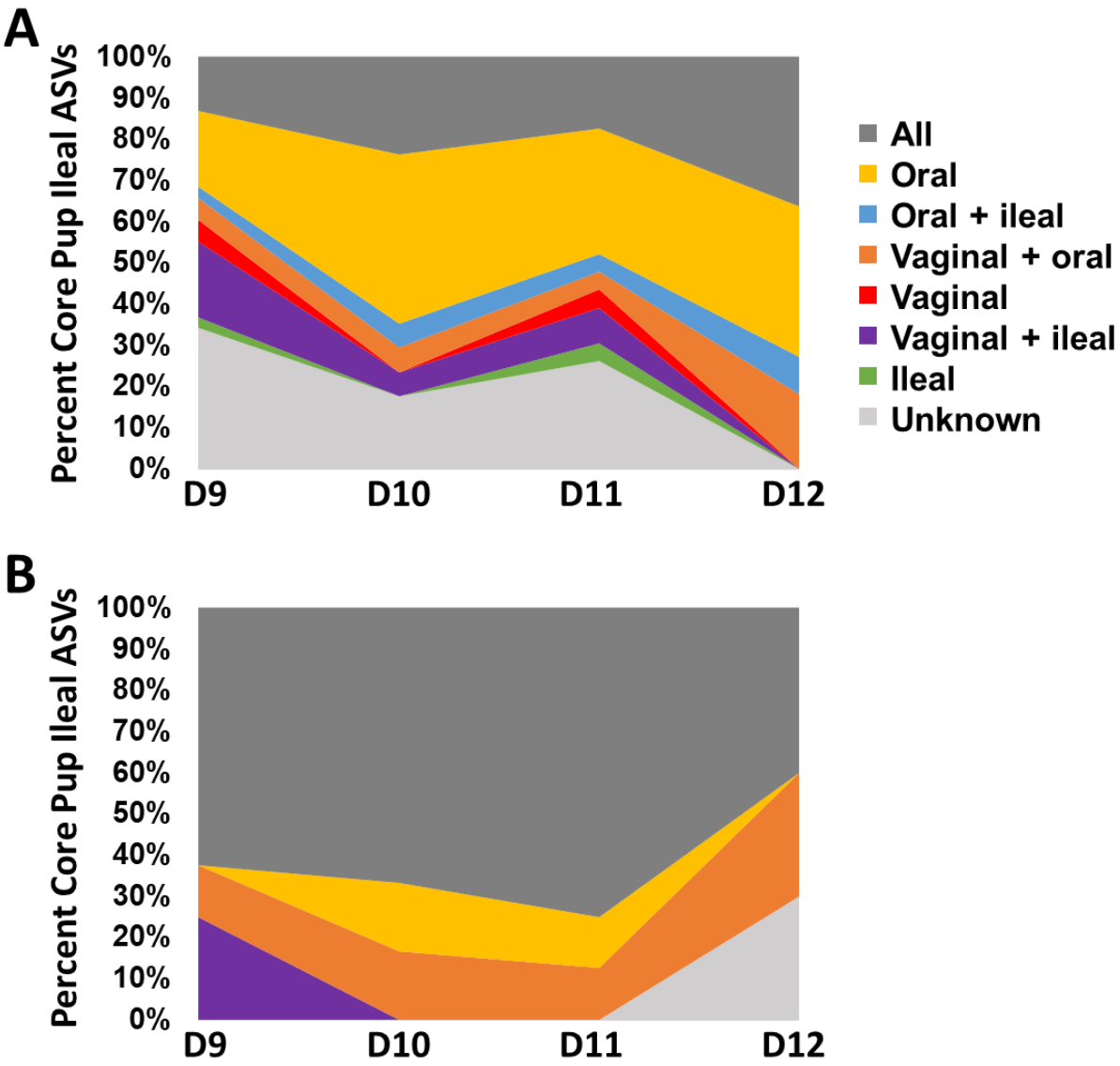

Supplemental Figure 3.5. Neonatal and maternal ileal core GMs share little to no unique ASVs with each other. Area graph depicting the proportion of amplicon sequence variants (ASV)s found in the pup ileal core microbiota at each timepoint, that are also found in maternal tissue core microbiota. Figure key is located to the right of the panel. **(A)** GM1 pup ileal core microbiota and, **(B)** GM4 pup ileal core microbiota.

CHAPTER 4 – THE GUT MICROBIOTA AND TARGETED PATHOBIONT EXPOSURE ALTERS TYPE 1 DIABETES PHENOTYPE IN NON-OBESE DIABETIC MICE

Introduction

Type 1 diabetes (T1D) is a chronic autoimmune disease that affects 1.9 million of Americans. The prevalence of T1D within the United States is dramatically increasing, as much as 30% from 2017 to 2020[143], thus there is an urgency to gain a more comprehensive understanding in hopes of developing new screening, mitigation, and therapeutic strategies. Disease onset is marked by infiltration of immune cells into the pancreatic islets of Langerhans, and subsequently attacking insulin producing beta cells within the islets, eventually leading to a complete loss of insulin production[144]. The exact etiology of T1D is not completely understood but current literature agrees that it is acquired through both genetic and environmental factors. Our current understanding is that genetics predispose individuals to the development of disease, but onset may be triggered by an array of environmental factors[145,146]. Various environmental factors have been attributed to contributing to the susceptibility of T1D, ranging from viral infections[147], maternal and neonatal antibiotic usage[148,149], cow milk consumption[150], metabolic profile of diet[151], and more. Seemingly, most environmental factors attributed to T1D susceptibility alter the gut microbiota (GM), and indeed, multiple studies in humans and animal models

of disease report that individuals with T1D have decreased GM diversity[152], increased intestinal permeability[153,154], and significant alterations of prevalent species within the GM from that of healthy individuals[155]. However, identifying a direct cause-and-effect relationship of specific environmental factors and T1D has been nearly impossible due to the complexity of genetic and environmental variability seen within the human population[156]. Thus, to better examine the intricate interactions of environmental factors on T1D development in a more controlled manner, animal models of T1D are utilized.

The Non-Obese Diabetic (NOD) mouse is the most utilized animal model of T1D due to its polygenetic inheritance of spontaneous insulin-dependent diabetes mellitus (IDDM), much like that seen in the human disease[156,157]. And although the utilization of the NOD mouse model has led to many new discoveries and therapies over its history, problems with the reproducibility of experimental outcomes using NOD mice have become evident over time[158,159]. NOD mice are notoriously susceptible to inter-institutional variability regarding T1D incidence and time of onset[158,159]. This has largely been attributed to environmental differences like diet[160,161], bedding[60,162], and many other colony husbandry factors [60,163]. These small changes over time converge and may result in a unique GM background. Yet these factors are markedly under-reported in the literature and poorly considered during experimental design, leading to conflicting experimental results between mouse colonies[158,163].

Additionally, there is evidence that single species of organisms can dramatically alter the survival of NOD mice colonies, such as segmented filamentous bacteria (SFB) and Murine Hepatitis Virus (MHV), which has been reported to ameliorate the T1D phenotype of NOD mice[56,162], and *Helicobacter hepaticus*, which reportedly decreases T1D prevalence[164]. To further complicate matters, there is a documented sex difference in disease prevalence between male and female mice within the same colony[165]. Male mice experience a lower incidence of disease and therefore go underutilized in experiments. However, studies that do utilized both sexes have reported that antibiotic treatment can intensify or reduce this sex-based difference in T1D[166], likely through a GM dependent mechanism[167]. Thus, not consistently utilizing male NOD mice and neglecting to develop experiments utilizing mice harboring various background GMs has limited our understanding of how GM composition and sex interact within NOD mice, and the subsequent effect it has on T1D development.

This study aimed to assess the effects of sex, background GM, and experimental inoculation of specific pathobionts, in combination, on the development and severity of T1D in NOD mice to gain a better understanding of how these factors interact to affect T1D outcome. To this means, two cohorts of NOD mice were utilized: to assess diabetes onset, one cohort was aged until up to 52 weeks to assess animal with disease, and the other cohort aged until 16 weeks to assess pre-diabetic changes. Mice harbored either a low richness GM, designated as GM1 and originating

from mice from the Jackson Laboratories, a high richness GM, designated as GM4 and originating from mice from Envigo, or GM1+SFB, the low richness GM1 mice that also harbored SFB. Mice were inoculated at 4 weeks of age with either a sham inoculum, *Helicobacter hepaticus,* an enterotropic strain of Murine Hepatitis Virus (MHV), *or* dual inoculation of *H. hepaticus* and MHV. This was in order to assess the effects of agents that are often removed from the GM of laboratory mice. *H. hepaticus is* a commensal bacteria found in laboratory and wild mice[169,170] and was chosen for inoculation due to its role as a provocateur of intestinal inflammation[168]. MHV is a virus that is clinically silent in immunocompetent mice[171,172] and is also a common commensal organism in wild mice[170]. Two cohorts of mice were utilized, one cohort was aged for 16 weeks and the other for 52 weeks to look at both pre-diabetic and diabetic disease development respectively. Mice were monitored for hyperglycemia bi-weekly using a glucometer starting at 10 weeks of age and euthanized if blood glucose levels (BGL) were ≥300 mg/dL for two consecutive days, BGLs of mice on the 52-week study were also collected at the time mice were put on study. Fecal samples were collected pre-inoculation and fecal and cecal samples were collected at euthanasia for 16S rRNA sequencing analysis to evaluate GM compositional changes. Pancreata were collected and scored for insulitis to assess disease severity, and survival time was used to determine differences in T1D incidence and onset. Study was designed to test the hypothesis stated that 1.) GM4 and GM1+SFB mice

would develop less T1D and score lower for insulitis than GM1 mice, 2.) *H. hepaticus* would increase disease incidence compared to control, 3.) MHV would decrease disease incidence, and 4.) male and female mice would react differently to colonization of SFB.

Methods

Colony Establishment

Male and Female genetic founder NODShiLt/J mice were provided by CL from Jackson Laboratories and allowed to acclimate for 1 week. After acclimation these mice were then cohoused as breeding pairs/trios and mated. Complex microbiota targeted rederivation was then performed by the University of Missouri Mutant Mouse Resource and Research Center as described previously[57]. Briefly, NODShiLt/J embryos were transferred into CD-1 surrogate dams harboring either a GM1 or GM4 microbiota. The resulting offspring were subsequently bred to generate NOD colonies harboring both complex microbiotas. A subset of NOD GM1 mice were inoculated via gastric gavage with 100 uL of SFB inoculum at 3-4 weeks of age. SFB inoculum was isolated utilizing a previously published method[173]. These inoculated mice were then bred to produce offspring harboring SFB at birth to create a NOD GM1+SFB colony. Feces from randomly selected mice were screened to ensure that colonization of SFB was established.

Mice

All experimental mice were randomly assigned to a pathobiont group and inoculated via gastric gavage at 3-4 weeks of age. Each of the 3 GMs used had 4 pathobiont groups (sham, *H. hepaticus*, MHV, *H. hepaticus* + MHV), equating to 12 unique groups. For the 52-week study 16 mice, (8 males and 8 females) were used for each pathobiont group equating to a total of 192 mice (n = 16 mice [8M, 8F] per pathobiont group × 12 groups). Five mice were removed from the study due to poor health without hyperglycemia and were excluded from analysis (total n = 187). For the 16-week experiment, 24 mice, 12 males and 12 females were used for each pathobiont group equating to a total of 288 mice (n = 24 mice [12M, 12F] per pathobiont group × 12 groups). Five mice were excluded from analysis due to hyperglycemic onset prior to 16-weeks (total n = 283).

To avoid cross-contamination and maintain biosecurity MHV-inoculated mice were housed in a separate facility from MHV-free mice; however, both groups were maintained with the same housing, bedding and diet. All mice were housed in microisolator cages on individually ventilated cage-racks (Thoren, Hazleton, PA), filled with autoclaved compressed paper (Paperchip Brand Laboratory Animal Bedding, Shepherd Specialty Paper) with ad libitum access to autoclaved rodent chow (BreederDiet 5058 Purina) and water, under a 12:12 light/dark cycle. The cages contained a nestlet for enrichment and 4 mice per cage. The water source differed between facilities with MHV-free and colony mice receiving autoclaved

sulfuric acid acidified water and MHV-inoculated mice receiving autoclaved HCl acidified water.

Experimental Inoculum

All mice were inoculated via gastric gavage at 3-4 weeks of age. Control mice were inoculated with 500 uL of autoclaved sterile Brucella broth as a sham inoculum. Mice selected for *H. hepaticus* and MHV+ *H. hepaticus* groups were administered 500 uL of *H. hepaticus* inoculum. This *Helicobacter hepaticus* strain, MU-94, was cultured using methods described previously[174]. After *H. hepaticus* inoculation, mice in the MHV+ *H. hepaticus* group were then transferred to a pathogen containment facility and inoculated with MHV the following day. Feces were collected from all mice inoculated with *H. hepaticus* two weeks post-inoculation to confirm colonization via PCR. MHV and MHV+ *H. hepaticus* mice were inoculated with MHV via gastric gavage of 100 uL DMEM containing MHV (2×10^5 pfu) obtained and cultured by Greg Purdy at IDEXX BioAnalytics (Columbia, Missouri) using a method previously described[175].

Blood Glucose Monitoring

Starting at 10 weeks of age, NOD study mice blood glucose levels were monitored bi-weekly for the remaining duration of the experiment. Mice were bled via saphenous vein while restrained in a decapicone and blood glucose levels were measured using an AlphaTRAK 2 Blood Glucose Monitoring System Kit using code 91. Two separate devices were calibrated and used at each facility where mice were held. For the 52-week study,

blood glucose levels were recorded at 3-4 weeks of age before receiving assigned inoculation. For both studies, if an animal measured 300 mg/dL or higher, it was again tested the following day and if levels remained elevated for two consecutive days, the animal was considered diabetic and humanely euthanized via inhaled carbon dioxide followed by cervical dislocation as a secondary method, in accordance with the AVMA Guidelines for the Euthanasia of Animals: 2013 Edition or 2020 Edition, depending on euthanasia date. Post euthanasia blood was collected by cardiac stick where approximately 0.4-0.6 mL of blood was collected and placed into a BD Microtainer® gold top SST. The tube was then placed on a blood sample oscillator for 30 minutes to allow blood to clot, then centrifuged at 10000 RPM for 5 minutes and serum was collected and placed into a 1.5mL Eppendorf tube for storage at -80˚ C. A subset of high-quality serum samples later submitted to IDEXX BioAnalytics where serum BGL was quantified. These measurements were compared back to BGL measurements taken from the glucometer and confirmed high agreement between methods of measuring BGL.

Sample Collection

One to two freshly evacuated fecal pellets were collected from mice immediately prior to inoculation at 3-4 weeks of age, and again two weeks post inoculation for *H. hepaticus*-inoculated mice. For collection, each mouse was place into a clean bedding-free microisolator cage in a class II biological safety cabinet and allowed to defecate. Fecal pellets were

collected with sterile toothpicks and transferred into 2.0 mL Eppendorf tubes with steel BBs and immediately placed on ice. For terminal collection, the most aboral fecal pellet was collected from the distal colon or rectum.

Cecal contents were collected from all mice post-euthanasia by creating a small incision at the tip of the cecum and squeezing contents from cecum directly into a sterile 2.0 mL Eppendorf tube containing a steel BB and immediately placed on ice. Whole pancreas was then removed and placed directly into a histological cassette and fixed in 10% neutral-buffered formalin for at least 24 hours. Pancreata were then submitted to IDEXX BioAnalytics for sample processing and H&E staining.

Insulitis Scoring

H&E-stained pancreata slides were analyzed by a trained veterinary pathologist (ALR) who was completely blinded to all categorical data of subjects. A slide for each subject was analyzed and each islet on an individual slide was scored for insulitis on a scale from 0-4 with a previously validated scoring system as followed: 0 – No insulitis, 1 – mild peri-insulitis, 2— peri-insulitis, 3—moderate intra-insulitis, 4—severe insulitis[176]. The overall score for each slide was calculated by taking the median of all insulitis scores for that slide. An independent observer who was also completely blinded confirmed all scores.

DNA Extraction

16-week study fecal and cecal samples were extracted using PowerFecal kits (Qiagen) and 52-week study fecal and cecal samples were

extracted using PowerFecal Pro kits (Qiagen). This difference in kit utilization was due to the availability of the kits from the manufacturer, as PowerFecal kits were discontinued between when study samples were extracted. DNA was extracted according to the manufacturer's instructions for the DNA extraction kit used, with the exception that samples were homogenized in 2.0 mL tubes containing a steel BB using a TissueLyser II (Qiagen, Venlo, Netherlands) for 10 minutes at 30/sec rather than utilizing the vortex adapter described in the manual protocol. Sample DNA was eluted in 100 uL of elution buffer (Qiagen) and DNA yields were quantified with fluorometry (Qubit 2.0, Invitrogen, Carlsbad, CA) via the quant-iT BR dsDNA reagent kits (Invitrogen) and normalized to a uniform concentration and volume before submission for sequencing.

Inoculation Confirmation

Two-week post *H. hepaticus* inoculation, fecal samples were collected from *H. hepaticus* and MHV + *H. hepaticus* inoculated mice. Fecal DNA was then extracted, and PCR was performed to ensure *H. hepaticus* presence in feces. For the 16-week samples, colonization was confirmed by PCR using a previously established protocol with primers specific for *H. hepaticus*[177]. For the 52-week samples, fecal DNA were submitted to IDEXX BioAnalytics for PCR confirmation of presence of *H. hepaticus* using the same primers and protocol. The difference in PCR processing was due to workload during the 52-week study, where analysis needed to be outsourced for timely results. Mice that were found to be negative for *H.*

hepaticus via PCR post-inoculation were removed from study. Eight *H. hepaticus* inoculated mice were removed from the 16-week study for being devoid of *H. hepaticus* (total n = 275).

Infection with MHV was confirmed via serology analysis. A single terminally collected serum sample was chosen at random to represent each cage, and a cage was considered positive if at least one mouse per cage tested positive for MHV. These randomly selected samples were submitted to IDEXX BioAnalytics for serologic analysis. For mice not inoculated with MHV, sentinel mice were utilized to monitor for MHV presence.

Colonization of SFB was confirmed via PCR analysis of pooled DNA from feces collected at the pre-inoculation timepoints for both studies. Samples were pooled by cage after DNA extraction, where sample DNA concentration was diluted to equally represent each animal in the cage at a concentration of 20 ng/uL. Pooled samples were submitted to the University of Missouri Metagenomic Center for PCR analysis, and all mice regardless of background GM were tested.

16s rRNA library preparation and sequencing

Extracted mouse fecal and cecal DNA were processed at the University of Missouri Genomic Technology Core Facility. Bacterial 16S rRNA amplicons were constructed by amplifying the V4 region of the 16S rRNA gene with universal primers (U515F/806R) flanked by Illumina standard adapter sequences using previously described methods[130,131]. Oligonucleotide sequences are stored for reference at proBase[178]. Forward

and reverse dual-indexed primers were using in all reactions. PCR reactions were performed at a volume of 50 uL and contained 100 ng metagenomic DNA, primers (0.2 uM each), dNTPS (200 uM each), and Phusion high fidelity DNA polymerase (1U, Thermo Fisher). Parameters for amplification were $98°C^{(3\ min)} + [98°C^{(15\ sec)} + 50°C^{(30\ sec)} + 72°C^{(30\ sec)}] \times 25$ cycles $+ 72°C^{(7\ min)}$. Amplicon pools at 5 uL/reaction were combined by thorough mixing and subsequently purified by adding Axygen Axyprep MagPCR clean-up beads to an equal volume of 50 uL and incubated at room temperature for 15 minutes. After purification, products received multiple washes of 80% ethanol and the dried pellet was resuspended in 32.5 uL EB buffer (Qiagen), incubated at room temperature for two minutes, and then placed on a magnetic stand for five minutes. The final amplicon pool was then evaluated using the Advanced Analytical Fragment Analyzer automated electrophoresis system, quantified using quant-iT HS dsDNA reagent kits, and finally diluted according to Illumina's standard sequencing protocol as 2x250 bp paired-end reads on the MiSeq instrument.

Informatics analysis.

Fecal and cecal DNA sequences were assembled and annotated at the University of Missouri Bioinformatics and Analytics Core Facility. Cutadapt[179] (https://github.com/marcelm/cutadapt) was used to removed primers, that were designed to match the 5' ends of the forward and reverse reads, from the 5' end of the of the forward read. Then, if found, the reverse complement of the primer to the reverse read was removed from the forward

read as were all bases downstream. This allowed a forward read to be trimmed at both ends if the insert was found to be shorter than the amplicon length. The same approach was repeated on the reverse read, but with the primers in the opposite roles. Read pairs were rejected if both pairs did not match a 5' primer, and an error-rate of 0.1 was allowed. Two passes over each read were made to ensure removal of the second primer. For removal of the primer sequence from the 3' end a minimal overlap of three bp was required.

The QIIME2[180] DADA2[181] plugin (version 1.18.0) was used to denoise, de-replicate, and count ASVs (amplicon sequence variants), incorporating the following parameters: 1) forward and reverse reads were truncated to 150 bases, 2) forward and reverse reads with number of expected errors higher than 2.0 were discarded, and 3) chimeras were detected using the "consensus" method and removed. Python version 3.8.10 and Biom version 2.1.10 were used in QIIME2. Taxonomies were assigned to final sequences using the Silva v138[182] database, using the classify-sklearn procedure. For downstream analysis, data from both studies were rarified at a depth of 15954 sequence reads.

Metagenome pathway analysis

Rarefied 16S rRNA sequencing data obtained from cecal contents of NOD mice from the 16-week old cohort were utilized for prediction of metagenome function using the PICRUst2[183] version 2.5.0 algorithm. Data was separated by GM for each sex and analyzed independently. Phylogenic

placement of reads was handled by gappa[184] version 0.8.0 with the alternative placement option SEPP[185] version 4.5.1. The R library Castor[186] version 1.7.3 functions were utilized for hidden state phylogenetic predictions, and MinPath[187] version 1.4.0 was used for pathway inference.

Statistics

For analysis of T1D onset in the 52-week study, Kaplan-Meier log rank analyses were utilized to determine statistical differences between onset of pathobiont groups harboring each GM composition within male and female mice. Then, to determine the overall effect of sex, GM, and pathobiont on hyperglycemic onset, a Cox proportional hazard analysis was utilized. All statistics for T1D onset were generated using SigmaPlot 13.0.0, and graphs were generated using the R package ggplot2[188] version 3.3.6.

Statistics for insulitis scores of mice from the 16-week cohort were calculated using a three-factor (sex, GM and pathobiont) analysis of variance (ANOVA) using R package rstatix[189] version 0.7.0. Holm-Sidak pairwise comparisons for pathobiont groups were generated using the R package emmeans[190] version 1.8.0.

Bray-Curtis distribution matricies were generated first for male and female 16-week NOD mouse from pre-inoculation fecal samples and terminal cecal content 16S rRNA sequencing data. One-way Permutational Multivariate Analysis of Variance (PERMANOVA)s were used to determine significance of GM and collection timepoint on beta diversity, and Bray-

Curtis post *hoc* analyses with Bonferroni adjustments were utilized to determine pairwise differences. Next, Bray-Curtis distributions and PERMANOVAs for pathobiont differences within each GM for male and female mice were utilized following the same statistical procedure. One-way PERMANOVAs were computed using the R package vegan[191] version 2.6.2, and pairwise comparison were generated with the R package ecole version 09-2021[192]. Principle coordinate analysis (PCoA)s graphs generated from Bray-Curtis distributions with the cailliez adjustment method via R package ape[193] version 5.6.2.

PICRUst2 metagenome pathway predictions were analyzed for significant differences between pathobiont groups within each GM and sex by utilizing a nested ANOVA on ranks test followed by a Dunn's post *hoc* with Benjamini-Hochberg corrections for pairwise comparison of pathobionts. The R package stats[194] version 4.2.1 was used to calculate these statistics.

Results

Hyperglycemic onset is driven by interactions between sex, GM, and pathobiont

The first aim was to determine if inoculation of NOD mice with pathobionts significantly altered hyperglycemic onset within a 52-week study. Kaplan-Meyer survival curves and log-rank tests were utilized to determine if there was an overall difference between pathobiont groups

within GMs for each sex. Analysis found no significant differences during long-rank analysis between pathobiont groups within female mice for GM1 (**Figure 4.1A**), GM1+SFB (**Figure 4.1B**), or GM4 (**Figure 4.1C**); and, for male GM1 mice (**Figure 4.1D**). Log-rank analysis did find an overall significant difference between pathobiont group T1D incidence for male GM1+SFB mice (**Figure 4.1E**), and post-hoc analysis revealed significant pairwise differences between *H. hepaticus*-inoculated mice and both MHV ($t = 13.9$, $p < 0.001$) and MHV + *H. hepaticus* ($t = 11.3$, $p = 0.004$)-inoculated mice, where *H. hepaticus* had significantly higher incidence of T1D. A significant log-rank analysis was also found within male GM4 mice and post-hoc analysis again found that *H. hepaticus*-inoculated mice had significantly higher incidence of T1D than MHV-inoculated mice ($t = 8.2$, $p = 0.037$).

To determine the overall effect of each factor on T1D incidence independently a Cox Proportional Hazards Regression Analysis was used (**Supplemental Figure 4.1**). Analysis found mice inoculated with *H. hepaticus* had significantly higher Wald Chi-squared statistic, and therefore a higher T1D incidence than both control ($\chi = 5.3$, $p = 0.021$) mice and MHV ($\chi = 12.2$, $p < 0.001$) inoculated mice. For differences between background GM composition, mice harboring a GM1 background had a higher incidence of T1D than either GM1+SFB ($\chi = 8.0$, $p = 0.005$) or GM4 ($\chi = 12.4$, $p < 0.001$) mice. As expected, female mice had significantly higher incidence of T1D than male mice ($\chi = 43.1$, $p < 0.001$).

H. hepaticus monoinoculation drives insulitis severity

To better understand how inoculation with various pathobionts affects disease development prior to hyperglycemic onset, insulitis severity was determined in a cohort of NOD mice at 16-weeks of age through histological scoring of individual islets for lymphocytic infiltration on a scale from 0-4, and a median score of all islets for each animal was given to represent overall insulitis severity in that mouse. A score of 0 represents no insulitis (**Figure 4.2A**), 1 represents mild peri-insulitis (**Figure 4.2B**), 2 represent moderate peri-insulitis (**Figure 4.2C**), 3 represent moderate insulitis (**Figure 4.2D**), and 4 represent severe insulitis (**Figure 4.2E**)[176]. Statistics were calculated using a 3-way ANOVA for the factors sex, GM, and pathobiont. Analysis of scores found a main effect of sex ($F = 24.1$, $p < 0.001$) and pathobiont ($F = 2.7$, $p = 0.046$) and interactions of sex, GM, and pathobiont ($F = 3.2$, $p = 0.005$). Specifically, analysis found that mice-inoculated with MHV regardless of GM or sex, had lower insulitis scores than *H. hepaticus*-inoculated mice ($t = 2.8$, $p = 0.031$). Next, to better analyze the effect of individual factors, pairwise comparisons of pathobiont groups were determined for insulitis scores of female and male mice within each GM background. Within female mice, there was no significant difference between pathobiont groups for either GM1 (**Figure 4.2F**) or GM1+SFB (**Figure 4.2G**). Within female GM4 mice (**Figure 4.2H**), MHV-inoculated mice had significantly lower insulitis scores than either control ($t = 2.7$, $p = 0.043$) or *H. hepaticus*-inoculated mice ($t = 3.1$, $p = 0.014$). For male mice, there was a significant pathobiont difference detected within

GM1 (**Figure 4.2I**), where *H. hepaticus*-inoculated mice developed higher insulitis scores than control mice (t = 2.6, p = 0.041), MHV inoculated mice (t = 3.3, p = 0.001) and MHV+*H. hepaticus* inoculated mice (t = 3.0, p = 0.014). There were no significant differences detected between pathobiont groups for male mice within either GM1+SFB (**Figure 4.2J**) or GM4 (**Figure 4.2K**).

Pathobiont inoculation alters cecal content beta diversity

To determine if inoculation with pathobiontss was associated with an altered gut microbiota composition, principal coordinate analyses (PCoAs) were utilized to visualize changes in Bray-Curtis beta diversity. For female mice, a PCoA examining all samples collected at each timepoint was visualized (**Figure 4.3A**). This revealed that beta diversity differed depending on GM present (F = 167.46, p = 0.010), with a significant difference between all three GM compositions, and between collection timepoints (F = 14.01, p = 0.001). Then, to examine changes in beta diversity related to pathobiont, PCoAs for pathobiont groups within each GM were generated for terminal cecal contents. For female mice within GM1 (**Figure 4.3B**), GM1+SFB, (**Figure 4.3C**), and GM4 (**Figure 4.3D**) PERMANOVAs revealed overall significant differences between pathobiont groups for all GMs analyzed (GM1: F = 4.01, p = 0.001; GM1+SFB: F = 4.39, p = 0.001; GM4: F = 2.69, p = 0.001). Within female GM1, *H. hepaticus* inoculation, alone (F = 4.78, p = 0.006) or in combination with MHV (F = 5.50, p = 0.018), significantly altered beta diversity compared to control

mice (**Figure 4.3B**), however, inoculation of MHV alone did not alter beta diversity from control (F = 2.33, p = 0.072). For female mice harboring GM1+SFB (**Figure 4.3C**), all pathobiont groups significantly differed from control (*H.hep*: F = 6.12, p = 0.006; MHV: F = 2.89, p = 0.030; MHV+*H.hep*: F = 5.18, p = 0.006). Inoculation of GM4 females (**Figure 4.3D**) with *H. hepaticus* alone (F = 3.59, p = 0.018) or in combination with MHV (F = 3.33, p = 0.006) significantly altered beta diversity compared to control, similar to GM1 females, and again MHV inoculated mice did not significantly affect beta diversity compared to control females (F = 1.96, p = 0.108).

The beta diversity of male mice pre-inoculation fecal samples and terminally collected cecal contents were also visualized via PCoA (**Figure 4.3E**). Within female mice, GM background composition separated along principal component 1 (F = 153.92, p = 0.001), and all GMs had significantly different beta diversity during post *hoc* analysis. The beta diversity between collection timepoints also varied significantly (F = 16.82, p = 0.001) and visually separated out on principal component 2 of the PCoA. Next analyzed was beta diversity of male terminal cecal contents between pathobiont groups within each GM. PERMANOVA found alterations in beta diversity based on pathobiont groups for GM1 (**Figure 4.3F**), GM1+SFB (**Figure 4.3G**), and GM4 (**Figure 4.3H**). When pathobiont groups beta diversities were analyzed via pairwise comparison, analysis found that there was a significant difference between all pathobiont groups, for all three GM compositions.

Colonization with *H. hepaticus* mediates predicted changes in metabolic function

Next, to determine if pathobiont group differences in 16S rRNA sequencing were associated with changes in predicted metabolic pathways, the PICRUst2 pipeline was utilized. PICRUst2 generated read counts for each ASV associated predicted pathway using 16S rRNA sequencing results. Data were analyzed for pathobiont groups differences within each GM for both female and male mice. Significant differences in predicted pathway read counts were determined for each analysis, and pathways that were significantly and consistently enriched were identified. The eight pathways included the TCA cycle IV (Helicobacter), 2-methylcitrate cycle I, ADP-L-glycero-β-D-*manno*-heptose biosynthesis, demethylmenaquinol-6 biosynthesis II, 2-methycitrate cycle II, Photorespiration I, ppGpp metabolism, and reductive TCA cycle I. Analysis found the GM1 female (**Figure 4.5A**) and GM1 male (**Figure 4.5B**) had the greatest variation in pathobiont associated pathways compared to GM1+SFB and GM4 male and female data (**Supplemental Table 4.1**). Of the 8 consistently significant pathways detected, 5 pathways had consistent differences in pathobiont groups during pairwise comparison: TCA cycle IV (Helicobacter), 2-methylcitrate cycle I, demethylmenaquinol-6 biosynthesis II, 2-methycitrate cycle II, and ppGpp metabolism. Of these, predicted pathways associated with control mice had significantly lower ASV associated read counts than MHV+*H. hepaticus*-inoculated mice for each analysis. Three pathways

consistently detected in control mice had significantly lower ASV associated read counts than *H. hepaticus* mice: 2-methycitrate cycle I, 2-methycitrate cycle II, and demethylmenaquinol-6 biosynthesis II.

Discussion

The pathological mechanisms responsible for T1D development are currently understood to involve both genetic and environmental factors. To better understand these factors that contribute to disease development, studies utilize animal models of disease, of which the NOD mouse model of disease is the most utilized for T1D research. However, NOD mice are a phenotypically variable model of T1D, leading to conflicting research findings and decreased translatability to humans. Our study aimed to address how previously suspected environmental drivers of phenotypic variability in the NOD mouse interact to affect NOD phenotypic outcome, and to provide insight to potential mechanisms of pathobiont driven T1D exacerbation for future studies. Our studies found that T1D severity is modulated by inoculation with pathobionts, particularly in male mice, and by background GM composition, particularly in female mice. Further, analysis revealed that pathobiont inoculation drove dysbiosis, and that this dysbiosis was associated with predicted changes in metabolic pathways.

The time of diabetic onset in NOD mice is highly variable, reportedly due to a variety of environmental factors. To assess how previously

speculated factors interact to effect NOD hyperglycemic onset, mice of both sexes were utilized, with differing GM background complexities, and these groups were inoculated with pathobionts reported to alter diabetic onset. After experimental inoculation mice were allowed 52 weeks to develop hyperglycemia, and disease onset was recorded (**Figure 4.1**). Results revealed that along with the long-established sex bias, that inoculation with *H. hepaticus* exacerbates disease onset. This was prevalent in the male mice, excluding GM1, and trended in females of all GMs. This corroborated the findings of a previous study by De Riva et al. that found their colony of NOD mice with a high incidence of T1D was colonized with *H. hepaticus*, while their low incidence colony was not[164]. The authors suggest that the male mice had more dramatic differences in onset between pathobiont inoculation due to their overall decreased susceptibility to T1D as compared to females, and thus a higher potential for changes in disease onset. In comparison, MHV inoculation tended to attenuate disease onset, again particularly in the male mice excluding GM1 (**Supplemental Figure 4.1**). This is consistent with a previous study by Wilberz et al. that reported a decreased incidence in NOD mice harboring MHV[56], however in contrast to Wilberz et al. findings', male mice were more affected than females in this study. Interestingly, when mice were colonized with both MHV and *H. hepaticus,* overall disease incidence was comparable to control mice. This highlights an example of the complexity and unpredictability of these select

pathobionts and their interaction with sex and background GM to mediated disease onset.

In T1D development of NOD mice, insulitis precedes hyperglycemic onset[195]. To determine if pathobiont exposure also altered T1D pathogenesis prior to hyperglycemic onset, insulitis severity was analyzed from a separate cohort of NOD mice at 16-weeks of age (**Figure 4.2**). Analysis found a significant effect of both sex and pathobiont on insulitis severity, and a significant interaction between sex, GM, and pathobiont. Here again we observed similar effects of pathobiont exposure consistent with the findings of hyperglycemic onset in the previous cohort, with *H. hepaticus* driving insulitis severity and MHV ameliorating insulitis. This contrasts with previous studies, which cited no difference in insulitis severity between NOD mice colonized with *H. hepaticus* and those devoid of *H. hepaticus*[164]. The authors speculate this discrepancy in findings may be due to differences in the background GM composition between studies, where SFB presence may be negating the negative effects of *H. hepaticus* in the de Riva et al. study, similar to what was observed in the GM1+SFB group, which were the only GM composition between males and females that did not experience a significant change in insulitis severity after pathobiont inoculation. Additionally, we are not aware of studies reporting MHVs effect on insulitis severity.

The presence of T1D is associated with significant changes in GM composition, termed dysbiosis, in both human T1D patients[152,155] and NOD

mice[145,196]. In this study pathobiont inoculation associated changes in beta diversity, a measurement used to determine dysbiosis, were identified in cecal samples collected terminally from our 16-week cohort (**Figure 4.3**). There was an overall effect of pathobiont inoculation in all GMs regardless of sex. Of interest, within the female mice, excluding those harboring a GM1+SFB background, sole inoculation of MHV did not alter beta diversity from that of control. In contrast, inoculation of *H. hepaticus*, with or without MHV inoculation, altered beta diversity from that of controls in mice of all GMs regardless of sex. These changes in beta diversity support previous findings that indicate *H. hepaticus* causes GM dysbiosis in immunologically susceptible mouse models[168,197]. In contrast, MHV has not been associated with gut dysbiosis within the literature, although the gut microbiota is often not analyzed in studies of the latter.

Development of T1D is associated with profound changes in metabolic function and protein metabolism[198]. To determine if pathobiont associated changes in beta diversity are also associated with changes in predicted host metagenomic function, PICRUSt2 was utilized. Analysis found changes in metabolic function associated with inoculation of *H. hepaticus*, with or without co-colonization with MHV (**Figure 4.4**, **Supplemental Table 4.1**), while MHV inoculation alone did not significantly alter most pathways from controls. Across the factors sex and GM, this *H. hepaticus* associated effect was most evident in male mice with GM1 background. Interestingly, the 8 metagenomic pathways that were

consistently different between pathobiont groups across both sex and GM were all pathways related to metabolic function such as biosynthesis of metabolites such as protein K^2, degradation of propionate, and TCA cycle regulation. These *H. hepaticus* associated changes in metabolism are consistent with reported literature in other immunocompromised models such as *H. hepaticus* inoculated Rag2$^{-/-}$ mice, which experience a downregulation of metabolites and changes in both the TCA cycle and short chain fatty acid production alongside exacerbation of disease[199]. Dysregulation of these same pathways have also been associated with T1D pathogenesis in previous studies, in both humans and NOD mice. For instance, dysregulation of the TCA cycle in NOD mice is associated with a pre-diabetic state[200]. It is therefore reasonable to conclude *H. hepaticus* associated perturbations in these mechanisms could therefore drive differences in T1D incidence and severity, although more research is needed to confirm these findings.

With regard to the role of MHV in these studies, it should be noted other environmental factors associated with differences in the facility where these mice were housed may also have contributed to phenotypic changes. While housing, bedding and diet were consistent, the methods of water sterilization differed as did husbandry staff. We have previously shown that water sterilization can result in subtle shifts in microbiota can occur, however it is unknown whether such small changes can impact model phenotypes[60]. Staff underwent appropriate measures to ensure that all

other husbandry and environment for these facilities were as similar as possible, but water purification methods remained out of the ability to control for. No significant compositional differences in beta diversity were found in the GM of mice housed at different facilities suggesting that the shifts in water purifications methods were insignificant (data not shown).

Due to the transient colonization of SFB prior to weaning, and the prevalence of SFB in the ileum rather than the colon[201], confirmation of SFB colonization was inconsistently detected in experimental mice with the available fecal samples. Therefore, GM1+SFB mice testing PCR negative for SFB were not removed from the study due to the lowered capacity to detect SFB within feces. However, the data collected from these mice showed significant changes in survival between GM1 and GM1+SFB colonies suggesting SFB was in fact present within the colony and was the driver of T1D onset differences between GM1 and GM1+SFB mice (**Supplemental Figure 4.1**).

It is to emphasize that PICRUst2[183] is not a tool for direct analysis of the metabolome or metagenomic function, but rather predicts potential differences in metagenomic function based on sequencing reads. This tool is useful for identifying potentially perturbed pathways, but additional metabolic driven studies are needed to confirm these differences. Further studies clarifying the mechanism in which *H. hepaticus* exacerbates T1D have potential to clarify the mechanism in which the gut microbiota and T1D development interact in the NOD model and could direct future research in

human T1D toward mechanistic inhibitors or other interventions to negate GM driven T1D development. The work described here supports that the NOD mouse model is variable, however with additional future research, scientists can harness this variability to improve overall translatability of the NOD model through manipulation of the GM to increase phenotypical similarity of the NOD model to human T1D incidence and severity.

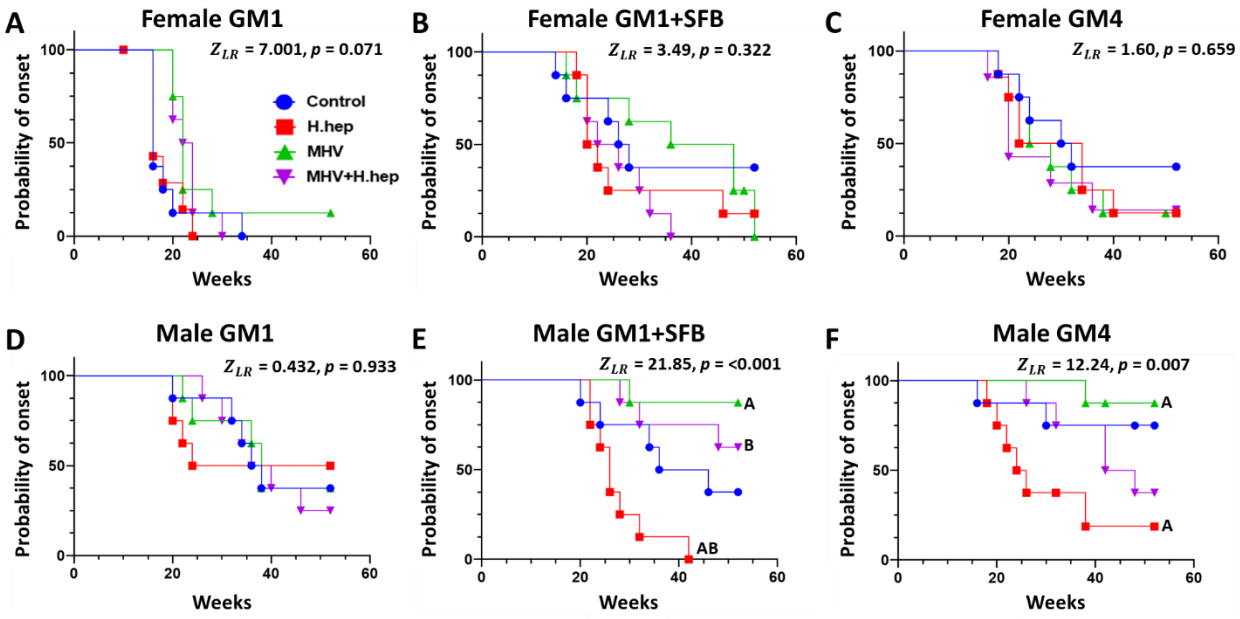

Figure 4.1. *Helicobacter hepaticus* drives T1D incidence. Kaplan-Meyer survival curves for incidence of type 1 diabetes over the course of 1 year (52 weeks). (A-C) Female mice harboring a GM background of **(A)** GM1, **(B)** GM1+SFB, and **(C)** GM4. Male mice harboring a GM background of **(D)** GM1, **(E)** GM1+SFB, and **(F)** GM4. Mice were considered diabetic after two consecutive blood glucose level reading of 300 mg/dL or higher. Statistics were generated using log-rank tests for each graph, and a Holm-Sidak post-hoc test was utilized to determine pairwise comparisons. Legend key overlaid on (A). *H.hep* – *Helicobacter hepaticus*, MHV+*H.hep* – dual inoculation of MHV and *H. hepaticus*

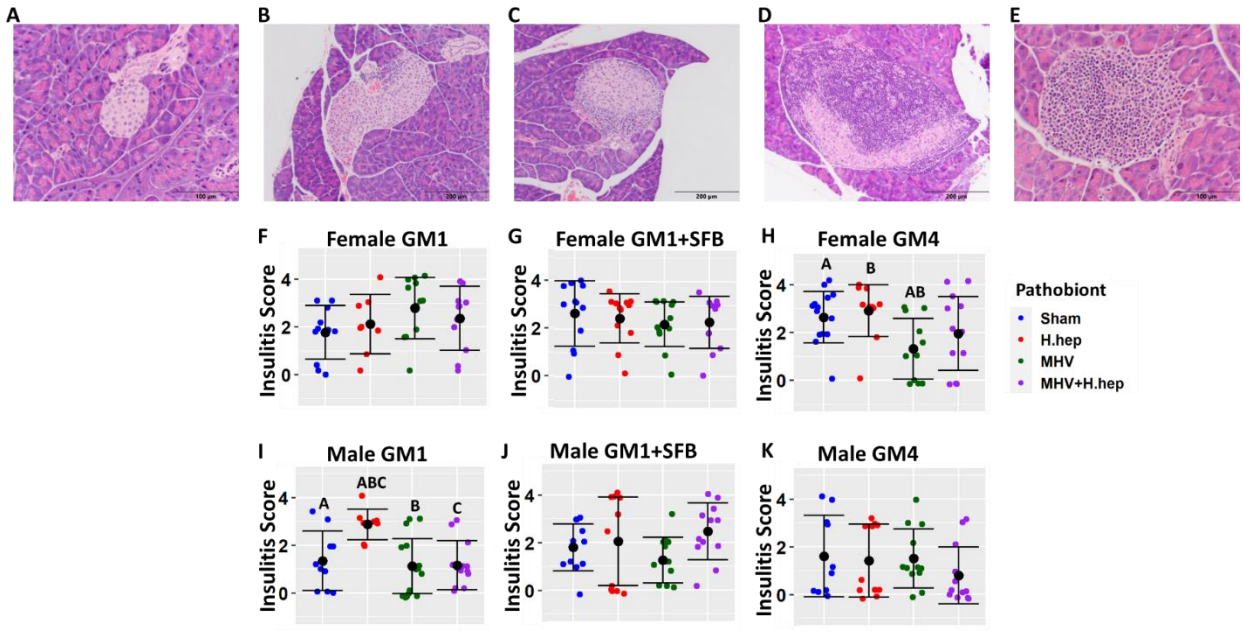

Figure 4.2. Insulitis severity is driven by interactions of sex, GM, and pathobiont inoculation. Pictural representation of insulitis scoring system utilized for quantification of insulitis from H&E histology slides (A-E). **(A)** Example of score 0 – No lymphocytic infiltration, **(B)** Example of score 1 – Mild peri-insulitis, **(C)** Example of score 2 – Peri-Insulitis, **(D)** Example of score 3 – Moderate insulitis, **(E)** Example of score 4 – Severe insulitis. Scales for each picture are overlaid on picture in lower right corner. Dot plot representing the overall insulitis scores of mice at 16-weeks on a 0-4 scale. (F-H) Female mouse insulitis scores within **(F)** GM1, **(G)** GM1+SFB, and **(H)** GM4. (I-K) Male mouse insulitis scores with **(I)** GM1, **(J)** GM1+SFB, and **(K)** GM4. Mean of groups depicted as black dots, error bars represent standard deviation or samples, legend key located to the right of figure. Scores analyze for significant interactions via a 3-factor (Sex, GM, Pathobiont) ANOVA with a Holm-Sidak post-hoc analysis for pairwise comparisons. Significant differences between pathobiont inoculated groups within each GM are designated with matching letters.

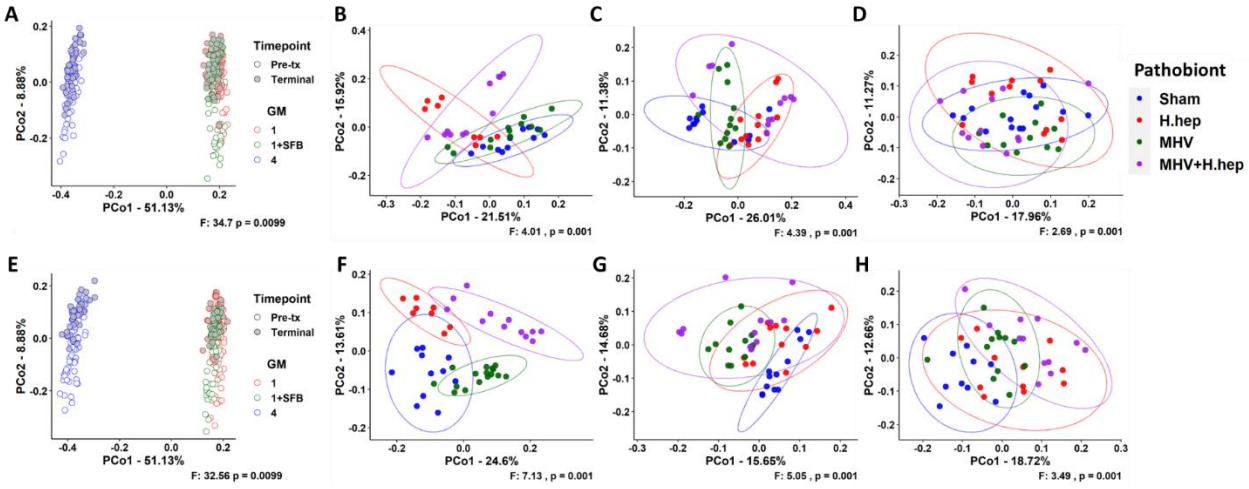

Figure 4.3. Pathobiont inoculation causes shift in beta-diversity. PCoA graphs depicting changes in sample beta diversity of 16-week-old NOD (A-D) female and (E-H) male mice. **(A)** pre-inoculation feces and terminal cecal content samples from female mice. Legend to right of graph. Terminally collected cecal content samples from females were visualized within each GM **(B)** GM1, **(C)** GM1+SFB, and **(D)** GM4. **(E)** pre-inoculation feces and terminal cecal content samples from male mice. Legend to right of graph. Terminally collected cecal content samples from males were visualized within each GM **(F)** GM1, **(G)** GM1+SFB, and **(H)** GM4. Legend for terminal graphs on right. Statistics were calculated using one-way PERMANOVAs.

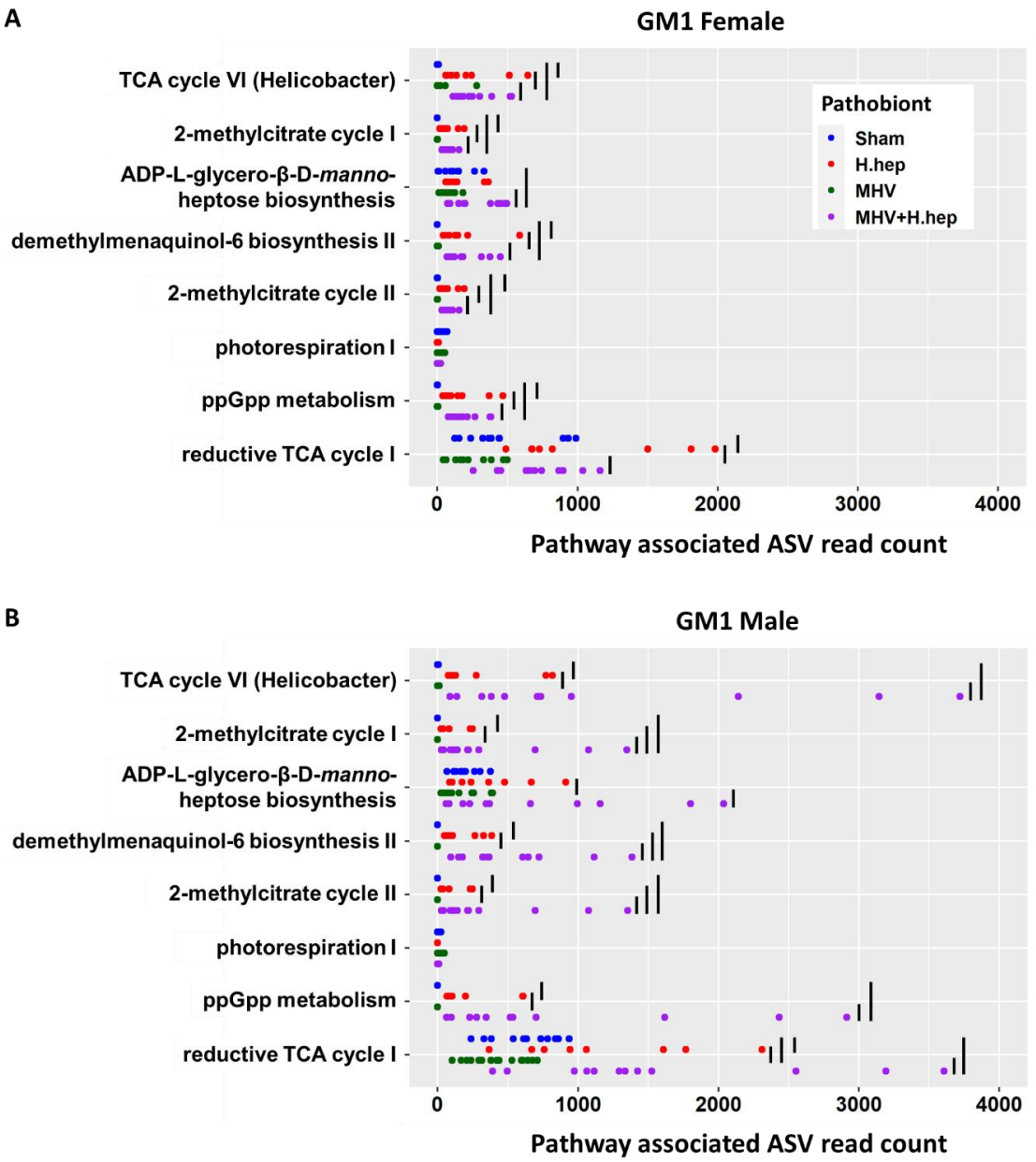

Figure 4.4. Inoculation of *H. hepaticus* alters predicted pathways. Metagenomic pathway associated ASV read counts of consistently differentially regulated pathways between pathobiont groups within cecal samples of **(A)** GM1 females and **(B)** GM1 males. Individual dots represent individual mice. Bars represent significant differences between groups as determined by a nested one-way ANOVA on ranks. Legend key overlaid on (A).

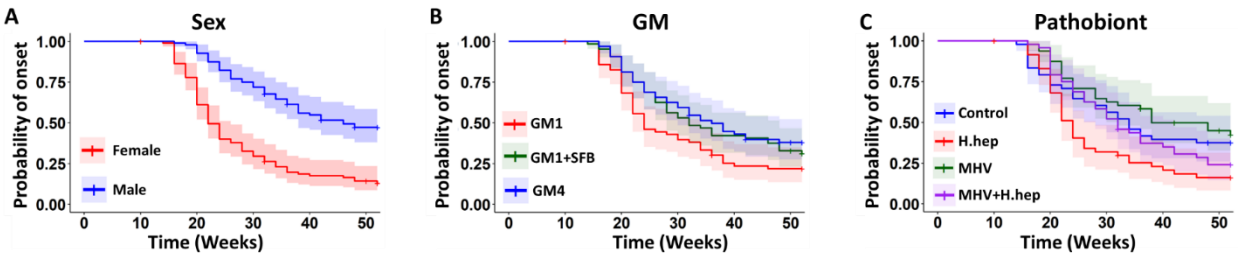

D

Factors	Reference	Comparison	Wald	P value	HR	95% CI
Sex	Female	Male	43.15	<0.001	0.29	0.20 - 0.42
GM	GM1	GM1+SFB	7.98	0.005	0.55	0.36 - 0.83
		GM4	12.37	<0.001	0.46	0.30 - 0.71
Pathobiont	H.hep	Control	5.33	0.021	0.57	0.35 - 0.92
		MHV	12.21	<0.001	0.41	0.25 - 0.68

Supplemental Figure 4.1. All factors significantly impact disease onset. (A-B) Kaplan-Meyer survival curves representing the univariate cox proportional hazards analysis on hyperglycemic onset of NOD mice from the 52-week cohort. Each factor was graphed: **(A)** Sex, **(B)** GM, and **(C)** pathobiont. Key for each graph is found overlaid on graph. Shading represents 95% confidence interval **(D)** Table representing the significant statistics generated via multivariate cox proportional hazards analysis. *H.hep* – *Helicobacter hepaticus*, MHV+*H.hep* – dual inoculation of MHV and *H. hepaticus*, Wald – Wald Chi-Squared test, P value – p value for Wald Chi-Squared test, HR – hazard ratio, 95% CI – 95% confidence interval for hazard ratio.

			Pathobiont Pathway Average RA			
pathway	**GM**	**Sex**	**Control**	**H.hep**	**MHV**	**MHV+H.hep**
TCA cycle IV (Helicobacter)	1	F	0.73	246.80	32.71	276.88
		M	1.15	299.31	1.09	1098.39
	1+SFB	F	1.46	441.05	0.00	286.18
		M	2.04	246.56	0.66	379.28
	4	F	1.75	109.16	2.91	158.81
		M	0.35	59.96	1.68	133.02
2-methycitrate cycle I	1	F	0.00	72.32	0.26	80.99
		M	0.00	89.65	0.00	363.94
	1+SFB	F	0.00	131.21	0.00	83.42
		M	0.00	72.34	0.14	112.77
	4	F	45.52	104.71	44.22	114.36
		M	17.92	71.71	18.19	113.56
ADP-L-glycero-β-D-*manno*-heptose biosynthesis	1	F	108.34	159.45	71.82	282.41
		M	212.85	377.54	133.78	689.92
	1+SFB	F	158.13	543.27	267.28	292.50
		M	176.00	425.04	117.69	345.89
	4	F	202.76	344.98	202.20	464.13
		M	112.07	298.87	95.35	369.58
Demethylmenaqionol-6 biosynthesis II	1	F	0.00	165.60	0.54	186.35
		M	0.00	167.86	0.00	521.19
	1+SFB	F	0.00	286.32	0.00	263.91
		M	0.00	203.22	0.00	376.03
	4	F	0.00	112.32	0.00	162.84
		M	0.00	63.11	0.00	129.57
2-methycitrate cycle II	1	F	0.04	72.37	0.24	81.18
		M	0.00	89.88	0.00	364.68
	1+SFB	F	0.00	131.28	0.00	83.45
		M	0.00	72.42	0.16	112.92
	4	F	45.58	104.81	44.30	114.51
		M	18.04	71.75	18.29	113.71
Photorespiration I	1	F	18.83	0.99	20.78	3.60
		M	7.95	0.00	11.82	1.33
	1+SFB	F	15.02	1.99	29.68	3.31
		M	31.39	3.28	27.26	2.65
	4	F	17.80	0.00	19.97	2.63
		M	12.57	1.68	8.77	1.33
ppGpp metabolism	1	F	0.05	177.57	0.47	198.04
		M	0.00	227.44	0.00	833.59
	1+SFB	F	0.00	320.01	0.00	201.86
		M	0.00	177.80	0.05	274.59
	4	F	7.67	84.76	7.12	138.76
		M	19.70	46.89	8.07	106.14
Reductive TCA Cycle I	1	F	472.84	1084.81	226.21	711.52
		M	625.99	1185.62	418.94	1580.59
	1+SFB	F	177.97	1092.91	169.35	867.78
		M	352.01	745.55	195.53	1001.55
	4	F	1023.33	1130.27	595.04	885.94
		M	1023.84	1178.40	621.96	890.61

Supplemental Table 4.1. *H. hepaticus* alters predicted pathways within all GMs. Metagenomic pathway associated ASV read counts of all consistently differentially enriched pathways between pathobiont inoculated groups within cecal samples of all mice

CHAPTER 5—CONCLUSIONS AND FUTURE DIRECTIONS

Animal models, specifically mouse models, have a long history of utilization in experimental research. Mouse models have proven to be an invaluable tool for the better understanding of human biology and physiology. Methods for better care and quality of the mouse model have developed over history, but there are still many aspects of the mouse model that we do not fully understand, and these qualities, such as the GM, can drastically alter the phenotype of various models, which lowers experimental replicability and translatability between studies. Ultimately, this leads to lowered translatability to the human condition. Without a thorough understanding of the factors that drive GM variability, animal models will continue to suffer from reduced translatability. In Chapter 1, the studies discussed attempt to capture the ongoing evolution of mouse model husbandry and best experimental practices, as well as highlighting important drivers of GM variability that have been identified in both the human and mouse model population were described. Ongoing research is required to determine potential drivers of GM variability within mouse models and the mechanisms involved in these alterations. The subsequent chapters of this dissertation attempt to uncover suspected drivers of GM variability through utilization of multiple mouse strains and stocks.

In Chapter 2, authors determined the effect of housing density on the ability to detect a statistical difference between antibiotic treated mice and sex and age-matched controls during antibiotic administration and 4 weeks

after cessation of these antibiotics. Results indicated a greater ability to detect statistical significance when mice were housed 2 mpc rather than 4 mpc. These results were replicated in two separate cohorts of mice, with each cohort receiving different antibiotic cocktails. Through utilization of multiple antibiotic cocktails, we were able to increase the validity of these findings by demonstrating replicability across antibiotics regardless of the underlying mechanisms of antibiotic intervention.

To further explore the implications of housing density on the gut microbiota there are still several avenues to be explored. First, it may be helpful to repeat this study in mice of a different GM composition such as those from mice obtained from Envigo or GM4 harboring mice, to represent a more complex microbiota as these compositions have shown to have greater colony resistance than lower diversity compositions. This might translate to smaller antibiotic induced changes and a greater ability to regain ASVs after the cessation of antibiotics, which may diminish the differences between housing 2 mpc versus 4 mpc. Another future direction could be to determine if 2 mpc continues to be better at detecting statistical significance than 4mpc during other experimental interventions such as pathogen exposure and changes in diet.

In Chapter 3 of this dissertation the transfer of maternal microbial sources to the composition of the neonatal mouse gut microbiota in two differently enriched GM backgrounds were analyzed. Results of this study are overall consistent with recent literature regarding gut microbiota development and

vertical transfer of various maternal microbiota sources. In conclusion, SPF mouse microbiotas undergo a dynamic and somewhat characteristic maturation process, culminating by roughly two to three weeks of age. Prior to that, the neonatal gut microbiota is more similar in composition to the maternal oral microbiota, as opposed to the vaginal or fecal microbiotas. Additionally, the maternal source microbiota that is transferred during gut microbiota development is dependent on the specific SPF microbiota of the mother. Further studies are needed to expand our knowledge regarding the effect of these developmental exposures on host development, and if additional maternal bacterial sources, such as the skin or milk, contribute significantly to GM development.

In Chapter 4, how GM background and select pathobiont inoculations interact to differentially influence T1D development in male and female NOD mice was determined. The hypothesis for this experiment was supported in that a higher richness background GM decreases T1D while a lower richness background GM increases T1D severity. Further, the hypothesis that pathobiont inoculation would alter T1D incidence was supported, where *H. hepaticus* exacerbated disease and MHV ameliorated disease. The effect of these environmental factors on T1D development depended on what combination of sex, GM, and pathobiont inoculations are present in the individual. Particularly, male mice are more susceptible to changes in pathobiont inoculation received, while female T1D incidence depends more on background GM composition. This study supports

previous findings that both GM richness and colonization of a single organism species can alter the T1D phenotype of NOD mice and provides new insight to potential metabolic pathways that these pathobionts influence that may also be implicated in T1D development in both humans and mice.

Future directions for the study in chapter 4 could include validation of the suggested differentially regulated pathways as detected by PiCRUST2 analysis. This could be achieved by metabolomic or proteomic analysis of the GM composition between *H. hepaticus* inoculated and control NOD mice. Validation of differences in these pathways could invoke further studies to evaluate the specific mechanisms implicated in the differential regulation of the pathway through utilization of KO mice for different genes involved in these pathways or direct inhibition of the pathway through inhibitors. This could help further our understanding of both mechanisms of T1D onset as well as the mechanisms in which *H. hepaticus* influences host health.

BIBLIOGRAPHY

1 Keeler, C. E. *The laboratory mouse; its origin, heredity, and culture*. (Harvard university press, 1931).

2 Phifer-Rixey, M. & Nachman, M. W. Insights into mammalian biology from the wild house mouse Mus musculus. *eLife* **4**, e05959, doi:10.7554/eLife.05959 (2015).

3 Dobson, G. P., Letson, H. L., Biros, E. & Morris, J. Specific pathogen-free (SPF) animal status as a variable in biomedical research: Have we come full circle? *EBioMedicine* **41**, 42-43, doi:10.1016/j.ebiom.2019.02.038 (2019).

4 Ericsson, A. C. & Franklin, C. L. The gut microbiome of laboratory mice: considerations and best practices for translational research. *Mamm Genome* **32**, 239-250, doi:10.1007/s00335-021-09863-7 (2021).

5 Ericsson, A. C. *et al.* Effects of vendor and genetic background on the composition of the fecal microbiota of inbred mice. *PLoS One* **10**, e0116704, doi:10.1371/journal.pone.0116704 (2015).

6 Ericsson, A. C., Crim, M. J. & Franklin, C. L. A brief history of animal modeling. *Mo Med* **110**, 201-205 (2013).

7 Ivy, A. C. The History and Ethics of the Use of Human Subjects in Medical Experiments. *Science* **108**, 1-5, doi:10.1126/science.108.2792.1 (1948).

8 FDA. *Animal Rule Information*, <https://www.fda.gov/emergency-preparedness-and-response/mcm-regulatory-science/animal-rule-information> (2022).

9 Duncan, I. J. H. in *Animal Welfeare: From Science to Law* 13-19 (Hild S. & Schweitzer L., 2019).

10 Franco, N. H. Animal Experiments in Biomedical Research: A Historical Perspective. *Animals (Basel)* **3**, 238-273, doi:10.3390/ani3010238 (2013).

11 Camenzind, S. Kantian Ethics and the Animal Turn. On the Contemporary Defence of Kant's Indirect Duty View. *Animals (Basel)* **11**, doi:10.3390/ani11020512 (2021).

12 Favre, D. & Tsang, V. The Development of the Anti-Cruelty Laws Duing the 1800's. *Detroit College of Law Review* (1993).

13 Bailey, J. Does the stress of laboratory life and experimentation on animals adversely affect research data? A critical review.

14 Russell, W. M. S. & Burch, R. L. *Principles of Humane Experimental Technique*. (1959).

15 Fenwick, N., Griffin, G. & Gauthier, C. The welfare of animals used in science: how the "Three Rs" ethic guides improvements. *Can Vet J* **50**, 523-530 (2009).

16 Meigs, L., Smirnova, L., Rovida, C., Leist, M. & Hartung, T. Animal testing and its alternatives – the most important omics is

economics. *ALTEX - Alternatives to animal experimentation* **35**, 275-305, doi:10.14573/altex.1807041 (2018).
17 Suntharalingam, G. *et al.* Cytokine storm in a phase 1 trial of the anti-CD28 monoclonal antibody TGN1412. *N Engl J Med* **355**, 1018-1028, doi:10.1056/NEJMoa063842 (2006).
18 Tacke, M., Hanke, G., Hanke, T. & Hunig, T. CD28-mediated induction of proliferation in resting T cells in vitro and in vivo without engagement of the T cell receptor: evidence for functionally distinct forms of CD28. *Eur J Immunol* **27**, 239-247, doi:10.1002/eji.1830270136 (1997).
19 Hunig, T. & Dennehy, K. CD28 superagonists: mode of action and therapeutic potential. *Immunol Lett* **100**, 21-28, doi:10.1016/j.imlet.2005.06.012 (2005).
20 Rosshart, S. P. *et al.* Laboratory mice born to wild mice have natural microbiota and model human immune responses. *Science* **365**, doi:10.1126/science.aaw4361 (2019).
21 Beura, L. K. *et al.* Normalizing the environment recapitulates adult human immune traits in laboratory mice. *Nature* **532**, 512-516, doi:10.1038/nature17655 (2016).
22 Storey, J., Gobbetti, T., Olzinski, A. & Berridge, B. R. A Structured Approach to Optimizing Animal Model Selection for Human Translation: The Animal Model Quality Assessment. *ILAR J* **62**, 66-76, doi:10.1093/ilar/ilac004 (2021).
23 Frangogiannis, N. G. Why animal model studies are lost in translation. *J Cardiovasc Aging* **2**, doi:10.20517/jca.2022.10 (2022).
24 Berridge, B. R. Animal Study Translation: The Other Reproducibility Challenge. *ILAR Journal* **62**, 1-6, doi:10.1093/ilar/ilac005 (2021).
25 Maggio-Price, L. *et al.* Helicobacter infection is required for inflammation and colon cancer in SMAD3-deficient mice. *Cancer Res* **66**, 828-838, doi:10.1158/0008-5472.CAN-05-2448 (2006).
26 Yu, Y., Zhu, S., Li, P., Min, L. & Zhang, S. Helicobacter pylori infection and inflammatory bowel disease: a crosstalk between upper and lower digestive tract. *Cell Death Dis* **9**, 961, doi:10.1038/s41419-018-0982-2 (2018).
27 Shahab, M. & Shahab, N. Coevolution of the Human Host and Gut Microbiome: Metagenomics of Microbiota. *Cureus* **14**, e26310, doi:10.7759/cureus.26310 (2022).
28 Maraci, Ö. *et al.* The Gut Microbial Composition Is Species-Specific and Individual-Specific in Two Species of Estrildid Finches, the Bengalese Finch and the Zebra Finch. *Frontiers in Microbiology* **12**, doi:10.3389/fmicb.2021.619141 (2021).
29 Priya, S. & Blekhman, R. Population dynamics of the human gut microbiome: change is the only constant. *Genome Biology* **20**, 150, doi:10.1186/s13059-019-1775-3 (2019).
30 Ahn, J. & Hayes, R. B. Environmental Influences on the Human Microbiome and Implications for Noncommunicable Disease. *Annu*

Rev Public Health **42**, 277-292, doi:10.1146/annurev-publhealth-012420-105020 (2021).
31 Leser, T. D. & Molbak, L. Better living through microbial action: the benefits of the mammalian gastrointestinal microbiota on the host. *Environ Microbiol* **11**, 2194-2206, doi:10.1111/j.1462-2920.2009.01941.x (2009).
32 Oliphant, K. & Allen-Vercoe, E. Macronutrient metabolism by the human gut microbiome: major fermentation by-products and their impact on host health. *Microbiome* **7**, 91, doi:10.1186/s40168-019-0704-8 (2019).
33 Wu, H. J. & Wu, E. The role of gut microbiota in immune homeostasis and autoimmunity. *Gut Microbes* **3**, 4-14, doi:10.4161/gmic.19320 (2012).
34 Takiishi, T., Fenero, C. I. M. & Camara, N. O. S. Intestinal barrier and gut microbiota: Shaping our immune responses throughout life. *Tissue Barriers* **5**, e1373208, doi:10.1080/21688370.2017.1373208 (2017).
35 Ducarmon, Q. R. *et al.* Gut Microbiota and Colonization Resistance against Bacterial Enteric Infection. *Microbiology and Molecular Biology Reviews* **83**, e00007-00019, doi:doi:10.1128/MMBR.00007-19 (2019).
36 de Jonge, N., Carlsen, B., Christensen, M. H., Pertoldi, C. & Nielsen, J. L. The Gut Microbiome of 54 Mammalian Species. *Front Microbiol* **13**, 886252, doi:10.3389/fmicb.2022.886252 (2022).
37 Bubier, J. A., Chesler, E. J. & Weinstock, G. M. Host genetic control of gut microbiome composition. *Mammalian Genome* **32**, 263-281, doi:10.1007/s00335-021-09884-2 (2021).
38 Valeri, F. & Endres, K. How biological sex of the host shapes its gut microbiota. *Frontiers in Neuroendocrinology* **61**, 100912, doi:https://doi.org/10.1016/j.yfrne.2021.100912 (2021).
39 Beresford-Jones, B. S. *et al.* The Mouse Gastrointestinal Bacteria Catalogue enables translation between the mouse and human gut microbiotas via functional mapping. *Cell Host & Microbe* **30**, 124-138.e128, doi:https://doi.org/10.1016/j.chom.2021.12.003 (2022).
40 Sender, R., Fuchs, S. & Milo, R. Revised Estimates for the Number of Human and Bacteria Cells in the Body. *PLoS Biol* **14**, e1002533, doi:10.1371/journal.pbio.1002533 (2016).
41 Nguyen, T. L., Vieira-Silva, S., Liston, A. & Raes, J. How informative is the mouse for human gut microbiota research? *Dis Model Mech* **8**, 1-16, doi:10.1242/dmm.017400 (2015).
42 Kieser, S., Zdobnov, E. M. & Trajkovski, M. Comprehensive mouse microbiota genome catalog reveals major difference to its human counterpart. *PLoS Comput Biol* **18**, e1009947, doi:10.1371/journal.pcbi.1009947 (2022).
43 Xiao, L. *et al.* A catalog of the mouse gut metagenome. *Nature Biotechnology* **33**, 1103-1108, doi:10.1038/nbt.3353 (2015).

44 Luczynski, P. *et al.* Growing up in a Bubble: Using Germ-Free Animals to Assess the Influence of the Gut Microbiota on Brain and Behavior. *Int J Neuropsychopharmacol* **19**, doi:10.1093/ijnp/pyw020 (2016).
45 Grenham, S., Clarke, G., Cryan, J. F. & Dinan, T. G. Brain-gut-microbe communication in health and disease. *Front Physiol* **2**, 94, doi:10.3389/fphys.2011.00094 (2011).
46 Lamousé-Smith, E. S., Tzeng, A. & Starnbach, M. N. The Intestinal Flora Is Required to Support Antibody Responses to Systemic Immunization in Infant and Germ Free Mice. *PLOS ONE* **6**, e27662, doi:10.1371/journal.pone.0027662 (2011).
47 Mosca, A., Leclerc, M. & Hugot, J. P. Gut Microbiota Diversity and Human Diseases: Should We Reintroduce Key Predators in Our Ecosystem? *Frontiers in Microbiology* **7**, doi:10.3389/fmicb.2016.00455 (2016).
48 Kriss, M., Hazleton, K. Z., Nusbacher, N. M., Martin, C. G. & Lozupone, C. A. Low diversity gut microbiota dysbiosis: drivers, functional implications and recovery. *Curr Opin Microbiol* **44**, 34-40, doi:10.1016/j.mib.2018.07.003 (2018).
49 Gong, D., Gong, X., Wang, L., Yu, X. & Dong, Q. Involvement of Reduced Microbial Diversity in Inflammatory Bowel Disease. *Gastroenterol Res Pract* **2016**, 6951091, doi:10.1155/2016/6951091 (2016).
50 Kang, D.-W. *et al.* Reduced Incidence of Prevotella and Other Fermenters in Intestinal Microflora of Autistic Children. *PLOS ONE* **8**, e68322, doi:10.1371/journal.pone.0068322 (2013).
51 Augustine, T., Kumar, M., Al Khodor, S. & van Panhuys, N. Microbial Dysbiosis Tunes the Immune Response Towards Allergic Disease Outcomes. *Clin Rev Allergy Immunol*, doi:10.1007/s12016-022-08939-9 (2022).
52 Karl, J. P. *et al.* Effects of Psychological, Environmental and Physical Stressors on the Gut Microbiota. *Front Microbiol* **9**, 2013, doi:10.3389/fmicb.2018.02013 (2018).
53 Rosshart, S. P. *et al.* Wild Mouse Gut Microbiota Promotes Host Fitness and Improves Disease Resistance. *Cell* **171**, 1015-1028 e1013, doi:10.1016/j.cell.2017.09.016 (2017).
54 Ericsson, A. C., Montonye, D. R., Smith, C. R. & Franklin, C. L. Modeling a Superorganism – Considerations Regarding the Use of “Dirty” Mice in Biomedical Research. *Yale Journal of Biology and Medicine* (2017).
55 Taguchi, F., Hirano, N., Kiuchi, Y. & Fujiwara, K. Difference in response to mouse hepatitis virus among susceptible mouse strains. *Jpn J Microbiol* **20**, 293-302, doi:10.1111/j.1348-0421.1976.tb00991.x (1976).
56 Wilberz, S., Partke, H. J., Dagnaes-Hansen, F. & Herberg, L. Persistent MHV (mouse hepatitis virus) infection reduces the

incidence of diabetes mellitus in non-obese diabetic mice. *Diabetologia* **34**, 2-5, doi:10.1007/BF00404016 (1991).
57 Hart, M. L. *et al.* Development of outbred CD1 mouse colonies with distinct standardized gut microbiota profiles for use in complex microbiota targeted studies. *Sci Rep* **8**, 10107-10107, doi:10.1038/s41598-018-28448-0 (2018).
58 Ericsson, A. C. *et al.* Supplier-origin mouse microbiomes significantly influence locomotor and anxiety-related behavior, body morphology, and metabolism. *Commun Biol* **4**, 716, doi:10.1038/s42003-021-02249-0 (2021).
59 Hart, M. L., Ericsson, A. C. & Franklin, C. L. Differing Complex Microbiota Alter Disease Severity of the IL-10−/− Mouse Model of Inflammatory Bowel Disease. *Frontiers in Microbiology* **8**, doi:10.3389/fmicb.2017.00792 (2017).
60 Bidot, W. A., Ericsson, A. C. & Franklin, C. L. Effects of water decontamination methods and bedding material on the gut microbiota. *PLoS One* **13**, e0198305, doi:10.1371/journal.pone.0198305 (2018).
61 Yatsunenko, T. *et al.* Human gut microbiome viewed across age and geography. *Nature* **486**, 222-227, doi:10.1038/nature11053 (2012).
62 Filardo, S. *et al.* Impact of Air Pollution on the Composition and Diversity of Human Gut Microbiota in General and Vulnerable Populations: A Systematic Review. *Toxics* **10** (2022).
63 Li, S., Yang, Z., Hu, D., Cao, L. & He, Q. Understanding building-occupant-microbiome interactions toward healthy built environments: A review. *Frontiers of Environmental Science & Engineering* **15**, 65, doi:10.1007/s11783-020-1357-3 (2020).
64 Bowyer, R. C. E. *et al.* Socioeconomic Status and the Gut Microbiome: A TwinsUK Cohort Study. *Microorganisms* **7**, doi:10.3390/microorganisms7010017 (2019).
65 Antinozzi, M. *et al.* Cigarette Smoking and Human Gut Microbiota in Healthy Adults: A Systematic Review. *Biomedicines* **10**, doi:10.3390/biomedicines10020510 (2022).
66 Day, A. W. & Kumamoto, C. A. Gut Microbiome Dysbiosis in Alcoholism: Consequences for Health and Recovery. *Frontiers in Cellular and Infection Microbiology* **12**, doi:10.3389/fcimb.2022.840164 (2022).
67 Singh, R. K. *et al.* Influence of diet on the gut microbiome and implications for human health. *J Transl Med* **15**, 73, doi:10.1186/s12967-017-1175-y (2017).
68 Zhang, M. & Yang, X. J. Effects of a high fat diet on intestinal microbiota and gastrointestinal diseases. *World J Gastroenterol* **22**, 8905-8909, doi:10.3748/wjg.v22.i40.8905 (2016).
69 Wang, L., Wang, H., Zhang, B., Popkin, B. M. & Du, S. Elevated Fat Intake Increases Body Weight and the Risk of Overweight and

Obesity among Chinese Adults: 1991-2015 Trends. *Nutrients* **12**, doi:10.3390/nu12113272 (2020).
70 Li, J., Wu, H., Liu, Y. & Yang, L. High fat diet induced obesity model using four strainsof mice: Kunming, C57BL/6, BALB/c and ICR. *Exp Anim* **69**, 326-335, doi:10.1538/expanim.19-0148 (2020).
71 Stott, N. L. & Marino, J. S. High Fat Rodent Models of Type 2 Diabetes: From Rodent to Human. *Nutrients* **12**, doi:10.3390/nu12123650 (2020).
72 Murphy, E. A., Velazquez, K. T. & Herbert, K. M. Influence of high-fat diet on gut microbiota: a driving force for chronic disease risk. *Curr Opin Clin Nutr Metab Care* **18**, 515-520, doi:10.1097/MCO.0000000000000209 (2015).
73 von Schwartzenberg, R. J. *et al.* Caloric restriction disrupts the microbiota and colonization resistance. *Nature* **595**, 272-277, doi:10.1038/s41586-021-03663-4 (2021).
74 Yang, L. *et al.* The varying effects of antibiotics on gut microbiota. *AMB Express* **11**, 116, doi:10.1186/s13568-021-01274-w (2021).
75 Schellekens, H. *et al.* Bifidobacterium longum counters the effects of obesity: Partial successful translation from rodent to human. *EBioMedicine* **63**, 103176, doi:10.1016/j.ebiom.2020.103176 (2021).
76 Korte, S. W., Dorfmeyer, R. A., Franklin, C. L. & Ericsson, A. C. Acute and long-term effects of antibiotics commonly used in laboratory animal medicine on the fecal microbiota. *Vet Res* **51**, 116, doi:10.1186/s13567-020-00839-0 (2020).
77 Kullberg, M. C. *et al.* Helicobacter hepaticus-induced colitis in interleukin-10-deficient mice: cytokine requirements for the induction and maintenance of intestinal inflammation. *Infect Immun* **69**, 4232-4241, doi:10.1128/IAI.69.7.4232-4241.2001 (2001).
78 Dieleman Levinus, A. *et al.* Helicobacter hepaticus Does Not Induce or Potentiate Colitis in Interleukin-10-Deficient Mice. *Infection and Immunity* **68**, 5107-5113, doi:10.1128/IAI.68.9.5107-5113.2000 (2000).
79 Pradhan, S. B. & Dali, S. Relation between gallbladder neoplasm and Helicobacter hepaticus infection. *Kathmandu Univ Med J (KUMJ)* **2**, 331-335 (2004).
80 Thurman, C. E. *et al.* Effect of Housing Condition and Diet on the Gut Microbiota of Weanling Immunocompromised Mice. *Comp Med* **71**, 485-491, doi:10.30802/AALAS-CM-21-000015 (2021).
81 Montonye, D. R. *et al.* Acclimation and Institutionalization of the Mouse Microbiota Following Transportation. *Front Microbiol* **9**, 1085, doi:10.3389/fmicb.2018.01085 (2018).
82 Zhang, C. *et al.* Transfer efficiency and impact on disease phenotype of differing methods of gut microbiota transfer. *Sci Rep* **12**, 19621, doi:10.1038/s41598-022-24014-x (2022).

83 Ericsson, A. C. *et al.* The influence of caging, bedding, and diet on the composition of the microbiota in different regions of the mouse gut. *Sci Rep* **8**, 4065, doi:10.1038/s41598-018-21986-7 (2018).
84 Hufeldt, M. R., Nielsen, D. S., Vogensen, F. K., Midtvedt, T. & Hansen, A. K. Variation in the gut microbiota of laboratory mice is related to both genetic and environmental factors. *Comp Med* **60**, 336-347 (2010).
85 Hart, M. L., Ericsson, A. C. & Franklin, C. L. Differing complex microbiota alter disease severity of the IL-10-/- mouse model of inflammatory bowel disease. *Frontiers in microbiology* **8**, doi:10.3389/fmcib.2017.00792 (2017).
86 Moskowitz, J. E., Andreatta, F. & Amos-Landgraf, J. The gut microbiota modulates differential adenoma suppression by B6/J and B6/N genetic backgrounds in Apc(Min) mice. *Mammalian genome : official journal of the International Mammalian Genome Society* **30**, 237-244, doi:10.1007/s00335-019-09814-3 (2019).
87 Denning, T. L. *et al.* Functional specializations of intestinal dendritic cell and macrophage subsets that control Th17 and regulatory T cell responses are dependent on the T cell/APC ratio, source of mouse strain, and regional localization. *J Immunol* **187**, 733-747, doi:10.4049/jimmunol.1002701 (2011).
88 Festing, M. F. & Altman, D. G. Guidelines for the design and statistical analysis of experiments using laboratory animals. *ILAR journal / National Research Council, Institute of Laboratory Animal Resources* **43**, 244-258, doi:10.1093/ilar.43.4.244 (2002).
89 Paigen, B. *et al.* Physiological effects of housing density on C57BL/6J mice over a 9-month period. *Journal of animal science* **90**, 5182-5192, doi:10.2527/jas.2012-5417 (2012).
90 Walters, W. *et al.* Improved Bacterial 16S rRNA Gene (V4 and V4-5) and Fungal Internal Transcribed Spacer Marker Gene Primers for Microbial Community Surveys. *mSystems* **1**, doi:10.1128/mSystems.00009-15 (2016).
91 Martin, M. Cutadapt removes adapter sequences from high-throughput sequencing reads. *EMBnet.journal* **17**, 10-12, doi:https://doi.org/10.14806/ej.17.1.200. (2011).
92 Bolyen, E. *et al.* Reproducible, interactive, scalable and extensible microbiome data science using QIIME 2. *Nat Biotechnol* **37**, 852-857, doi:10.1038/s41587-019-0209-9 (2019).
93 Callahan, B. J. *et al.* DADA2: High-resolution sample inference from Illumina amplicon data. *Nature methods* **13**, 581-583, doi:10.1038/nmeth.3869 (2016).
94 Van Loo, P. L., Mol, J. A., Koolhaas, J. M., Van Zutphen, B. F. & Baumans, V. Modulation of aggression in male mice: influence of group size and cage size. *Physiol Behav* **72**, 675-683, doi:10.1016/s0031-9384(01)00425-5 (2001).

95 Laber, K., Veatch, L. M., Lopez, M. F., Mulligan, J. K. & Lathers, D. M. Effects of housing density on weight gain, immune function, behavior, and plasma corticosterone concentrations in BALB/c and C57BL/6 mice. *J Am Assoc Lab Anim Sci* **47**, 16-23 (2008).
96 Nicholson, A. *et al.* The response of C57BL/6J and BALB/cJ mice to increased housing density. *J Am Assoc Lab Anim Sci* **48**, 740-753 (2009).
97 Morgan, J. L. *et al.* Effects of housing density in five inbred strains of mice. *PloS one* **9**, e90012, doi:10.1371/journal.pone.0090012 (2014).
98 Peters, A. & Festing, M. Population density and growth rate in laboratory mice. *Laboratory animals* **24**, 273-279, doi:10.1258/002367790780866227 (1990).
99 Peng, X., Lang, C. M., Drozdowicz, C. K. & Ohlsson-Wilhelm, B. M. Effect of cage population density on plasma corticosterone and peripheral lymphocyte populations of laboratory mice. *Laboratory animals* **23**, 302-306, doi:10.1258/002367789780746042 (1989).
100 O'Malley, J., Dambrosia, J. M. & Davis, J. A. Effect of housing density on reproductive parameters and corticosterone levels in nursing mice. *J Am Assoc Lab Anim Sci* **47**, 9-15 (2008).
101 Smith, A. L., Mabus, S. L., Muir, C. & Woo, Y. Effects of housing density and cage floor space on three strains of young adult inbred mice. *Comp Med* **55**, 368-376 (2005).
102 Smith, A. L., Mabus, S. L., Stockwell, J. D. & Muir, C. Effects of housing density and cage floor space on C57BL/6J mice. *Comp Med* **54**, 656-663 (2004).
103 Bogatyrev, S. R., Rolando, J. C. & Ismagilov, R. F. Self-reinoculation with fecal flora changes microbiota density and composition leading to an altered bile-acid profile in the mouse small intestine. *Microbiome* **8**, 19, doi:10.1186/s40168-020-0785-4 (2020).
104 Hildebrand, F. *et al.* Inflammation-associated enterotypes, host genotype, cage and inter-individual effects drive gut microbiota variation in common laboratory mice. *Genome biology* **14**, R4, doi:10.1186/gb-2013-14-1-r4 (2013).
105 Walker, M. *et al.* Mixed-strain housing for female C57BL/6, DBA/2, and BALB/c mice: validating a split-plot design that promotes refinement and reduction. *BMC Med Res Methodol* **16**, 11, doi:10.1186/s12874-016-0113-7 (2016).
106 Robertson, S. J. *et al.* Comparison of Co-housing and Littermate Methods for Microbiota Standardization in Mouse Models. *Cell Rep* **27**, 1910-1919 e1912, doi:10.1016/j.celrep.2019.04.023 (2019).
107 Ericsson, A. C. & Franklin, C. L. The gut microbiome of laboratory mice: considerations and best practices for translational research. *Mammalian genome : official journal of the International*

Mammalian Genome Society, doi:10.1007/s00335-021-09863-7 (2021).
108 Basson, A. R. *et al.* Artificial microbiome heterogeneity spurs six practical action themes and examples to increase study power-driven reproducibility. *Scientific reports* **10**, 5039, doi:10.1038/s41598-020-60900-y (2020).
109 Stinson, L. F., Boyce, M. C., Payne, M. S. & Keelan, J. A. The Not-so-Sterile Womb: Evidence That the Human Fetus Is Exposed to Bacteria Prior to Birth. *Frontiers in Microbiology* **10**, doi:10.3389/fmicb.2019.01124 (2019).
110 Nagpal, R. *et al.* Sensitive Quantitative Analysis of the Meconium Bacterial Microbiota in Healthy Term Infants Born Vaginally or by Cesarean Section. *Frontiers in Microbiology* **7**, doi:10.3389/fmicb.2016.01997 (2016).
111 Ferretti, P. *et al.* Mother-to-Infant Microbial Transmission from Different Body Sites Shapes the Developing Infant Gut Microbiome. *Cell Host & Microbe* **24**, 133-145.e135, doi:https://doi.org/10.1016/j.chom.2018.06.005 (2018).
112 Mortensen, M. S. *et al.* Modeling transfer of vaginal microbiota from mother to infant in early life. *eLife* **10**, e57051, doi:10.7554/eLife.57051 (2021).
113 Beller, L. *et al.* Successional Stages in Infant Gut Microbiota Maturation. *mBio* **12**, e01857-01821, doi:doi:10.1128/mbio.01857-21 (2021).
114 Zhang, C. *et al.* The Effects of Delivery Mode on the Gut Microbiota and Health: State of Art. *Frontiers in Microbiology* **12**, doi:10.3389/fmicb.2021.724449 (2021).
115 Hansen, C. H. F. *et al.* Mode of Delivery Shapes Gut Colonization Pattern and Modulates Regulatory Immunity in Mice. *The Journal of Immunology* **193**, 1213, doi:10.4049/jimmunol.1400085 (2014).
116 Stewart, C. J. *et al.* Temporal development of the gut microbiome in early childhood from the TEDDY study. *Nature* **562**, 583-588, doi:10.1038/s41586-018-0617-x (2018).
117 Levi Mortera, S. *et al.* Monitoring Perinatal Gut Microbiota in Mouse Models by Mass Spectrometry Approaches: Parental Genetic Background and Breastfeeding Effects. *Frontiers in Microbiology* **7**, doi:10.3389/fmicb.2016.01523 (2016).
118 Reyman, M. *et al.* Effects of early-life antibiotics on the developing infant gut microbiome and resistome: a randomized trial. *Nature Communications* **13**, 893, doi:10.1038/s41467-022-28525-z (2022).
119 Ran, X., He, Y., Ai, Q. & Shi, Y. Effect of antibiotic-induced intestinal dysbacteriosis on bronchopulmonary dysplasia and related mechanisms. *Journal of Translational Medicine* **19**, 155, doi:10.1186/s12967-021-02794-6 (2021).

120 Sanidad, K. Z. & Zeng, M. Y. Neonatal gut microbiome and immunity. *Current Opinion in Microbiology* **56**, 30-37, doi:https://doi.org/10.1016/j.mib.2020.05.011 (2020).
121 Koenig Jeremy, E. *et al.* Succession of microbial consortia in the developing infant gut microbiome. *Proceedings of the National Academy of Sciences* **108**, 4578-4585, doi:10.1073/pnas.1000081107 (2011).
122 Hughes, K. R. *et al.* The early life microbiota protects neonatal mice from pathological small intestinal epithelial cell shedding. *The FASEB Journal* **34**, 7075-7088, doi:https://doi.org/10.1096/fj.202000042R (2020).
123 Robertson, R. C., Manges, A. R., Finlay, B. B. & Prendergast, A. J. The Human Microbiome and Child Growth – First 1000 Days and Beyond. *Trends in Microbiology* **27**, 131-147, doi:https://doi.org/10.1016/j.tim.2018.09.008 (2019).
124 Sela, D. A. & Mills, D. A. Nursing our microbiota: molecular linkages between bifidobacteria and milk oligosaccharides. *Trends in Microbiology* **18**, 298-307, doi:https://doi.org/10.1016/j.tim.2010.03.008 (2010).
125 Bezirtzoglou, E. The Intestinal Microflora During the First Weeks of Life. *Anaerobe* **3**, 173-177, doi:https://doi.org/10.1006/anae.1997.0102 (1997).
126 Fallani, M. *et al.* Determinants of the human infant intestinal microbiota after the introduction of first complementary foods in infant samples from five European centres. *Microbiology* **157**, 1385-1392, doi:https://doi.org/10.1099/mic.0.042143-0 (2011).
127 Asnicar, F. *et al.* Studying Vertical Microbiome Transmission from Mothers to Infants by Strain-Level Metagenomic Profiling. *mSystems* **2**, e00164-00116, doi:10.1128/mSystems.00164-16.
128 Preidis, G. A. *et al.* Composition and function of the undernourished neonatal mouse intestinal microbiome. *The Journal of Nutritional Biochemistry* **26**, 1050-1057, doi:https://doi.org/10.1016/j.jnutbio.2015.04.010 (2015).
129 Meng, Q. *et al.* Single-Cell Transcriptome Sequencing and Proteomics Reveal Neonatal Ileum Dynamic Developmental Potentials.
130 Walters, W. A. *et al.* PrimerProspector: de novo design and taxonomic analysis of barcoded polymerase chain reaction primers. *Bioinformatics* **27**, 1159-1161, doi:10.1093/bioinformatics/btr087 (2011).
131 Caporaso, J. G. *et al.* Global patterns of 16S rRNA diversity at a depth of millions of sequences per sample. *Proceedings of the National Academy of Sciences* **108**, 4516-4522, doi:10.1073/pnas.1000080107 (2011).
132 Hammer, Ø., Harper, D. A. T. & Ryan, P. D. PAST: PALEONTOLOGICAL STATISTICAL SOFTWARE PACKAGE FOR

EDUCATION AND DATA ANALYSIS. *Palaeontologia Electronica* **4**, 1-9 (2001).
133 Risely, A. Applying the core microbiome to understand host–microbe systems. *Journal of Animal Ecology* **89**, 1549-1558, doi:https://doi.org/10.1111/1365-2656.13229 (2020).
134 Schloss, P. D. *et al.* Stabilization of the murine gut microbiome following weaning. *Gut Microbes* **3**, 383-393, doi:10.4161/gmic.21008 (2012).
135 Albenberg, L. *et al.* Correlation between intraluminal oxygen gradient and radial partitioning of intestinal microbiota. *Gastroenterology* **147**, 1055-1063 e1058, doi:10.1053/j.gastro.2014.07.020 (2014).
136 Oliphant, K. *et al.* Bacteroidota and Lachnospiraceae integration into the gut microbiome at key time points in early life are linked to infant neurodevelopment.
137 Alderete, T. A.-O. *et al.* Early life gut microbiota is associated with rapid infant growth in Hispanics from Southern California.
138 Cabrera-Rubio, R. *et al.* The human milk microbiome changes over lactation and is shaped by maternal weight and mode of delivery.
139 Underwood, M. A. *et al.* Human milk oligosaccharides in premature infants: absorption, excretion, and influence on the intestinal microbiota.
140 Mirpuri, J. *et al.* Proteobacteria-specific IgA regulates maturation of the intestinal microbiota. *Gut Microbes* **5**, 28-39, doi:10.4161/gmic.26489 (2014).
141 Machado Prado, M. R. & Boller, C. in *Discovery and Development of Anti-Inflammatory Agents from Natural Products* (ed Goutam Brahmachari) 259-282 (Elsevier, 2019).
142 Michel, C. & Blottiere, H. M. Neonatal Programming of Microbiota Composition: A Plausible Idea That Is Not Supported by the Evidence. *Front Microbiol* **13**, 825942, doi:10.3389/fmicb.2022.825942 (2022).
143 Prevention, C. f. D. C. a. National Diabetes Statistics Report 2020. (2020).
144 van Belle, T. L., Coppieters, K. T. & von Herrath, M. G. Type 1 diabetes: etiology, immunology, and therapeutic strategies. *Physiol Rev* **91**, 79-118, doi:10.1152/physrev.00003.2010 (2011).
145 Zheng, P., Li, Z. & Zhou, Z. Gut microbiome in type 1 diabetes: A comprehensive review. *Diabetes Metab Res Rev* **34**, e3043, doi:10.1002/dmrr.3043 (2018).
146 Paun, A., Yau, C. & Danska, J. S. The Influence of the Microbiome on Type 1 Diabetes. *J Immunol* **198**, 590-595, doi:10.4049/jimmunol.1601519 (2017).
147 Filippi, C. M. & von Herrath, M. G. Viral trigger for type 1 diabetes: pros and cons. *Diabetes* **57**, 2863-2871, doi:10.2337/db07-1023 (2008).

148 Zhang, X. S. *et al.* Antibiotic-induced acceleration of type 1 diabetes alters maturation of innate intestinal immunity. *Elife* **7**, doi:10.7554/eLife.37816 (2018).
149 Hu, Y. *et al.* Maternal Antibiotic Treatment Protects Offspring from Diabetes Development in Nonobese Diabetic Mice by Generation of Tolerogenic APCs. *J Immunol* **195**, 4176-4184, doi:10.4049/jimmunol.1500884 (2015).
150 Lamb, M. M. *et al.* The effect of childhood cow's milk intake and HLA-DR genotype on risk of islet autoimmunity and type 1 diabetes: the Diabetes Autoimmunity Study in the Young. *Pediatr Diabetes* **16**, 31-38, doi:10.1111/pedi.12115 (2015).
151 Marino, E. *et al.* Erratum: Gut microbial metabolites limit the frequency of autoimmune T cells and protect against type 1 diabetes. *Nat Immunol* **18**, 1271, doi:10.1038/ni1117-1271c (2017).
152 Vatanen, T. *et al.* The human gut microbiome in early-onset type 1 diabetes from the TEDDY study. *Nature* **562**, 589-594, doi:10.1038/s41586-018-0620-2 (2018).
153 Bosi, E. *et al.* Increased intestinal permeability precedes clinical onset of type 1 diabetes. *Diabetologia* **49**, 2824-2827, doi:10.1007/s00125-006-0465-3 (2006).
154 Secondulfo, M. *et al.* Ultrastructural mucosal alterations and increased intestinal permeability in non-celiac, type I diabetic patients. *Dig Liver Dis* **36**, 35-45, doi:10.1016/j.dld.2003.09.016 (2004).
155 de Goffau, M. C. *et al.* Aberrant gut microbiota composition at the onset of type 1 diabetes in young children. *Diabetologia* **57**, 1569-1577, doi:10.1007/s00125-014-3274-0 (2014).
156 Chatzigeorgiou, A., Halapas, A., Kalafatakis, K. & Kamper, E. The use of animal models in the study of diabetes mellitus. *In Vivo* **23**, 245-258 (2009).
157 Chen, Y. G., Mathews, C. E. & Driver, J. P. The Role of NOD Mice in Type 1 Diabetes Research: Lessons from the Past and Recommendations for the Future. *Front Endocrinol (Lausanne)* **9**, 51, doi:10.3389/fendo.2018.00051 (2018).
158 Shoda, L. K. *et al.* A comprehensive review of interventions in the NOD mouse and implications for translation. *Immunity* **23**, 115-126, doi:10.1016/j.immuni.2005.08.002 (2005).
159 Baxter, A. G., Koulmanda, M. & Mandel, T. E. High and low diabetes incidence nonobese diabetic (NOD) mice: origins and characterisation. *Autoimmunity* **9**, 61-67, doi:10.3109/08916939108997125 (1991).
160 Funda, D. P., Kaas, A., Bock, T., Tlaskalova-Hogenova, H. & Buschard, K. Gluten-free diet prevents diabetes in NOD mice. *Diabetes Metab Res Rev* **15**, 323-327, doi:10.1002/(sici)1520-7560(199909/10)15:5<323::aid-dmrr53>3.0.co;2-p (1999).

161 Marino, E. *et al.* Gut microbial metabolites limit the frequency of autoimmune T cells and protect against type 1 diabetes. *Nat Immunol* **18**, 552-562, doi:10.1038/ni.3713 (2017).
162 Fahey, J. R. *et al.* Antibiotic-associated Manipulation of the Gut Microbiota and Phenotypic Restoration in NOD Mice. *Comp Med* **67**, 335-343 (2017).
163 Franklin, C. L. & Ericsson, A. C. Microbiota and reproducibility of rodent models. *Lab Anim (NY)* **46**, 114-122, doi:10.1038/laban.1222 (2017).
164 De Riva, A. *et al.* Regulation of type 1 diabetes development and B-cell activation in nonobese diabetic mice by early life exposure to a diabetogenic environment. *PLoS One* **12**, e0181964, doi:10.1371/journal.pone.0181964 (2017).
165 Bao, M., Yang, Y., Jun, H.-S. & Yoon, J.-W. Molecular Mechanisms for Gender Differences in Susceptibility to T Cell-Mediated Autoimmune Diabetes in Nonobese Diabetic Mice. *The Journal of Immunology* **168**, 5369-5375, doi:10.4049/jimmunol.168.10.5369 (2002).
166 Candon, S. *et al.* Antibiotics in early life alter the gut microbiome and increase disease incidence in a spontaneous mouse model of autoimmune insulin-dependent diabetes. *PloS one* **10**, e0125448-e0125448, doi:10.1371/journal.pone.0125448 (2015).
167 Yurkovetskiy, L. *et al.* Gender bias in autoimmunity is influenced by microbiota. *Immunity* **39**, 400-412, doi:10.1016/j.immuni.2013.08.013 (2013).
168 Fox, J. G. Helicobacter bilis: bacterial provocateur orchestrates host immune responses to commensal flora in a model of inflammatory bowel disease. *Gut* **56**, 898-900, doi:10.1136/gut.2006.115428 (2007).
169 Wasimuddin *et al.* High prevalence and species diversity of Helicobacter spp. detected in wild house mice. *Appl Environ Microbiol* **78**, 8158-8160, doi:10.1128/AEM.01989-12 (2012).
170 Parker, S. E., Malone, S., Bunte, R. M. & Smith, A. L. Infectious diseases in wild mice (Mus musculus) collected on and around the University of Pennsylvania (Philadelphia) Campus. *Comp Med* **59**, 424-430 (2009).
171 Barthold, S. W. & Smith, A. L. Duration of mouse hepatitis virus infection: studies in immunocompetent and chemically immunosuppressed mice.
172 Körner, R. W., Majjouti, M., Alcazar, M. A. A. & Mahabir, E. Of Mice and Men: The Coronavirus MHV and Mouse Models as a Translational Approach to Understand SARS-CoV-2. *Viruses* **12**, 880, doi:10.3390/v12080880 (2020).
173 Ericsson, A. C., Davis, D. J., Franklin, C. L. & Hagan, C. E. Exoelectrogenic capacity of host microbiota predicts lymphocyte

recruitment to the gut. *Physiol Genomics* **47**, 243-252, doi:10.1152/physiolgenomics.00010.2015 (2015).
174 Hillhouse, A. E., Myles, M. H., Taylor, J. F., Bryda, E. C. & Franklin, C. L. Quantitative trait loci in a bacterially induced model of inflammatory bowel disease. *Mammalian Genome* **22**, 544-555, doi:10.1007/s00335-011-9343-5 (2011).
175 Bauer, B. A. *et al.* Influence of Rack Design and Disease Prevalence on Detection of Rodent Pathogens in Exhaust Debris Samples from Individually Ventilated Caging Systems. *Journal of the American Association for Laboratory Animal Science : JAALAS* **55**, 782-788 (2016).
176 Jain, R. *et al.* Innocuous IFNgamma induced by adjuvant-free antigen restores normoglycemia in NOD mice through inhibition of IL-17 production. *J Exp Med* **205**, 207-218, doi:10.1084/jem.20071878 (2008).
177 Drazenovich, N. L., Franklin, C. L., Livingston, R. S. & Besselsen, D. G. Detection of rodent Helicobacter spp. by use of fluorogenic nuclease polymerase chain reaction assays. *Comp Med* **52**, 347-353 (2002).
178 Loy, A., Maixner, F., Wagner, M. & Horn, M. probeBase--an online resource for rRNA-targeted oligonucleotide probes: new features 2007. *Nucleic acids research* **35**, D800-804, doi:10.1093/nar/gkl856 (2007).
179 Martin, M. Cutadapt removes adapter sequences from high-throughput sequencing reads. *EMBnet.journal; Vol 17, No 1: Next Generation Sequencing Data AnalysisDO - 10.14806/ej.17.1.200* (2011).
180 Bolyen, E. *et al.* Reproducible, interactive, scalable and extensible microbiome data science using QIIME 2. *Nature Biotechnology* **37**, 852-857, doi:10.1038/s41587-019-0209-9 (2019).
181 Callahan, B. J. *et al.* DADA2: High-resolution sample inference from Illumina amplicon data. *Nature Methods* **13**, 581-583, doi:10.1038/nmeth.3869 (2016).
182 Pruesse, E. *et al.* SILVA: a comprehensive online resource for quality checked and aligned ribosomal RNA sequence data compatible with ARB. *Nucleic acids research* **35**, 7188-7196, doi:10.1093/nar/gkm864 (2007).
183 Douglas, G. M. *et al.* PICRUSt2 for prediction of metagenome functions. *Nature Biotechnology* **38**, 685-688, doi:10.1038/s41587-020-0548-6 (2020).
184 Czech, L., Barbera, P. & Stamatakis, A. Genesis and Gappa: processing, analyzing and visualizing phylogenetic (placement) data. *Bioinformatics* **36**, 3263-3265, doi:10.1093/bioinformatics/btaa070 (2020).
185 Mirarab, S., Nguyen, N. & Warnow, T. in *Biocomputing 2012* 247-258 (WORLD SCIENTIFIC, 2011).

186 Louca, S. & Doebeli, M. Efficient comparative phylogenetics on large trees. *Bioinformatics* **34**, 1053-1055, doi:10.1093/bioinformatics/btx701 (2018).
187 Ye, Y. & Doak, T. G. A Parsimony Approach to Biological Pathway Reconstruction/Inference for Genomes and Metagenomes. *PLOS Computational Biology* **5**, e1000465, doi:10.1371/journal.pcbi.1000465 (2009).
188 ggplot2: Elegant Graphics for Data Analysis (Springer-Verlag New York, 2016).
189 rstatix: Pipe-Friendly Framework for Basic Statistical Tests (2021).
190 Lenth, R. V. emmeans: Estimated Marginal Means, aka Least-Squares Means. (2022).
191 vegan: Community Ecology Package (2022).
192 ecole: ecole: School of Ecology Package (2021).
193 ape 5.0: an environment for modern phylogenetics and evolutionary analyses in {R} (2018).
194 R: A Language and Environment for Statistical Computing (R Foundation for Statistical Computing, 2022).
195 Chen, Y.-G., Mathews, C. E. & Driver, J. P. The Role of NOD Mice in Type 1 Diabetes Research: Lessons from the Past and Recommendations for the Future. *Frontiers in Endocrinology* **9**, doi:10.3389/fendo.2018.00051 (2018).
196 Durazzo, M., Ferro, A. & Gruden, G. Gastrointestinal Microbiota and Type 1 Diabetes Mellitus: The State of Art. *J Clin Med* **8**, doi:10.3390/jcm8111843 (2019).
197 Ray, A. *et al.* Gut Microbial Dysbiosis Due to Helicobacter Drives an Increase in Marginal Zone B Cells in the Absence of IL-10 Signaling in Macrophages. *J Immunol* **195**, 3071-3085, doi:10.4049/jimmunol.1500153 (2015).
198 Hebert, S. L. & Nair, K. S. Protein and energy metabolism in type 1 diabetes. *Clin Nutr* **29**, 13-17, doi:10.1016/j.clnu.2009.09.001 (2010).
199 Lu, K., Knutson, C. G., Wishnok, J. S., Fox, J. G. & Tannenbaum, S. R. Serum metabolomics in a Helicobacter hepaticus mouse model of inflammatory bowel disease reveal important changes in the microbiome, serum peptides, and intermediary metabolism. *J Proteome Res* **11**, 4916-4926, doi:10.1021/pr300429x (2012).
200 Madsen, R., Banday, V. S., Moritz, T., Trygg, J. & Lejon, K. Altered metabolic signature in pre-diabetic NOD mice. *PLoS One* **7**, e35445, doi:10.1371/journal.pone.0035445 (2012).
201 Ericsson, A. C. *et al.* Isolation of segmented filamentous bacteria from complex gut microbiota. *Biotechniques* **59**, 94-98, doi:10.2144/000114319 (2015).

VITA

Amber Russell grew up in the small town of Platte City, MO. Here she discovered her love for biology by exploring the outdoors. Her favorite hobbies were flipping rocks to find bugs and memorizing all the dog breeds in her favorite book *The complete dog book* by the American Kennel Club. She knew at an early age that she wanted to study biology and was fascinated with all things living. She was often found at recess playing in the grass under her favorite tree, protecting the tree from other children who would pull off the branches. She saw the importance of nature at a young age and has always sought to protect it, as was passed down to her from her maternal grandmother, a woman proud of her Oglala Lakota decent.

Amber was eager to continue her studies, graduating from Platte County High School early and moving to Maryville, MO at age 17 to start her undergraduate degree. Here she started her journey as a first-generation college student, where she would lead study sessions for her biology 101 course and helped her classmates improve their grades dramatically. Desiring more challenging and diverse courses, she promptly transferred to the University of Missouri to finish her undergraduate degree in Biological Sciences. During her undergraduate career she worked in various laboratories helping with dishes and other various tasks to help keep the laboratories operating smoothly. Towards the end of her undergraduate career, she was allowed the opportunity to conduct research under the guidance of Dr. Aaron Ericsson, presenting her research *Effect*

of Segmented Filamentous Bacteria on Fecal Microbiota Transfer in CD1 mice at various conferences. Being provided the opportunity to conduct research, she realized her life-long dream of becoming a scientist was in fact exactly what she hoped it would be.

Amber then went on to continue working under Dr. Aaron Ericsson for her dissertation research with the goal of obtaining a PhD in veterinary pathobiology. She found herself surrounded by a group of likeminded people who challenged her appropriately and helped her grow as a scientist and a person. Amber faced numerous health challenges during this time which almost ended not only her pursuit for education, but also her life journey. Thankfully, Amber won the battle with her health and was able to continue her research, which other members of her lab dutifully managed in her absence. Amber is forever grateful for the grace and patience she received from her colleagues and committee members during this period of her life.

Upon receiving her PhD, Amber hopes to continue her career as a scientist. She has particular interest in bioinformatics and data analysis and is seeking positions in industry. She wishes to find a position that will allow her to continue making “way too many graphs” and diversify her repertoire of scientific techniques. Further down the road, Amber hopes to be a primary investigator that utilizes animal models for comparative medicine. No matter where life takes her, she will no doubt bring her Chihuahuas and enthusiasm for life.